# Feasibility of Bauxite Residue in Pollution Mitigation and Resource Recovery

**A Dissertation Presented for the**
**Doctor of Philosophy**
**Degree**
**The University of Tennessee, Knoxville**

**Yongfeng Wang**
**December 2018**

Copyright © 2018 by Yongfeng Wang.
All rights reserved.

# ACKNOWLEDGEMENTS

Firstly, I would like to sincerely thank my Ph.D. advisor, Dr. Qiang He. He invests lots of time in my study and gives tremendous help for the encouragement of scientific thinking and exploration new area. Besides, he likes to give some suggestions and tips about my life that make me adapt to the new environment easily.

I'm very grateful for the advice and comments from my committee members, Dr. Michael Essington, Dr. Chris Cox, Dr. Jie Zhuang. Thank you for your valuable suggestions and patience for answering my questions. These suggestions and comments inspire me to think deeply about my research.

I would like to thank Dr. Jie Zhuang again. He led the FEED program and gave me the opportunity to study in University of Tennessee, Knoxville.

I would like to thank Dr. Rong Ji as my courtesy committee member and master's advisor. He led me to the road for the scientific research. During my pursuing my Ph.D., you also give me some supports and encouragements.

Thank you to my labmates, Lu Yang, Liu Cao, Yabing Li, Songyi Liu, and Clifford Swanson, and previous member in Dr. He's lab, Dr. Si Chen, Dr. Kristen Wykoff, Tianxue Yang. Thank you to Dr. Kate Manz, Dr. Adrian Gonzales, Sharon Hale for the providing the assistance for my experiments. I also want to thank my friends for their support and help in my study and life.

Finally, I would like to thank my parents, Yanling Wang and Ling Nie, and my girlfriend, Ying Liu for your love, support, and encouragement.

# ABSTRACT

Bauxite residue is an industrial waste generated from the alumina refining industry, raising great concerns about environmental pollution. The primary problem for bauxite residue is its high alkalinity and salinity. This beneficial reuse of bauxite residue is desirable for the sustainable management of this waste stream. Bauxite residues can be used as an option of flue gas desulfurization to reduce the toxicity associated with high alkalinity. In this dissertation, it was first identified the linkage between the characteristics of the bauxite residues and their acid neutralization capacity (ANC). Further options of beneficial use were investigated according to the characteristics of bauxite residues. With the iron oxide-rich mineralogy, bauxite residue exhibited excellent capabilities to remove aqueous phosphate at environmentally relevant concentrations. Given that phosphate is an important nutrient, the removal and concentration of phosphorus with bauxite residue could be a strategy for the recovery of phosphorus as a resource. With its cation exchange capacity, bauxite residues were also found to be able to remove ciprofloxacin as an extensively used antibiotic and potential water pollutant. These findings show that bauxite residues could be used as feasible sorbents for pollution mitigation as well as resource recovery. The beneficial use was further demonstrated in the utilization of bauxite residues as an additive in anaerobic digestion, which is frequently implemented for the stabilization of organic waste and the production of biogas as a renewable energy source. My work shows that bauxite residues could be readily neutralized

by the buffering capacity of the digestate in the anaerobic digestion without negatively impacting process performance. More importantly, the addition of bauxite residue could enhance the availability of phosphorus in the digestate which is desirable for the land application of anaerobic digestate as a soil supplement. In summary, this work has developed multiple pathways for the sustainable management of bauxite residue as a hazardous material with integrated applications in pollution mitigation and resource recovery.

# TABLE OF CONTENTS

CHAPTER I Introduction and Overview ..... 1
Introduction ..... 2
The origin and characteristics of bauxite residue ..... 2
The management of bauxite residue ..... 3
Utilization of bauxite residue ..... 4
Introduction to anaerobic digestion ..... 7
Buffering capacity in anaerobic digestion ..... 7
Critical factors in anaerobic digestion ..... 8
Approach to improve anaerobic digestion ..... 10
Land application of digestate ..... 11
Overview ..... 11
References ..... 15
Appendix ..... 22
CHAPTER II Characterization of Acid Neutralization Capacity (ANC) of Bauxite Residue from Three Sources ..... 23
Abstract ..... 24
Introduction ..... 25
Materials and Methods ..... 27
Bauxite residue ..... 27
Experimental design ..... 27
Acid digestion procedure ..... 28
Other analysis ..... 29
Results and Discussion ..... 29
Acid neutralization capacity ..... 29
Environmental evaluation of bauxite residue leachate after neutralization ..... 31
Elemental and mineralogical composition ..... 31
SEM imaging ..... 32
Conclusion ..... 33
References ..... 34
Appendix ..... 35
CHAPTER III Potential of Neutralized Bauxite Residue in the Removal of Aqueous Phosphorus ..... 46
Abstract ..... 47
Introduction ..... 48
Materials and Methods ..... 50
Bauxite residue ..... 50
Retention kinetics ..... 51
Batch phosphate removal experiment ..... 53
Data analysis ..... 54
Results and Discussion ..... 54
Characteristics of bauxite residue ..... 54
Phosphate retention kinetics of bauxite residue ..... 55

Effect of sulfate ..... 57
Effect of pH ..... 58
Effect of phosphate amount ..... 60
Conclusion ..... 61
References ..... 62
Appendix ..... 65
CHAPTER IV Feasibility of Bauxite Residue for the Removal of Ciprofloxain in the Aqueous Solution ..... 72
Abstract ..... 73
Introduction ..... 74
Methods and Materials ..... 77
Materials ..... 77
Retention kinetics ..... 77
Batch removal study ..... 78
Adsorption isotherm ..... 78
Analysis methods ..... 79
Data analysis ..... 80
Results and Discussion ..... 82
Retention kinetics ..... 82
The effect of some parameters in batch removal experiment ..... 84
Adsorption isotherm ..... 87
Conclusion ..... 87
References ..... 89
Appendix ..... 93
CHAPTER V Effects of Bauxite Residue as an Additive on Biogas Production and Phosphorus Recovery in Anaerobic Digester ..... 100
Abstract ..... 101
Introduction ..... 103
Materials and Methods ..... 106
Materials ..... 106
Batch experiment ..... 106
Analytic method ..... 107
Phosphorus fraction ..... 107
Data analysis ..... 108
Results and Discussion ..... 109
Impact of bauxite residue on the methane production ..... 109
The content of soluble cation in the anaerobic digester ..... 110
Impact of bauxite residue on the bioavailability of phosphorus in the digestate ..... 112
Conclusion ..... 113
References ..... 115
Appendix ..... 118
CHAPTER VI Summary ..... 124
VITA ..... 127

# LIST OF TABLES

Table 1.1. The optional approaches for the bauxite residue utilization. .....22
Table 2.1. Concentration of inorganic chemicals in the leachate solution.....45
Table 3.1. The chemical composition of three types of bauxite residue.....65
Table 3.2. The major characteristics of three types of bauxite residue. .....65
Table 3.3. Removal kinetics parameters regressed by four different models.....68
Table 4.1. The major characteristics of two types of raw and neutralized bauxite residue.....93
Table 4.2. Retention kinetics parameters on bauxite residue. .....95
Table 4.3. Adsorption isotherm parameters on bauxite residue.....99
Table 5.1. The major composition of two types of bauxite residue. .....118
Table 5.2. Parameters of methane production calculated from Gompertz equation.....118

# LIST OF FIGURES

Figure 1.1. Water–energy–food nexus framework linked with the utilization of bauxite residue. ..... 22
Figure 2.1. Photograph of bauxite residue from three sources. ..... 35
Figure 2.2. Titration curves for the different alkaline materials. ..... 35
Figure 2.3. Accumulative curves of ANC (pH 7.0 and 5.5) for three types of bauxite residue. ..... 36
Figure 2.4. Dissolved percentage from raw bauxite residue after washing, neutralization and acidification. ..... 37
Figure 2.5. Chemical composition of raw bauxite residue and bauxite residue after treatment of washing, neutralization and acidification. ..... 38
Figure 2.6. XRD patterns of BR1, Neutralized BR1 and Acidified BR1. ..... 39
Figure 2.7. XRD patterns of BR2, Neutralized BR2 and Acidified BR2. ..... 40
Figure 2.8. XRD patterns of BR3, Neutralized BR3 and Acidified BR3. ..... 41
Figure 2.9. SEM micrographs of BR1 and materials after washing, neutralization and acidification. ..... 42
Figure 2.10. SEM micrographs of BR2 and materials after washing, neutralization and acidification. ..... 43
Figure 2.11. SEM micrographs of BR3 and materials after washing, neutralization and acidification. ..... 44
Figure 3.1. XRD patterns of three types of bauxite residue. ..... 66
Figure 3.2. SEM patterns of three types of bauxite residue. ..... 67
Figure 3.3. Phosphate retention kinetics by bauxite residue. ..... 67
Figure 3.4. Effect of sulfate on phosphate removal by bauxite residue. ..... 69
Figure 3.5. Phosphate removal by bauxite residue with different pH and pH in equilibrium solution. ..... 70
Figure 3.6. Phosphate removal by bauxite residue with different phosphate concentration. ..... 71
Figure 4.1. CIP retention kinetics by bauxite residue. The line was the data fitted by first-order kinetics, parallel-first-order kinetics and second order kinetics. ..... 94
Figure 4.2. The effect of ionic strength on CIP removal by bauxite residue. ..... 96
Figure 4.3. The effect of pH on CIP removal (left axis) and final solution pH (right axis). The solid lines represent the amount of CIP removed and dash lines represent the final solution pH, respectively. ..... 97
Figure 4.4. The effect of CIP concentration on CIP removal amount (left axis) and removal percentage (right axis). The solid lines represent the amount of CIP removed and dash lines represent the removal percentage, respectively. .. 98
Figure 5.1. Influence of the addition of different dosages of bauxite residue on the VFA (left axis) and pH (dotted line, right axis) in the anaerobic digester. The error bars indicate the standard deviation with duplicates. ..... 119

Figure 5.2. Influence of the addition of different dosages of bauxite residue on soluble cations in the anaerobic digester. The error bars indicate the standard deviation with duplicates. ..... 120
Figure 5.3. Influence of the addition of different dosages of bauxite residue on Fe in the anaerobic digester. The error bars indicate the standard deviation with duplicates..... 121
Figure 5.4. Influence of the addition of different dosages of bauxite residue on P concentration in the liquid of anaerobic digester. The error bars indicate the standard deviation with duplicates. ..... 122
Figure 5.5. Influence of the addition of different dosages of bauxite residue on P fraction in the digestate..... 123

# CHAPTER I
# INTRODUCTION AND OVERVIEW

# Introduction

***The origin and characteristics of bauxite residue***

Bauxite residue (red mud) is a type of industrial waste from the alumina refining process. To produce per ton alumina, 1-2.5 tons of bauxite residue is generated based on the origin of bauxite ore (Paramguru et al., 2005). The alumina industry started to develop over one century ago. Predictions by Power et al. (2011) suggest that over 3.9 billion tons of bauxite residue are stored in the earth until 2017. The Bayer process as the main way for extraction of alumina utilizes the sodium hydroxide to treat the bauxite ore, leading to the production of caustic bauxite residue. With high alkalinity and high salinity, the disposal and storage of bauxite residue remain an important issue. The 2010 dam failure incident in Ajka, Hungary unleashed about 600,000-700,000 $m^3$ bauxite residue, causing severe injury, property damage and environmental contamination (Ruyters et al., 2011).

The main characteristic of bauxite residue is high alkalinity (pH ≈ 11.3) derived from some alkaline anions, such as $HCO_3^-/CO_3^{2-}$, $Al(OH)_4^-$ and $OH^-$, and high salinity (electrical conductivity ≈ 7.4 mS $cm^{-1}$) contributed by exchangeable sodium ($[Na^+]$ ≈ 101.4 mmol $L^{-1}$) (Grafe et al., 2011). The dried bauxite residue is the fine-grained particle with particle sized ranged from 2 to 100 μm. The average specific surface area is 32.7 $m^2$ $g^{-1}$ and bulk density is 2.5 g $cm^{-3}$ (Santini and Banning, 2016).

Bauxite ore origin impacts the chemical and mineralogical composition of bauxite residue. Bauxite residue is commonly comprised of ferric oxide ($Fe_2O_3$),

aluminum oxide ($Al_2O_3$), silicon oxide ($SiO_2$), titanium oxide ($TiO_2$), calcium oxide (CaO), sodium oxide ($Na_2O$) paired with a wide range of other oxides (Klauber et al., 2011). Using the powder X-ray diffraction (powder-XRD), the crystalline components and the amorphous fraction can be identified. From the mineralogical view, bauxite residue consists of different minerals, like goethite (α-FeOOH), hematite (α-$Fe_2O_3$), gibbsite ($Al(OH)_3$), boehmite (γ-AlOOH), sodalite ($Na_8[Al_6Si_6O_{24}][(OH)_2]$), cancrinite ($Na_6[Al_6Si_6O_{24}]\cdot 2CaCO_3$), perovskite ($CaTiO_3$) (Grafe et al., 2011).

***The management of bauxite residue***

Storage and disposal of bauxite residue pose a great challenge due to the large amounts of production and high environmental risk. Prior to the 1970s, marine discharge and lagooning were the only two available disposal methods and use of these methods gradually decreased and ceased due to potential environmental impact (Power et al., 2011). The current method has shifted from the wet treatment toward dry stacking or dry cake disposal (Nikraz et al., 2007). Drying treatment can reduce the moisture content and diminish the leachability of bauxite residue. As the ultimate way, “cap and store” strategies and in situ remediation approaches are considered as the most promising management of bauxite residue by converting wastes to novel geological materials (Santini and Banning, 2016).

Neutralization is also an important management approach for remediating the alkaline hazard. Many materials have been studied and developed as the

neutralizing agent. Seawater has been verified to effectively neutralize the alkalinity of bauxite residue (Despland et al., 2010; Couperthwaite et al., 2014). Seawater neutralization primarily eliminates carbonate and bicarbonate alkalinity by forming insoluble solids. Besides seawater, gypsum ($CaSO_4$) can also neutralize the alkalinity of bauxite residue by precipitating carbonate (Kopittke et al., 2004). The acid material is another sort of neutralizing agent. Mineral acid remediation using hydrochloric, nitric or sulfuric acid has been investigated (Liang et al., 2014). These strong acids can rapidly neutralize the alkalinity of bauxite residue and extent of neutralization can be effectively controlled by the acid consumption. The acid gas such as $CO_2$ (Bonenfant et al., 2008; Yadav et al., 2010) or $SO_2$ (Wang et al., 2015) was also the remediation materials. These processes not only remediate the alkalinity of bauxite residue but also fulfill the desulfurization. The bauxite residue desulfurization system had been successfully applied in Japan (Sumitomo) and Italy (Eurallumina) for flue gas treatment (Grafe et al., 2011). Besides chemical neutralization, bioremediation by fermentation and extracellular polymeric substance production are also the promising ways of neutralizing the alkalinity for bauxite residue (Santini et al., 2015).

***Utilization of bauxite residue***

Recycle and reuse of bauxite residue can exploit more value of the waste stream and facilitate the sustainable management. To date, the attempts to reuse of bauxite residue can be classified into three categories, including building

construction and industrial material, metal recovery and environmental pollutant treatment listed in Table 1.1. Bauxite residue could be used as the additive to Portland cement (Tsakiridis et al., 2004). The stabilized bauxite residue could enhance performance as a road base material (Jitsangiam et al., 2008). The bauxite residue has also been investigated to apply for the ceramic brick construction industry (Dodoo-Arhin, 2013) and geopolymers (Dimas et al., 2009). For industrial material, bauxite residue has been explored in different aspects, such as pigments (Pera et al., 1997) and catalysts (Kim et al., 2015). Moreover, metal recovery is another important recycle approach, including major metal (iron, aluminum, and titanium) (Paramguru et al., 2005, Kumar et al., 2006) and minor metal (rare earth elements) (Smirnov and Molchanova, 1997).

Recent efforts have focused on applying bauxite residue in pollution mitigation. Using its alkalinity, bauxite residue can be applied not only for flue gas desulfurization as described above but also for the amendment of acid mine drainage and acid soils (Klauber et al., 2011). Moreover, using the excessive surface area, and high quantity of aluminum oxide and ferric oxide, bauxite residue can be utilized for wastewater treatment as adsorbents, coagulants, and flocculants (Wang et al., 2008).

As a low-cost adsorbent, bauxite residue exhibits strong removal capacity for some pollutants that makes it possible for effective wastewater treatment (Wang et al., 2008; Bhatnagar et al., 2011). As nutrient pollutants, phosphate (Li et al., 2006; Huang et al., 2008) and nitrate (Cengeloglu et al., 2006) can be

adsorbed by bauxite residue. The removal of toxic anions by bauxite residue, such as fluoride (Cengeloglu et al., 2002; Tor et al., 2009) and arsenate (Genc-Fuhrman et al., 2003; Genc-Fuhrman et al., 2004; Genc-Fuhrman et al., 2005) have also been given more concerns. Heavy metal such as copper, cadmium, chromium, lead, and zinc can also be removed from the solution with bauxite residue (Gupta and Sharma, 2002; Bertocchi et al., 2006; Garau et al., 2007; Nadaroglu et al., 2010). Bauxite residue can additionally be used to remove the organic compounds such as dyes (Wang et al., 2005; Ratnamala et al., 2012; Shirzad-Siboni et al., 2014), phenol (Tor et al., 2006) and chlorophenol (Gupta et al., 2004).

To improve the capacity of wastewater treatment, bauxite residue can be modified by some activation approaches. After acid and heat activation, bauxite residue can show more surface adsorption sites and positive charge in surface area to improve the phosphate adsorption (Li et al., 2006; Huang et al., 2008; Antunes et al., 2012). Some research attempted to treat the bauxite residue by different types of acids such as hydrochloric, nitric acid (Huang et al., 2008), or sulfuric acid (Koumanova et al., 1997). The combined acid-heat activation could obviously improve the efficiency of wastewater treatment (Liu et al., 2007; Ye et al., 2015). Furthermore, the bauxite residue granular adsorbents were made by sintering with additives such as bentonite, starch, straw, and hydroxypropyl methylcellulose (HPMC), further increasing adsorption capacity for phosphate (Yue et al., 2010; Zhao et al., 2012; Ye et al., 2015).

### *Introduction to anaerobic digestion*

Anaerobic digestion is the only biological waste treatment technology that produces energy in the form of biogas (methane). Anaerobic digestion can utilize the agricultural, industrial, and municipal wastes under anaerobic digestion (Angenent et al., 2004; Hartmann and Ahring, 2006). The significant benefit of anaerobic digestion is to stabilize the organic waste and to produce renewable energy. Other benefits include reductions of odors, pathogens, and greenhouse gas emissions during the storage of organic waste (Mitchell et al., 2013). Moreover, extracting nitrogen and phosphorus from anaerobic digestion can recover the nutrient (Li et al., 2015). The digestate as digested residue can be used as fertilizer for plant growth that can reuse the nutrients from anaerobic digestion.

### *Buffering capacity in anaerobic digestion*

Anaerobic digestion consists of four pivotal procedures, hydrolysis, acidogenesis, acetogenesis, and methanogenesis. Methanogenesis mainly involves two pathways, i.e., acetolactic methanogenesis and hydrogenotrophic methanogenesis (Appels et al., 2008). The hydrolysis step degrades the insoluble organic materials into soluble organic matter such as amino acids and fatty acids. Due to the existence of some complex resistant organic matter, such as cellulose, semicellulose and lignin, the hydrolysis is commonly considered as the rate-limiting step. Then acidogenesis step converts these soluble organic substances into volatile fatty acid. The organic acid and alcohol are converted

into acetic acid, carbon dioxide, and hydrogen gas by acetogenesis. Finally, methane and carbon dioxide are produced via methanogenesis. The four procedures require four special microbial groups, hydrolyzing bacteria, fermenting bacteria, acetogenic bacteria and methanogenic archaea (Angenent et al., 2004). Anaerobic digestion strongly relies on syntrophic processes among the involved microorganisms.

Carbonic acid and bicarbonate mainly contribute to the buffering capacity in anaerobic digestion. The percentage of carbon dioxide in biogas is approximately 40%. According to pH in the solution, carbonic acid and bicarbonate concentration change to adjust the buffer capacity in anaerobic digestion. Volatile fatty acid can also adjust the alkalinity in anaerobic digestion. Fermentative microorganisms have been studied to remediate the alkalinity of bauxite residue by producing some organic acids (Santini et al., 2016).

***Critical factors in anaerobic digestion***

Although anaerobic digestion is an attractive technique with many benefits, applications are still limited by low methane yields and process instability. Instability is caused by reaction complexity and strict requirements of operation condition such as temperature, organic loading rate, solids and hydraulic retention time (Gunaseelan, 1997; Mata-Alvarez et al., 2000). Temperature needs to be controlled between 30 °C and 38 °C for the mesophilic digester, and between 50 and 57 °C for the thermophilic digester (Appels et al., 2008). pH is another important factor for the anaerobic microbial community and the optimal

pH for anaerobic digestion is between 6.8 and 7.2 (Ward et al., 2008). Methanogenic microbes with an optimum pH between 6.5 and 7.2 are more sensitive to pH than other microorganisms in anaerobic digestion (Appels et al., 2008).

Besides of reaction complexity and strict requirements of operation condition, another primary problem in anaerobic digestion is the process inhibition (Chen et al., 2008). One of the most important inhibitors is ammonia, which can significantly inhibit the growth of methanogens (Kayhanian, 1994). Ammonia is derived from the degradation of substrates with high protein and urea (Kayhanian, 1999), such as poultry waste (Kelleher et al., 2002). The toxicity is made by free ammonia nitrogen compared to the ammonium ion, thus ammonia inhibition is subjected to pH and temperature that can determine the balance of ammonia and ammonium in solution (Rajagopal et al., 2013). Associated with operation condition, the threshold concentration of ammonia inhibition ranged from 2500 mg/L to 6000 mg/L of total ammonia nitrogen (Rajagopal et al., 2013; Yenigun and Demirel, 2013). Antibiotics are also important inhibitor due to the antibiotics are widely used for animal husbandry and can be detected in the animal waste (Kemper, 2008). Antibiotics can obviously inhibit the methane yield and microbial community (Alvarez et al., 2010; Mitchell et al., 2013). High concentrations of cations and heavy metal can cause the bacterial cells to dehydrate and affect the enzyme activity (Sterritt and Lester, 1980; Yerkes et al., 1997). The overproduction of short chain fatty

alcohols and acids, and aromatic organic compounds were also found as inhibitors in anaerobic digestion (Heipieper et al., 1994; Blume et al., 2010).

***Approach to improve anaerobic digestion***

Optimizing of operation is the primary way to maintain the stability of anaerobic digestion. Anaerobic co-digestion that simultaneously treat different wastes is considered as the most valid way to improve biogas yield and substrate utilization (Mata-Alvarez et al., 2014). Some biological or chemical additives are added to enhance biogas yield in anaerobic digestion. Biological additives, such as microbial consortium and enzymes, can be used to increase cellulose and hemicellulose availability (Mao et al., 2015). On the other hand, alkali reagent, acid reagent, and oxidative reagent can be also used for pretreatment of lignocelluloses, improving the biodegradation and bioavailability of lignocelluloses (Mao et al., 2015). The addition of macronutrients and trace elements can also stimulate the treatment efficiency by stimulating the growth of microorganisms (Banks et al., 2012). Adding rusty scrap iron into anaerobic digestion was proposed to enhance anaerobic sludge digestion as induced microbial iron reduction accelerated the anaerobic hydrolysis–acidification processes (Zhang et al., 2014). To recover from ammonia inhibition, zeolite, glauconite, and activated carbon were considered as the additives (Yenigun and Demirel, 2013). Biochar used as an adsorbent can mitigate inhibition by adsorbing the inhibitor and supply a habitat for the methanogenic microflora (Mumme et al., 2014; Fagbohungbe et al., 2016).

### *Land application of digestate*

Land application of digestate can bring various benefits, such as nutrient recycling, reduction of mineral fertilizer consumption, and water pollution mitigation (Holm-Nielsen et al., 2009). As compared with undigested manure, Insam et al. (2015) concluded that digestate had more positive effects on the climate, environment, and agriculture. Animal waste is an important source of atmospheric methane (Sommer et al., 2007). After anaerobic digestion, animal waste is converted into digestate, and organic carbon is reduced and stabilized. Therefore, the land application of digestate mean the reduction of greenhouse gas production from manure (Insam and Wett, 2008); however, the land application of digestate is limited by the regulations from different countries due to the negative effects on the environment, such as heavy metals, pathogens, antibiotics, and overloading of nutrients (Insam et al., 2015). Therefore, the ecological influence should be considered when the digestate is used as fertilizer. The seed germination and elongation of root and shoot tests are primary approaches for phytotoxicity assessment, of which seed germination test is the fastest test (Di Salvatore et al., 2008). These methods can be easily used for evaluating the environmental risk of land application of digestate.

## Overview

Solid waste management is an important issue for the sustainable development of society. The solid waste comes from the municipal, agricultural and industrial activities. To treat these wastes appropriately, waste management needs to

follow the basic “three R’s” principle, i.e. reduce, reuse and recycle. Integrated solid waste management meets the great challenge. This study is aimed to explore the feasibility of bauxite residue in pollution mitigation and resource recovery combined with anaerobic digestion. The flowchart of the integrated treatment of bauxite residue and bio-waste is shown in Figure 1.1.

Bauxite residue is a byproduct of the alumina refining process as the mineral waste and is mostly comprised of various minerals. The high alkalinity and salinity make it bring the great environmental risk (Grafe et al., 2011). The dry stacking or dry cake disposal is the major approach for management of bauxite residue currently (Nikraz et al., 2007). More concerns have been given to the reuse and recycle of bauxite residue (Wang et al., 2008). The alumina refining process requires the electricity that needs to be supplied by the power plant. Using the alkalinity of bauxite residue can achieve the desulfurization of flue gas from the power plant. This approach can simultaneously neutralize the alkalinity of bauxite residue with the acidity of flue gas. In chapter II, the sulfuric acid ($H_2SO_4$) neutralization and acidification by three types of bauxite residue were used to simulate the flue gas desulfurization. Characterization of three kinds of bauxite residue and their acid neutralization capacity (ANC) were studied. During the neutralization and acidification, the leachate would not pose an extra environmental risk.

Even though these bauxite residues have been neutralized, the storage is still a problem due to the occupancy of space. Therefore, it is important to find

the right way to reuse them. The neutralized bauxite residue has been verified for the strong removal capacity of pollutants (Wang et al., 2008; Bhatnagar et al., 2011). Therefore, the neutralized bauxite residue can be considered to the removal of inorganic and organic pollutants. In chapter III and IV, the feasibility of $H_2SO_4$ neutralized bauxite residue in the removal of aqueous phosphorus and antibiotics were investigated.

Animal waste such as cattle manure, dairy manure or poultry manure comes from agriculture production and contains large amounts of organic matter. The storage of untreated animal waste can lead to serious environmental pollution, such as nutrient leaching, ammonia evaporation, and pathogen contamination (Holm-Nielsen et al., 2009). Anaerobic digestion is a valid approach to treat and convert them into biogas (methane and carbon dioxide). After post-treatment, methane content in biogas can be improved to meet the requirement of transportation in pipeline and utilization as bioenergy. On the other hand, the digestate derived from the anaerobic digestion can be further used for land application as fertilizer. The grass can be used for the feedstock of livestock, and other crops can be used for food. Then the biowaste from the animal waste or food waste can be treated in anaerobic digestion. This practice is an important way of recycling animal waste.

The anaerobic digestion as a buffering system can produce carbon dioxide and organic acids, which may bioremediate the alkalinity of bauxite residue. The anaerobic digestate with bauxite residue will be feasible as a

nutrient-rich and slow-releasing nutrient supplement in agricultural application. In chapter V, the effect of bauxite residue as an additive on biogas production and phosphorus fraction in anaerobic digester were investigated. Adding the bauxite residue into anaerobic digestion can integrate the mineral waste and biowaste management. This integrated waste management can improve the recycling efficiency of these two kinds of waste. On the other hand, this integrated waste management combined two industrial and agricultural closed-loop systems together.

## References


Alvarez JA, Otero L, Lema JM, Omil F. 2010. The effect and fate of antibiotics during the anaerobic digestion of pig manure. Bioresource Technol 101(22): 8581-8586.

Angenent LT, Karim K, Al-Dahhan MH, Domiguez-Espinosa R. 2004. Production of bioenergy and biochemicals from industrial and agricultural wastewater. Trends Biotechnol 22(9): 477-485.

Antunes MLP, Couperthwaite SJ, Da Conceicao FT, De Jesus CPC, Kiyohara PK, Coelho ACV, Frost RL. 2012. Red mud from brazil: thermal behavior and physical properties. Ind Eng Chem Res 51(2): 775-779.

Appels L, Baeyens J, Degreve J, Dewil R. 2008. Principles and potential of the anaerobic digestion of waste-activated sludge. Prog Energ Combust 34(6): 755-781.

Banks CJ, Zhang Y, Jiang Y, Heaven S. 2012. Trace element requirements for stable food waste digestion at elevated ammonia concentrations. Bioresource Technol 104: 127-135.

Bertocchi AF, Ghiani M, Peretti R, Zucca A. 2006. Red mud and fly ash for remediation of mine sites contaminated with As, Cd, Cu, Pb and Zn. J Hazard Mater 134(1-3): 112-119.

Bhatnagar A, Vilar VJP, Botelho CMS, Boaventura RAR. 2011. A review of the use of red mud as adsorbent for the removal of toxic pollutants from water and wastewater. Environ Technol 32(3): 231-249.

Blume F, Bergmann I, Nettmann E, Schelle H, Rehde G, Mundt K, Klocke M. 2010. Methanogenic population dynamics during semi-continuous biogas fermentation and acidification by overloading. J Appl Microbiol 109(2): 441-450.

Bonenfant D, Kharoune L, Sauve S, Hausler R, Niquette P, Mimeault M, Kharoune M. 2008. $CO_2$ sequestration by aqueous red mud carbonation at ambient pressure and temperature. Ind Eng Chem Res 47(20): 7617-7622.

Cengeloglu Y, Kir E, Ersoz M. 2002. Removal of fluoride from aqueous solution by using red mud. Sep Purif Technol 28(1): 81-86.

Cengeloglu Y, Tor A, Ersoz M, Arslan G. 2006. Removal of nitrate from aqueous solution by using red mud. Sep Purif Technol 51(3): 374-378.

Chen Y, Cheng JJ, Creamer KS. 2008. Inhibition of anaerobic digestion process: A review. Bioresource Technol 99(10): 4044-4064.

Couperthwaite SJ, Johnstone DW, Mullett ME, Taylor KJ, Millar GJ. 2014. Minimization of bauxite residue neutralization products using nanofiltered Seawater. Ind Eng Chem Res 53(10): 3787-3794.

Despland LM, Clark MW, Aragno M, Vancov T. 2010. Minimising alkalinity and pH spikes from Portland cement-bound bauxsol (Seawater-Neutralized Red Mud) pellets for pH circum-neutral waters. Environ Sci Technol 44(6): 2119-2125.

Di Salvatore M, Carafa AM, Carratù G. 2008. Assessment of heavy metals phytotoxicity using seed germination and root elongation tests: A comparison of two growth substrates. Chemosphere 73(9): 1461-1464.

Dimas DD, Giannopoulou IP, Panias D. 2009. Utilization of alumina red mud for synthesis of inorganic polymeric materials. Miner Process Extr M 30(3): 211-239.

Dodoo-Arhin D, Konadu DS, Annan E, Buabeng FP, Yaya A, Agyei-Tuffour B. 2013. Fabrication and characterization of Ghanaian bauxite red mud-clay composite bricks for construction applications. American Journal of Materials Science 3(5): 110-119.

Fagbohungbe MO, Herbert BMJ, Hurst L, Li H, Usmani SQ, Semple KT. 2016. Impact of biochar on the anaerobic digestion of citrus peel waste. Bioresource Technol 216: 142-149.

Garau G, Castaldi P, Santona L, Deiana P, Melis P. 2007. Influence of red mud, zeolite and lime on heavy metal immobilization, culturable heterotrophic microbial populations and enzyme activities in a contaminated soil. Geoderma 142(1-2): 47-57.

Genc-Fuhrman H, Bregnhoj H, McConchie D. 2005. Arsenate removal from water using sand-red mud columns. Water Res 39(13): 2944-2954.

Genc-Fuhrman H, Tjell JC, McConchie D. 2004. Adsorption of arsenic from water using activated neutralized red mud. Environ Sci Technol 38(8): 2428-2434.

Genc H, Tjell JC, McConchie D, Schuiling O. 2003. Adsorption of arsenate from water using neutralized red mud. J Colloid Interf Sci 264(2): 327-334.

Grafe M, Power G, Klauber C. 2011. Bauxite residue issues: III. Alkalinity and associated chemistry. Hydrometallurgy 108(1-2): 60-79.

Gunaseelan VN. 1997. Anaerobic digestion of biomass for methane production: A review. Biomass Bioenerg 13(1-2): 83-114.

Gupta VK, Ali I, Saini VK. 2004. Removal of chlorophenols from wastewater using red mud: An aluminum industry waste. Environ Sci Technol 38(14): 4012-4018.

Gupta VK, Sharma S. 2002. Removal of cadmium and zinc from aqueous solutions using red mud. Environ Sci Technol 36(16): 3612-3617.

Hartmann H, Ahring BK. 2006. Strategies for the anaerobic digestion of the organic fraction of municipal solid waste: an overview. Water Sci Technol 53(8): 7-22.

Heipieper HJ, Weber FJ, Sikkema J, Keweloh H, Debont JAM. 1994. Mechanisms of resistance of whole cells to toxic organic-solvents. Trends Biotechnol 12(10): 409-415.

Holm-Nielsen JB, Al Seadi T, Oleskowicz-Popiel P. 2009. The future of anaerobic digestion and biogas utilization. Bioresource Technol 100(22): 5478-5484.

Huang WW, Wang SB, Zhu ZH, Li L, Yao XD, Rudolph V, Haghseresht F. 2008. Phosphate removal from wastewater using red mud. J Hazard Mater 158(1): 35-42.

Insam H, Gomez-Brandon M, Ascher J. 2015. Manure-based biogas fermentation residues - Friend or foe of soil fertility? Soil Biol Biochem 84: 1-14.

Insam H, Wett B. 2008. Control of GHG emission at the microbial community level. Waste Manage 28(4): 699-706.

Jitsangiam P, Nikraz H, Jamieson E. 2008. Pozzolanic-Stabilised Mixture (PSM) for red sand as road base materials. Proc Monogr Eng Wate 1-2: 647-651.

Kayhanian M. 1994. Performance of a high-solids anaerobic-digestion process under various ammonia concentrations. J Chem Technol Biot 59(4): 349-352.

Kayhanian M. 1999. Ammonia inhibition in high-solids biogasification: An overview and practical solutions. Environ Technol 20(4): 355-365.

Kelleher BP, Leahy JJ, Henihan AM, O'Dwyer TF, Sutton D, Leahy MJ. 2002. Advances in poultry litter disposal technology - a review. Bioresource Technol 83(1): 27-36.

Kemper N. 2008. Veterinary antibiotics in the aquatic and terrestrial environment. Ecol Indic 8(1): 1-13.

Kim SC, Nahm SW, Park YK. 2015. Property and performance of red mud-based catalysts for the complete oxidation of volatile organic compounds. J Hazard Mater 300: 104-113.

Klauber C, Grafe M, Power G. 2011. Bauxite residue issues: II. options for residue utilization. Hydrometallurgy 108(1-2): 11-32.

Kopittke PM, Menzies NW, Fulton IM. 2004. Gypsum solubility in seawater, and its application to bauxite residue amelioration. Aust J Soil Res 42(8): 953-960.

Koumanova B, Drame M, Popangelova M. 1997. Phosphate removal from aqueous solutions using red mud wasted in bauxite Bayer's process. Resour Conserv Recy 19(1): 11-20.

Kumar S, Kumar R, Bandopadhyay A. 2006. Innovative methodologies for the utilisation of wastes from metallurgical and allied industries. Resour Conserv Recy 48(4): 301-314.

Li WW, Yu HQ, Rittmann BE. 2015. Chemistry: Reuse water pollutants. Nature 528(7580): 29-31.

Li YZ, Liu CJ, Luan ZK, Peng XJ, Zhu CL, Chen ZY, Zhang ZG, Fan JH, Jia ZP. 2006. Phosphate removal from aqueous solutions using raw and activated red mud and fly ash. J Hazard Mater 137(1): 374-383.

Liang WT, Couperthwaite SJ, Kaur G, Yan C, Johnstone DW, Millar GJ. 2014. Effect of strong acids on red mud structural and fluoride adsorption properties. J Colloid Interf Sci 423: 158-165.

Liu CJ, Li YZ, Luan ZK, Chen ZY, Zhang ZG, Jia ZP. 2007. Adsorption removal of phosphate from aqueous solution by active red mud. J Environ Sci-China 19(10): 1166-1170.

Mao CL, Feng YZ, Wang XJ, Ren GX. 2015. Review on research achievements of biogas from anaerobic digestion. Renew Sust Energ Rev 45: 540-555.

Mata-Alvarez J, Dosta J, Romero-Guza MS, Fonoll X, Peces M, Astals S. 2014. A critical review on anaerobic co-digestion achievements between 2010 and 2013. Renew Sust Energ Rev 36: 412-427.

Mata-Alvarez J, Mace S, Llabres P. 2000. Anaerobic digestion of organic solid wastes. An overview of research achievements and perspectives. Bioresource Technol 74(1): 3-16.

Mitchell SM, Ullman JL, Teel AL, Watts RJ, Frear C. 2013. The effects of the antibiotics ampicillin, florfenicol, sulfamethazine, and tylosin on biogas production and their degradation efficiency during anaerobic digestion. Bioresource Technol 149: 244-252.

Mumme J, Srocke F, Heeg K, Werner M. 2014. Use of biochars in anaerobic digestion. Bioresource Technol 164: 189-197.

Nadaroglu H, Kalkan E, Demir N. 2010. Removal of copper from aqueous solution using red mud. Desalination 251(1-3): 90-95.

Nikraz HR, Bodley AJ, Cooling DJ, Kong PYL, Soomro M. 2007. Comparison of physical properties between treated and untreated bauxite residue mud. J Mater Civil Eng 19(1): 2-9.

Paramguru RK, Rath PC, Misra VN. 2005. Trends in red mud utilization - A review. Miner Process Extr M 26(1): 1-29.

Pera J, Boumaza R, Ambroise J. 1997. Development of a pozzolanic pigment from red mud. Cement Concrete Res 27(10): 1513-1522.

Power G, Grafe M, Klauber C. 2011. Bauxite residue issues: I. Current management, disposal and storage practices. Hydrometallurgy 108(1-2): 33-45.

Rajagopal R, Masse DI, Singh G. 2013. A critical review on inhibition of anaerobic digestion process by excess ammonia. Bioresource Technol 143: 632-641.

Ratnamala GM, Shetty KV, Srinikethan G. 2012. Removal of Remazol Brilliant Blue Dye from dye-contaminated water by adsorption using red mud: equilibrium, kinetic, and thermodynamic studies. Water Air Soil Poll 223(9): 6187-6199.

Ruyters S, Mertens J, Vassilieva E, Dehandschutter B, Poffijn A, Smolders E. 2011. The red mud accident in Ajka (Hungary): plant toxicity and trace metal bioavailability in red mud contaminated soil. Environ Sci Technol 45(4): 1616-1622.

Santini TC, Banning NC. 2016. Alkaline tailings as novel soil forming substrates: reframing perspectives on mining and refining wastes. Hydrometallurgy 164: 38-47.

Santini TC, Kerr JL, Warren LA. 2015. Microbially-driven strategies for bioremediation of bauxite residue. J Hazard Mater 293: 131-157.

Santini TC, Malcolm LI, Tyson GW, Warren LA. 2016. pH and organic carbon dose rates control microbially driven bioremediation efficacy in alkaline bauxite residue. Environ Sci Technol 50(20): 11164-11173.

Shirzad-Siboni M, Jafari SJ, Giahi O, Kim I, Lee SM, Yang JK. 2014. Removal of acid blue 113 and reactive black 5 dye from aqueous solutions by activated red mud. J Ind Eng Chem 20(4): 1432-1437.

Smirnov DI, Molchanova TV. 1997. The investigation of sulphuric acid sorption recovery of scandium and uranium from the red mud of alumina production. Hydrometallurgy 45(3): 249-259.

Sommer SG, Petersen SO, Sorensen P, Poulsen HD, Moller HB. 2007. Methane and carbon dioxide emissions and nitrogen turnover during liquid manure storage. Nutr Cycl Agroecosys 78(1): 27-36.

Sterritt RM, Lester JN. 1980. Interactions of heavy-metals with bacteria. Sci Total Environ 14(1): 5-17.

Tor A, Cengeloglu Y, Aydin ME, Ersoz M. 2006. Removal of phenol from aqueous phase by using neutralized red mud. J Colloid Interf Sci 300(2): 498-503.

Tor A, Danaoglu N, Arslan G, Cengeloglu Y. 2009. Removal of fluoride from water by using granular red mud: Batch and column studies. J Hazard Mater 164(1): 271-278.

Tsakiridis PE, Agatzini-Leonardou S, Oustadakis P. 2004. Red mud addition in the raw meal for the production of Portland cement clinker. J Hazard Mater 116(1-2): 103-110.

Wang SB, Ang HM, Tade MO. 2008. Novel applications of red mud as coagulant, adsorbent and catalyst for environmentally benign processes. Chemosphere 72(11): 1621-1635.

Wang SB, Boyjoo Y, Choueib A, Zhu ZH. 2005. Removal of dyes from aqueous solution using fly ash and red mud. Water Res 39(1): 129-138.

Wang XK, Zhang YH, Lv FZ, An Q, Lu RR, Hu P, Jiang SB. 2015. Removal of alkali in the red mud by $SO_2$ and simulated flue gas under mild conditions. Environ Prog Sustain 34(1): 81-87.

Ward AJ, Hobbs PJ, Holliman PJ, Jones DL. 2008. Optimisation of the anaerobic digestion of agricultural resources. Bioresource Technol 99(17): 7928-7940.

Yadav VS, Prasad M, Khan J, Amritphale SS, Singh M, Raju CB. 2010. Sequestration of carbon dioxide ($CO_2$) using red mud. J Hazard Mater 176(1-3): 1044-1050.

Ye J, Cong XN, Zhang PY, Hoffmann E, Zeng GM, Wu Y, Zhang HB, Fan W. 2015. Phosphate adsorption onto granular-acid-activated-neutralized red mud: parameter optimization, kinetics, isotherms, and mechanism analysis. Water Air Soil Poll 226: 306.

Ye J, Cong XN, Zhang PY, Hoffmann E, Zeng GM, Wu Y, Zhang HB, Fang W. 2015. Preparation of a new granular acid-activated neutralized red mud and evaluation of its performance for phosphate adsorption. Acs Sustain Chem Eng 3(12): 3324-3331.

Yenigun O, Demirel B. 2013. Ammonia inhibition in anaerobic digestion: A review. Process Biochem 48(5-6): 901-911.

Yerkes DW, Boonyakitsombut S, Speece RE. 1997. Antagonism of sodium toxicity by the compatible solute betaine in anaerobic methanogenic systems. Water Sci Technol 36(6-7): 15-24.

Yue QY, Zhao YQ, Li Q, Li WH, Gao BY, Han SX, Qi YF, Yu H. 2010. Research on the characteristics of red mud granular adsorbents (RMGA) for phosphate removal. J Hazard Mater 176(1-3): 741-748.

Zhang YB, Feng YH, Yu QL, Xu ZB, Quan X. 2014. Enhanced high-solids anaerobic digestion of waste activated sludge by the addition of scrap iron. Bioresource Technol 159: 297-304.

Zhao YQ, Yue QY, Li Q, Xu X, Yang ZL, Wang XJ, Gao BY, Yu H. 2012. Characterization of red mud granular adsorbent (RMGA) and its performance on phosphate removal from aqueous solution. Chem Eng J 193: 161-168.

# Appendix

**Table 1.1. The optional approaches for the bauxite residue utilization.**

| Application area | Utilization case |
|---|---|
| Building construction and industrial material | Additive to Portland cement and road base material; ceramic brick construction industry and geopolymers; pigments and catalysts |
| Metal recovery | Major metal (iron, aluminum and titanium) and rare earth elements (scandium, uranium and thorium) |
| Environmental pollutant treatment | Treatment of acid mine drainage and wastewater treatment as adsorbents, coagulants and flocculants; waste gas treatment; soil amendment |

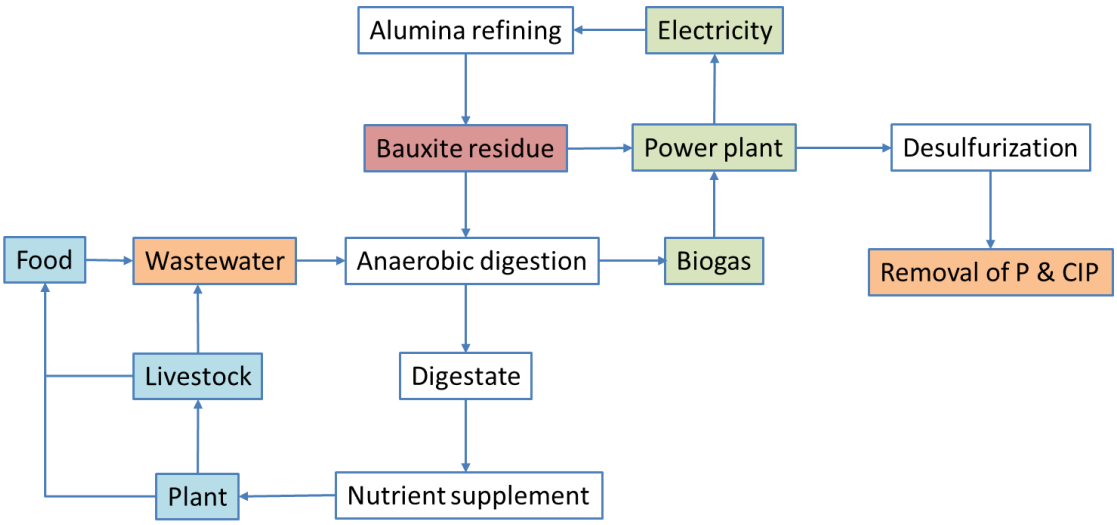


**Figure 1.1. Water–energy–food nexus framework linked with the utilization of bauxite residue.**

# CHAPTER II
# CHARACTERIZATION OF ACID NEUTRALIZATION CAPACITY (ANC) OF BAUXITE RESIDUE FROM THREE SOURCES

## Abstract

Bauxite residue (BR) as the byproduct of bauxite refining process has been characterized with high alkalinity, which could be exploited for use as the base chemical in flue gas desulfurization. In this study, bauxite residue from three sources were tested for acid neutralization capacity (ANC) as well as its linkage to mineralogy. The ANC (pH 7.0) of BR2 was the greatest among the three bauxite residues, while the ANC (pH 5.5) of BR1 was found to be the greatest among the three bauxite residues. According to the chemical and mineral composition of the raw bauxite residue as well as the neutralized or acidified bauxite residue, the ANC (pH 7.0) of BR2 could be attributed primarily to readily dissolved alkalinity in the form of sodium hydroxide (NaOH) or sodium carbonate ($Na_2CO_3$). In comparison, the ANC (pH 5.5) of BR1 and BR3 was likely attributable to mineral alkalinity, such as sodalite and calcite. Following the release of sodium (Na) and calcium (Ca) from bauxite residue after neutralization or acidification, the level of iron (Fe) increased in the solid phase. The increase in iron oxides content in bauxite residue is expected to enhance the utility of this material as an effective sorbent for pollutant removal, which would be further evaluated.

# Introduction

Bauxite residue (BR) is the alkaline byproduct from the bauxite refining process. Due to its high alkalinity, the bauxite residue is a hazardous material with corrosive characteristics. The disposal and storage of bauxite residue has resulted in major environmental and safety concerns. For example, after the dam collapse of the bauxite residue reservoir in Hungary in 2010, a series of problems emerged in the contaminated area, including plant toxicity, trace metal toxicity and soil deterioration (Ruyters et al., 2011). The alkalinity of bauxite residue is primarily derived from a number of alkaline anions, such as $HCO_3^-/CO_3^{2-}$, $Al(OH)_4^-$ and $OH^-$ (Grafe et al., 2011).

Some materials have been developed to neutralize the alkalinity of bauxite residue, e.g. seawater (Couperthwaite et al., 2014), gypsum (Kopittke et al., 2004), microbial function (Krishna et al., 2005), $CO_2$ (Sahu et al., 2010) and $SO_2$ (Wang et al., 2015). The alkalinity neutralization by $SO_2$ is combined with flue gas desulfurization. The aluminum industry consumes large amounts of energy in the form of electricity. During power generation in coal-fired power plants, the flue gas emission from coal power plant is an important air pollution issue. All types of coal contain sulfur. Thus, coal combustion is a large source of sulfur dioxide, an acidic pollutant gas that contributes to the production of acid rain, among other negative environmental impacts. Given the oxidation of $SO_2$, $SO_3$ also exists in the flue gas. Sulfuric acid ($H_2SO_4$) as a surrogate of $SO_2$ in flue gas was also considered as the neutralizing agent for the alkalinity of bauxite residue.

After neutralization, bauxite residue has been utilized for some environmental-friendly applications and one of the main applications is building materials, e.g. aggregates, bricks, cement, concrete and road materials (Klauber et al., 2011). In addition, the neutralized or acidified bauxite residue has been applied to solve environmental and agronomic problems (Wang et al., 2008; Klauber et al., 2011) due to that neutralized bauxite residue showed better performance with some special characteristics. For example, neutralized bauxite residue provides more surface adsorption sites and positive charges in surface area to enhance the adsorption capacity of phosphate (Li et al., 2006) and fluoride (Liang et al., 2014).

Due to the different origins of bauxite ores, there are some differences in the characteristics of bauxite residue. Based on the results in the review (Grafe et al., 2011), for different types of bauxite residue, pH can range from 9.7 to 12.8; electrical conductivity from 1.4 mS $cm^{-1}$ to 28.4 mS $cm^{-1}$; and sodium concentration from 8.9 mmol $L^{-1}$ to 225.8 mmol $L^{-1}$. Additionally, the chemical and mineral composition varied mostly according to the source of bauxite. On the other hand, the property of bauxite residue would change with acidification and neutralization. Currently, there still lacks the comparison between different types of neutralized or acidified bauxite residue.

In this study, we used $H_2SO_4$ neutralization of bauxite residue to simulate flue gas desulfurization by bauxite residue. This study aims to investigate the

acid neutralization capacity (ANC) of bauxite residue from three sources and characterize the neutralized bauxite residue.

## Materials and Methods

### *Bauxite residue*

The three bauxite residues included alumina refining facilities located in Shandong, Guangxi and Pingguo, China. They were respectively designated as BR1, BR2 and BR3. The appearance of the three types of bauxite residue of different sources was shown in figure 2.1.

### *Experimental design*

The raw materials were rinsed firstly with DI water for three times and dried in a fume hood. To measure the acid titration curve, the bauxite residue (4 g) with 100 ml DI water was titrated with 0.1 N $H_2SO_4$ as a surrogate of $SO_2$ to simulate flue gas desulfurization by bauxite residue. Then, 10 ml solution was taken and centrifuged. After centrifugation, the supernatant was acidified by 5% $HNO_3$ and analyzed for inorganic chemicals including copper (Cu), zinc (Zn), arsenic (As), chromium (Cr), selenium (Se), barium (Ba), Cadmium (Cd), Lead (Pb), Sliver (Ag) by inductively coupled atomic emission spectrometry (Thermo Electron Intrepid II ICP-AES).

To measure the acid neutralization capacity at long-term, the bauxite residue (1 g) with 25 ml DI water was titrated to pH 7.0 and 5.5 with 0.1 N $H_2SO_4$. The solid residues were respectively considered as the neutralized bauxite

residue and acidified bauxite residue after the bauxite residue was titrated to pH 7.0 and 5.5. pH in solution was measured by Oakton pH 700 Meter. After the equilibrium, the solution was centrifuged at 16000 g/min for 15 min. Then the supernatant was stored by acidifying by $HNO_3$ as acid leaching sample and analyzed by ICP-AES. The solid residues were rinsed with DI water for three times and dried in a fume hood, and then was digested to analyze the chemical composition in a microwave accelerated reaction system (CEM MARS 5) (see below).

***Acid digestion procedure***

The solid residue (0.4 g) was placed in a perfluoroalkoxy alkanes (PFA) liner and added with 9 mL of nitric acid (68%, m:V), 3 mL of hydrofluoric acid (48%, m:V) and 3 mL of hydrochloric acid (37%, m:V). After vigorous reaction stopped, the container was tightly capped and then placed into the microwave oven. The microwave oven was heated at 180 °C for 30 min. After cooling down for at least 5 min, the container was uncapped and 10 mL of boric acid neutralization solution (4.7%, m:V) was quickly added. The container was then re-capped, returned to the oven and heated at 170 °C for 20 min. A blank solution without solid was added containing the same amount of nitric acid, hydrofluoric acid, hydrochloric acid and boric acid, and set as control treatment with the same acid digestion procedure. After the acid digestion, the solution was centrifuged at 16000 g/min for 15 min. Then the supernatant was diluted with nitric acid (1%, m:V) and analyzed by ICP-AES.

### *Other analysis*

To identify the mineral composition, X-ray diffraction (XRD) patterns were collected using a Panalytical Empyrean with Cu Kα radiation at 45 kV and 40 mA. Scanning electron microscope (SEM, Zeiss AURIGA) is used to analyze the morphology.

## Results and Discussion

### *Acid neutralization capacity*

The titration curves of bauxite residue were shown in figure 2.2. Compared with bauxite residue, some industrial wastes had also been used for flue gas desulfurization (Cheng et al., 2009). The calcium carbide residue, mainly composed of $Ca(OH)_2$, was selected to compare the amounts of acid consumption with bauxite residue. According to the titration curve, the initial pH of the calcium carbide residue was 12.8, which was significantly greater than three bauxite residues. When titrated to neutral status, calcium carbide residue required more acid than bauxite residue. Thus, for desulfurization, the calcium carbide residue had greater capacity than bauxite residue. However, for removing the alkalinity, the bauxite residue performed better than calcium carbide residue. Due to the dissolution of fluoride, calcium carbide residue was not a benign material for desulfurization. For the three types of bauxite residue, the initial pH of BR1, BR2 and BR3 were respectively 9.7, 9.6 and 8.4. According to the titration curves in figure 2.2, the capacities of acid consumption were comparable for bauxite residue and the amounts of acid consumption were

related to the initial pH of bauxite residue. Therefore, BR1 and BR2 performed better than BR3 for the amounts of acid consumption.

ANC is used to measure the amount of acid required to reach a specific pH endpoint, and pH 5.5 and 7.0 are usually considered as the pH endpoint. The ANC of bauxite residue in the long term were shown in figure 3.3. After 24 days (6 times) titration, the ANC of bauxite residue was relatively steady. The ANC (pH 7.0) for BR1, BR2 and BR3 were 1.89 mol $H^+$/kg, 2.70 mol $H^+$/kg and 1.58 mol $H^+$/kg, respectively. The ANC (pH 5.5) for BR1, BR2 and BR3 were 4.55 mol $H^+$/kg, 3.75 mol $H^+$/kg and 3.95 mol $H^+$/kg, respectively. These results were consistent with other literatures with average 0.94 mol $H^+$/kg for ANC at pH 7.0 and 4.56 mol $H^+$/kg for ANC at pH 5.5 (Grafe et al., 2011). On the other hand, the slow releasing capacity of alkalinity was consistent with the basic characteristics of bauxite residue (Liu et al., 2007). The neutralization reaction is instantaneous, and the slow releasing process of alkalinity is determined by the dissolution of the mineral phase that determines the equilibrium during the measurement of ANC of bauxite residue.

Comparing the ANC of these three types of bauxite residue, there were some obvious differences. The ANC of BR1 and BR2 reached steady more quickly than BR3, indicating that BR1 and BR2 had some more readily releasing alkalinity. For BR2, the ANC (pH 7.0) was the greatest, but ANC (pH 5.5) was the lowest. These results suggested that BR2 contained the most dissolved alkalinity, such as $OH^-$ and $HCO_3^-$/$CO_3^{2-}$, and lack of mineral alkalinity.

Acidification can dissolve the sodalite for BR1, while acidification can dissolve the calcite for BR3. The dissolution of these alkaline minerals leaded to the slow-releasing alkalinity during the acidification.

***Environmental evaluation of bauxite residue leachate after neutralization***

To evaluate the environmental effect of these three types of bauxite residue leachate, the concentration of Cu, Zn, As, Cr and Se were measured in table 2.1. The concentrations of these inorganic chemicals were below the Extraction toxicity limit (GB5085.3-2007, China) and Toxicity Characteristic Leaching Procedure (TCLP) limit (40 Code of Federal Regulations 261.24, U.S. Environmental Protection Agency) described in table 2.1. Other elements such as Ba, Cd, Pb and Ag were not detected. Therefore, it was safe for bauxite residue leachate after neutralization and acidification.

***Elemental and mineralogical composition***

According to the XRD patterns in figure 3.6, 3.7 and 3.8, the three types of bauxite residue primarily consisted of hematite ($Fe_2O_3$), sodalite ($Na_{7.88}(Al_6Si_6O_{24})(CO_3)_{0.93}$) and calcite ($CaCO_3$). For chemical composition after acid digestion, the Al, Ca, Fe, Mg, Na, Si and Ti were the main elements in bauxite residue in figure 2.5. In addition, more than 10% existed in the loss on ignition (LOI), representing volatile substances that were chemically bound with the minerals, such as water, organic and inorganic carbon.

After washing, neutralization and acidification, the sodium and calcium were dissolved most in solution for bauxite residue in figure 2.4. For BR1, dissolved sodium reached 8.4% of the raw material in weight after acidification, indicating that BR1 had the most available alkalinity, thus ANC (pH 5.5) of BR1 was greatest among the three types of bauxite residue.

After acidification, the sodium was dissolved not only from the strong base but also partly from the mineral alkali. For BR1, sodalite ($Na_{7.88}(Al_6Si_6O_{24})(CO_3)_{0.93}$) was transferred to tamarugite ($NaAl(SO_4)_2 \cdot 6H_2O$). That was consistent with the result in another study that the dissolution of sodalite reacted with sulfuric acid was predicted to generate the $Na_2SO_4$, $Al_2(SO_4)_3$ and $Si(OH)_4$ (Liang et al., 2014). For BR2 and BR3, there was no sodalite found in XRD patterns, but after acidification, the calcite ($CaCO_3$) was transferred to gypsum ($CaSO_4 \cdot 2H_2O$). Due to the dissolution of Na, Al and Ca, the ratio of Fe in the bauxite residue increased with neutralization and acidification in figure 3.5 and the XRD intensity of hematite increased in figure 3.6, 3.7 and 3.8. The ratio of Al after acidification in solid was greater than that after neutralization that was due to that the dissolved Al can generate the $Al(OH)_3(s)$, which was quite stable at neutral status.

***SEM imaging***

According to the SEM imaging in figure 3.9, 3.10 and 3.11, the morphology of bauxite residue was shown. Bauxite residue contained the fine particle material. After neutralization and acidification, the aggregates are formed. By comparing

the SEM of three types of bauxite residue, the BR1 contained smaller particle than the other two bauxite residues.

## Conclusion

Bauxite residue as the byproduct of bauxite refining process has been characterized with high alkalinity, which could be exploited for use as the base chemical in flue gas desulfurization. In this study, bauxite residue from three sources were tested for acid neutralization capacity (ANC) as well as its linkage to minerology. The ANC (pH 7.0) of BR2 was the highest among the three bauxite residues, while the ANC (pH 5.5) of BR1 was found to be the greatest among the three types of bauxite residues. According to the chemical and mineral composition of the raw bauxite residue as well as the neutralized or acidified bauxite residue, the ANC (pH 7.0) of BR2 could be attributed primarily to readily dissolved alkalinity in the form of sodium hydroxide (NaOH) or sodium carbonate ($Na_2CO_3$). In comparison, the ANC (pH 5.5) of BR1 and BR3 was likely contributed from the mineral alkalinity, such as sodalite and calcite. Following the release of sodium (Na) and calcium (Ca) from bauxite residue after neutralization or acidification, the level of iron (Fe) increased in the solid phase and minerology changed. After acidification, sodalite ($Na_{7.88}(Al_6Si_6O_{24})(CO_3)_{0.93}$) was transferred to tamarugite ($NaAl(SO_4)_2 \cdot 6H_2O$) for BR1, while the calcite ($CaCO_3$) was transferred to gypsum ($CaSO_4 \cdot 2H_2O$) for BR2 and BR3.

## References


Cheng J, Zhou JH, Liu JZ, Cao XY, Cen KF. 2009. Physicochemical characterizations and desulfurization properties in coal combustion of three calcium and sodium industrial wastes. Energ Fuel 23: 2506-2516.

Couperthwaite SJ, Johnstone DW, Mullett ME, Taylor KJ, Millar GJ. 2014. Minimization of bauxite residue neutralization products using nanofiltered Seawater. Ind Eng Chem Res 53(10): 3787-3794.

Klauber C, Grafe M, Power G. 2011. Bauxite residue issues: II. options for residue utilization. Hydrometallurgy 108(1-2): 11-32.

Kopittke PM, Menzies NW, Fulton IM. 2004. Gypsum solubility in seawater, and its application to bauxite residue amelioration. Aust J Soil Res 42(8): 953-960.

Krishna P, Reddy MS, Patnaik SK. 2005. *Aspergillus Tubingensis* reduces the pH of the bauxite residue (Red mud) amended soils. Water Air Soil Poll 167(1-4): 201-209.

Li YZ, Liu CJ, Luan ZK, Peng XJ, Zhu CL, Chen ZY, Zhang ZG, Fan JH, Jia ZP. 2006. Phosphate removal from aqueous solutions using raw and activated red mud and fly ash. J Hazard Mater 137(1): 374-383.

Liu Y, Lin CX, Wu YG. 2007. Characterization of red mud derived from a combined Bayer Process and bauxite calcination method. J Hazard Mater 146(1-2): 255-261.

Ruyters S, Mertens J, Vassilieva E, Dehandschutter B, Poffijn A, Smolders E. 2011. The red mud accident in Ajka (Hungary): plant toxicity and trace metal bioavailability in red mud contaminated soil. Environ Sci Technol 45(4): 1616-1622.

Sahu RC, Patel RK, Ray BC. 2010. Neutralization of red mud using $CO_2$ sequestration cycle. J Hazard Mater 179(1-3): 28-34.

Wang SB, Ang HM, Tade MO. 2008. Novel applications of red mud as coagulant, adsorbent and catalyst for environmentally benign processes. Chemosphere 72(11): 1621-1635.

Wang XK, Zhang YH, Lv FZ, An Q, Lu RR, Hu P, Jiang SB. 2015. Removal of alkali in the red mud by $SO_2$ and simulated flue gas under mild conditions. Environ Prog Sustain 34(1): 81-87.

# Appendix

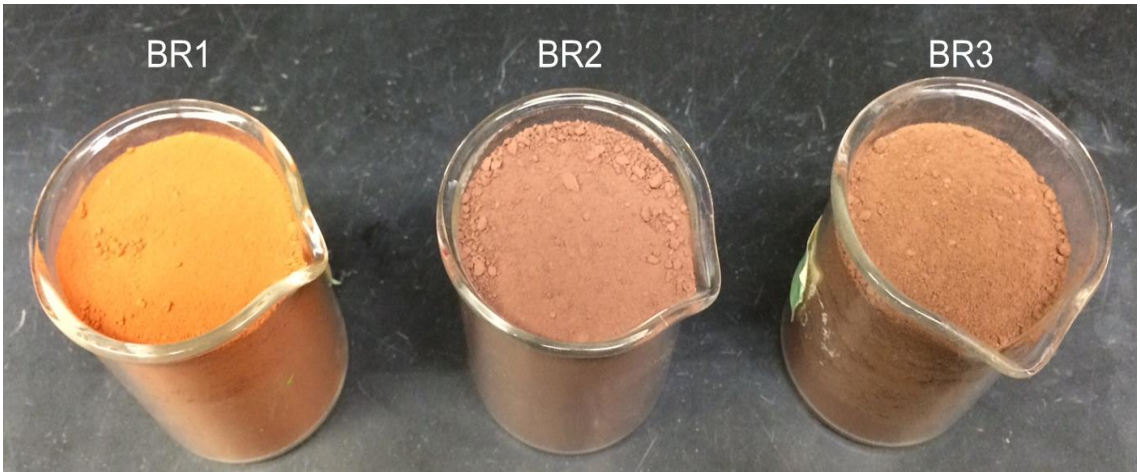


**Figure 2.1. Photograph of bauxite residue from three sources.**

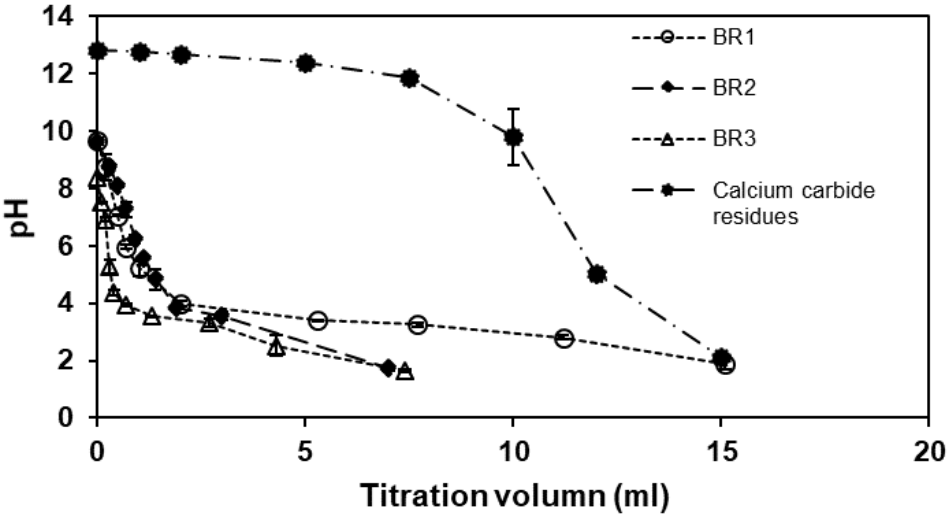


**Figure 2.2. Titration curves for the different alkaline materials.**

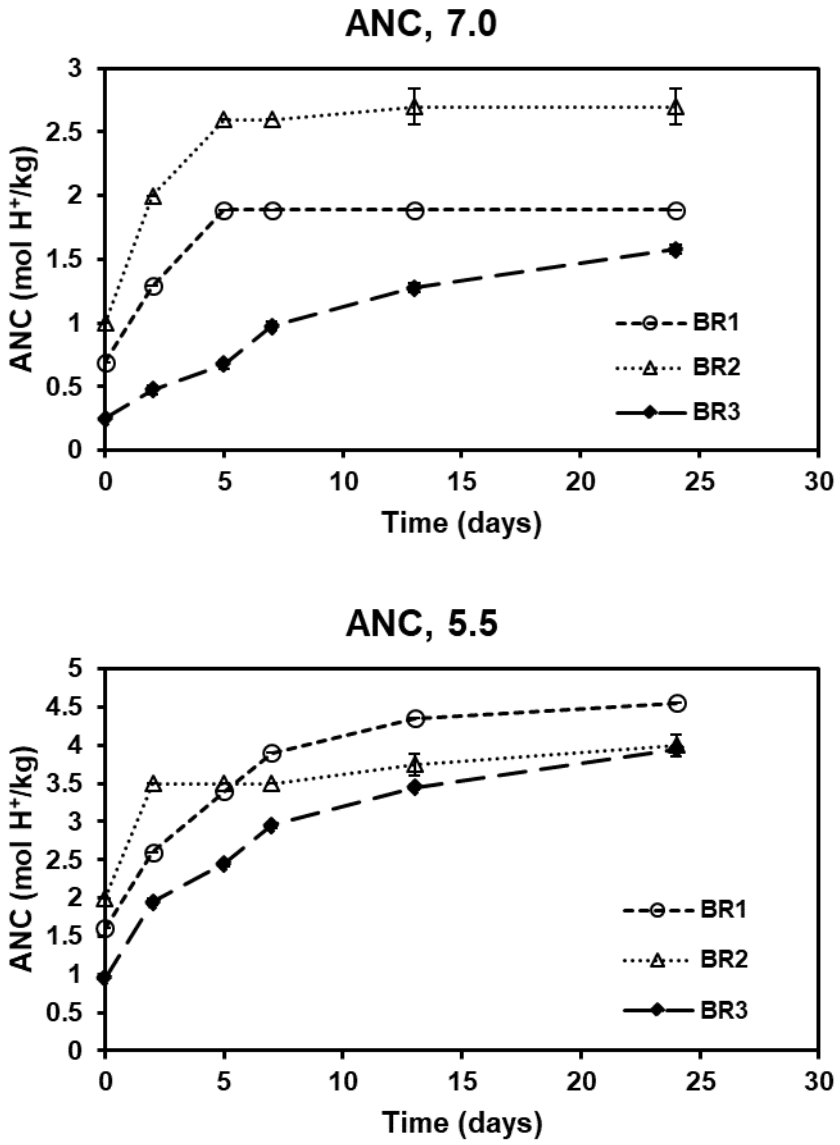


**Figure 2.3. Accumulative curves of ANC (pH 7.0 and 5.5) for three types of bauxite residue.**

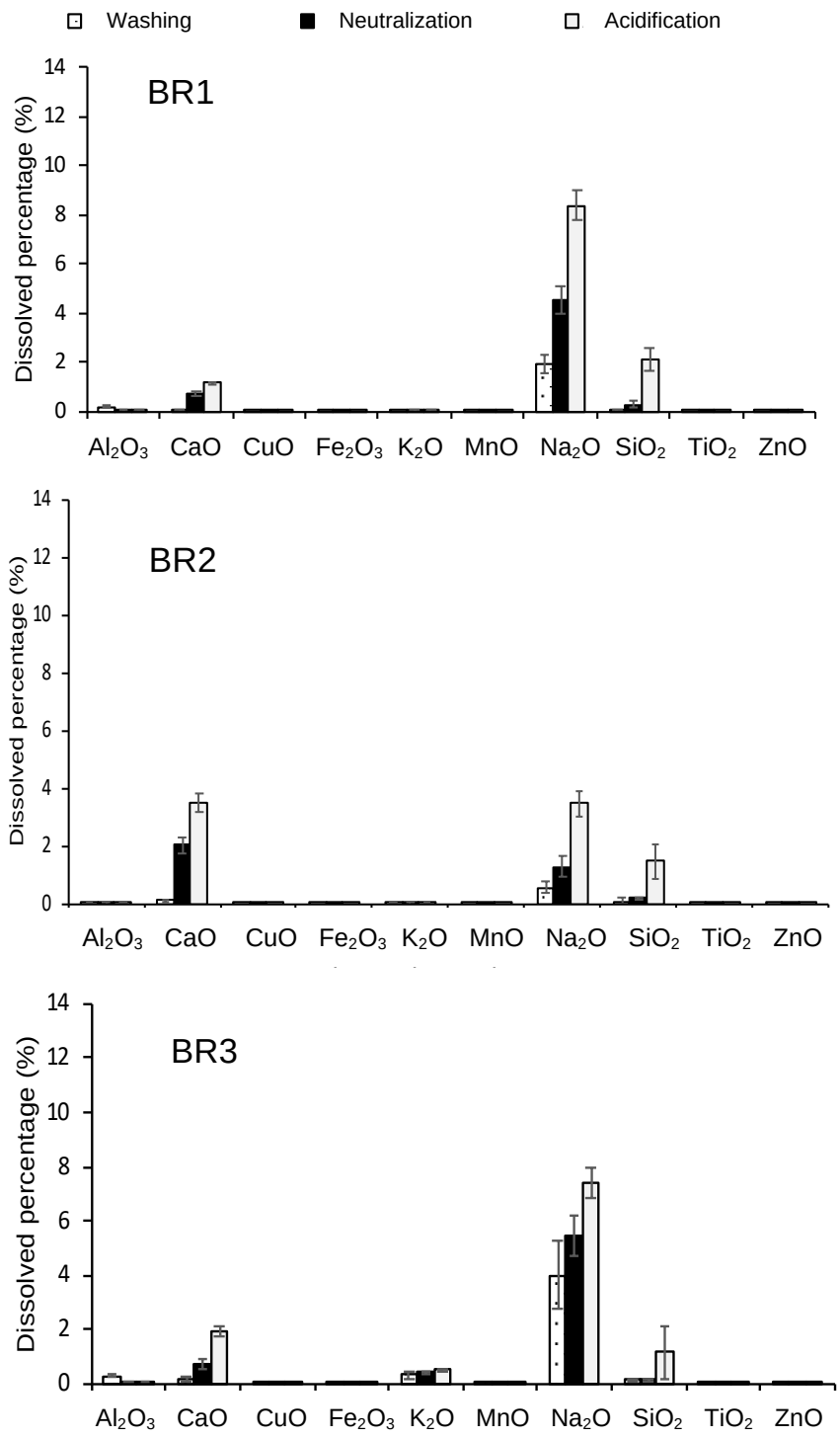


**Figure 2.4. Dissolved percentage from raw bauxite residue after washing, neutralization and acidification.**

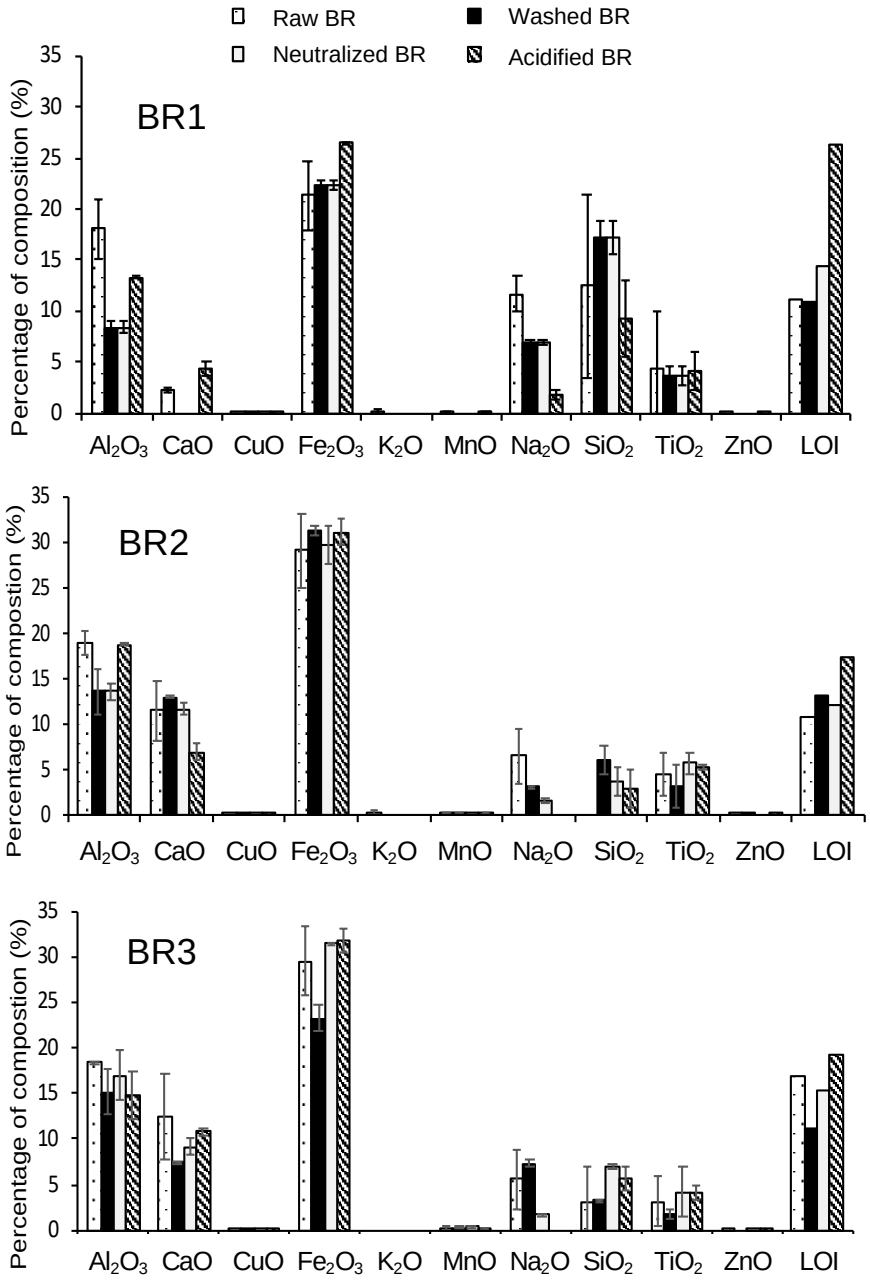


**Figure 2.5. Chemical composition of raw bauxite residue and bauxite residue after treatment of washing, neutralization and acidification.**

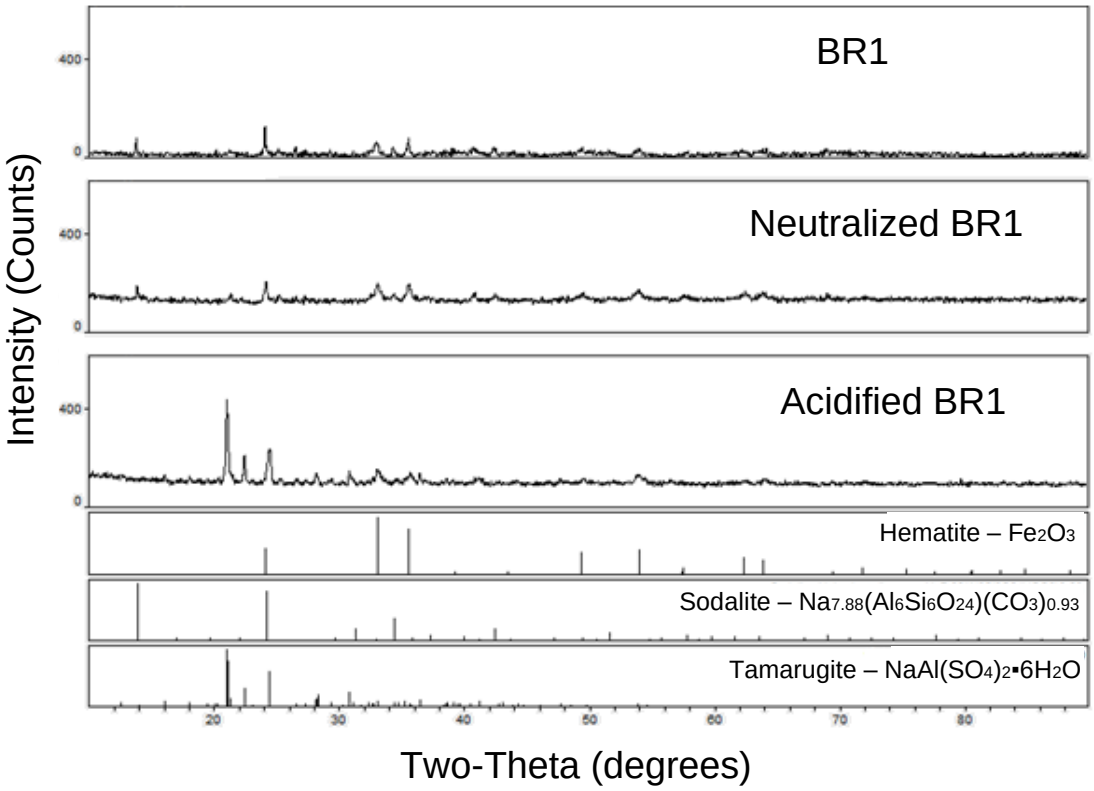


**Figure 2.6. XRD patterns of BR1, Neutralized BR1 and Acidified BR1.**

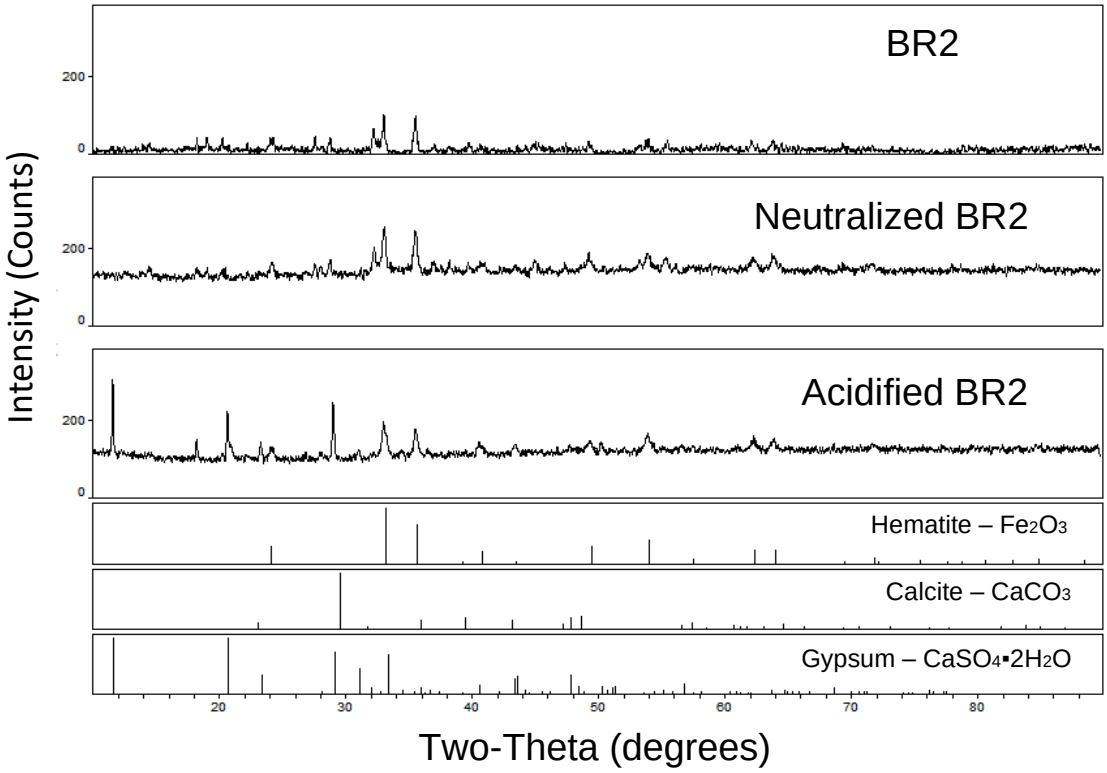


**Figure 2.7. XRD patterns of BR2, Neutralized BR2 and Acidified BR2.**

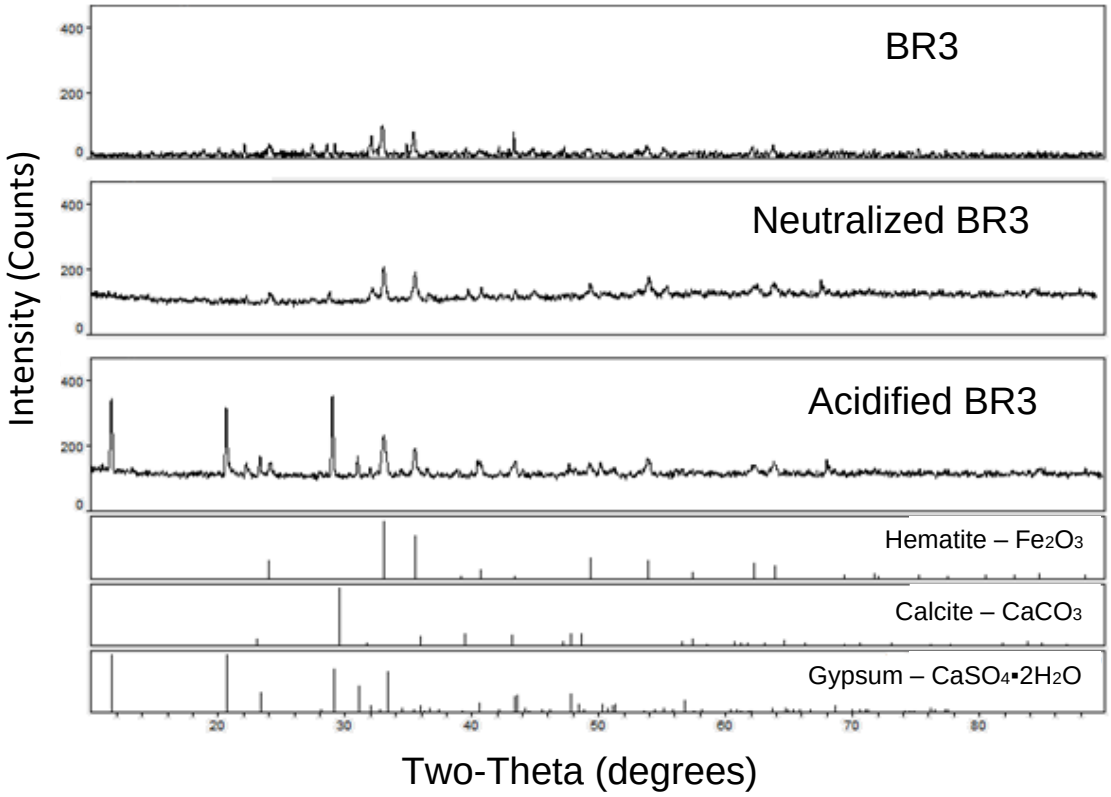


**Figure 2.8. XRD patterns of BR3, Neutralized BR3 and Acidified BR3.**

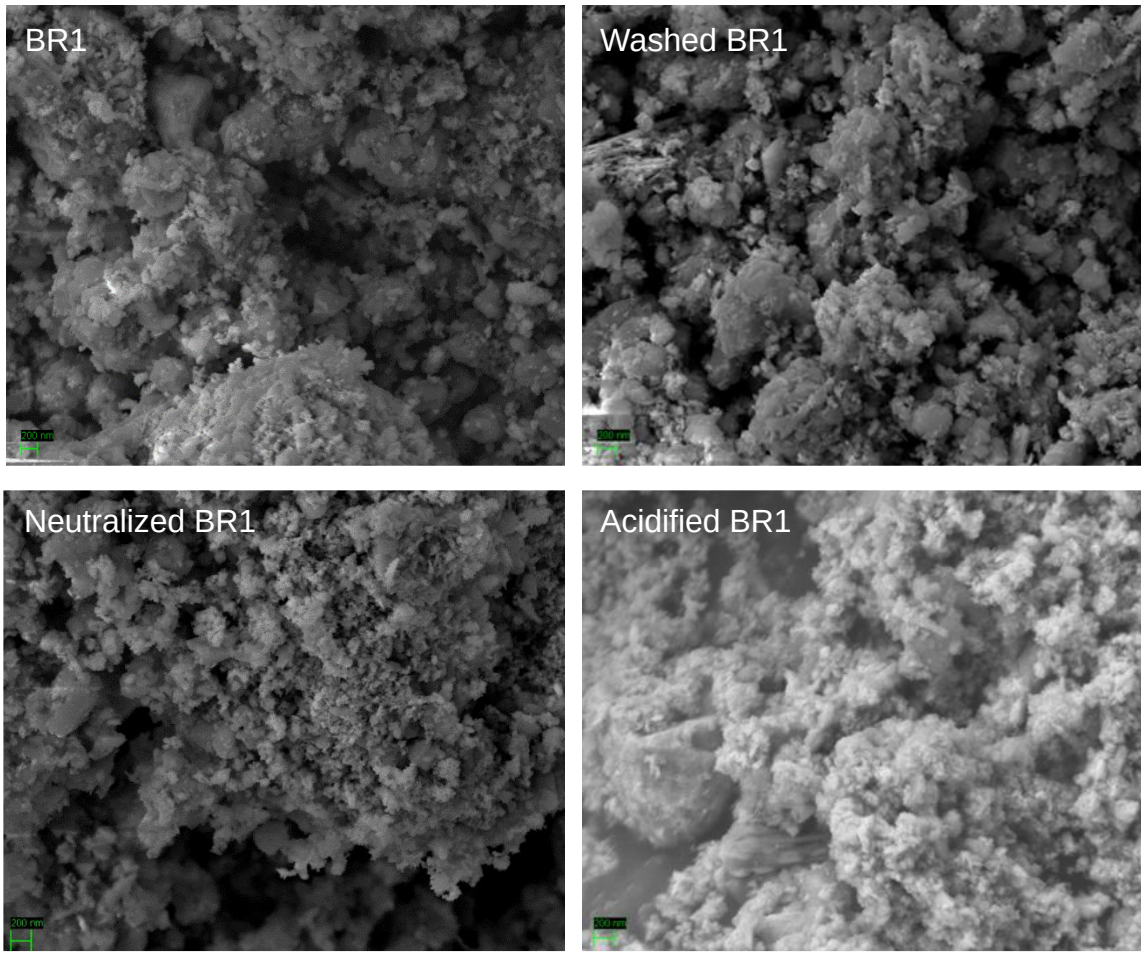


**Figure 2.9. SEM micrographs of BR1 and materials after washing, neutralization and acidification.**

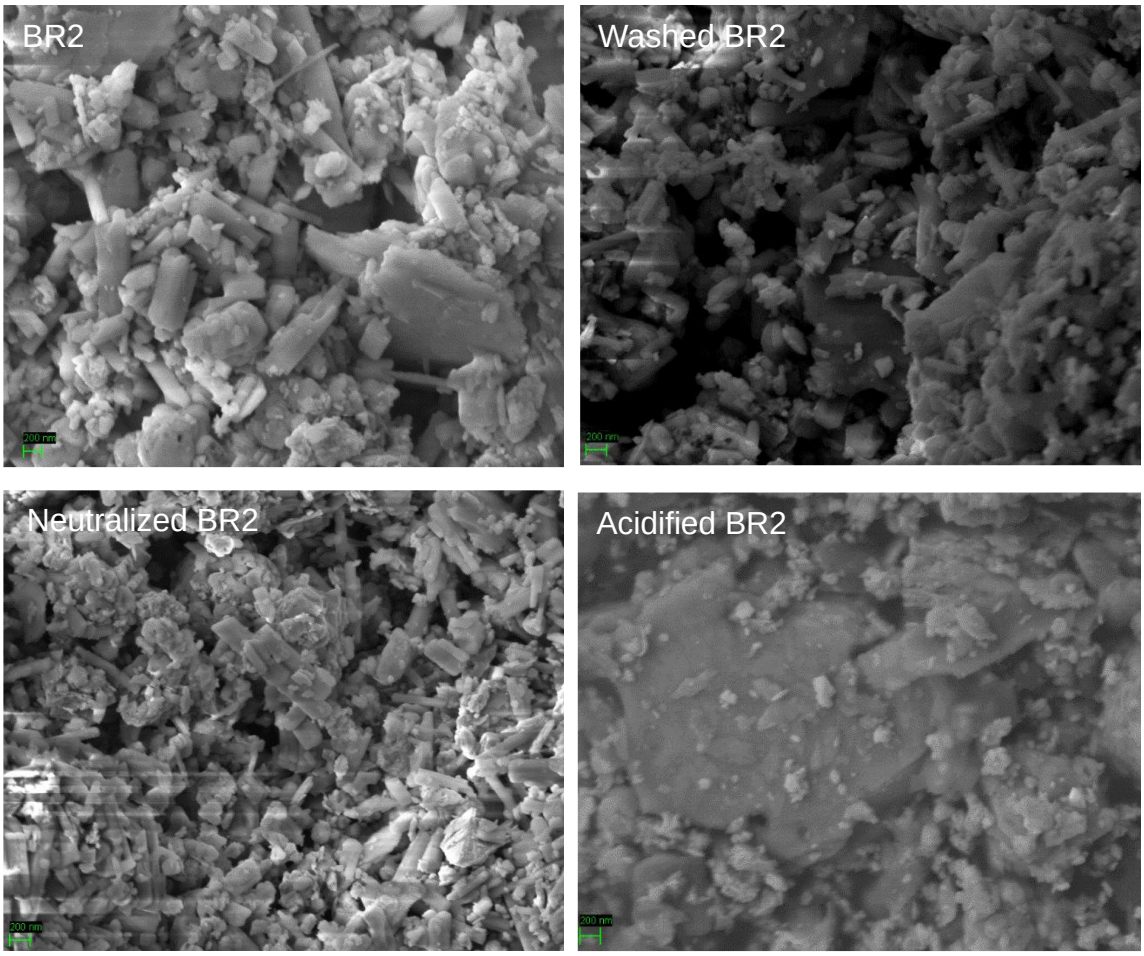


**Figure 2.10. SEM micrographs of BR2 and materials after washing, neutralization and acidification.**

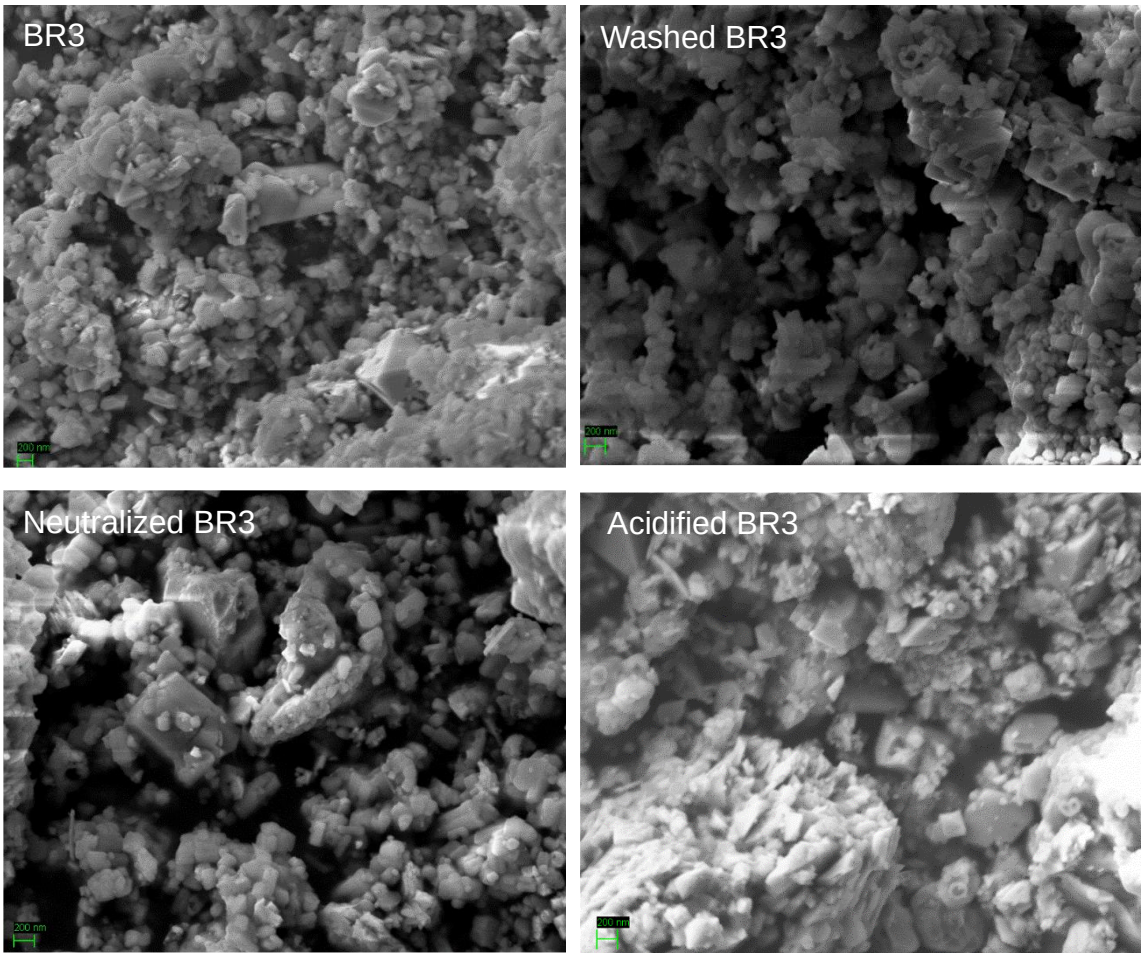


**Figure 2.11. SEM micrographs of BR3 and materials after washing, neutralization and acidification.**

**Table 2.1. Concentration of inorganic chemicals in the leachate solution.**

| Sample | treatment | Inorganic chemicals (mg $L^{-1}$) | | | | |
|---|---|---|---|---|---|---|
| | | Cu | Zn | As | Cr | Se |
| BR1 | pH=7.02 | 0.06 | 0.08 | 0.01 | 0.00 | 0.02 |
| | pH=5.41 | 0.09 | 0.16 | 0.01 | 0.00 | 0.01 |
| BR2 | pH=7.06 | 0.02 | 0.04 | 0.02 | 0.00 | 0.01 |
| | pH=5.56 | 0.03 | 0.10 | 0.01 | 0.00 | 0.02 |
| BR3 | pH=7.05 | 0.02 | 0.04 | 0.04 | 0.03 | 0.01 |
| | pH=5.49 | 0.03 | 0.10 | 0.01 | 0.02 | 0.01 |
| China EPA- Extraction toxicity limit (GB5085.3-2007) | | 100 | 100 | 5 | 15 | 1 |
| U.S. EPA-TCLP leaching limit (40 CFR 261.24) | | N/A | N/A | 5 | 5 | 1 |

# CHAPTER III
# POTENTIAL OF NEUTRALIZED BAUXITE RESIDUE IN THE REMOVAL OF AQUEOUS PHOSPHORUS

## Abstract

Phosphorus is a nonrenewable resource for crop and food production. The recovery of phosphorus from the natural environment is critical for the sustainable supply of this important fertilizer. Given the high content of iron oxides, it could be hypothesized that bauxite residue would be a feasible material for the removal of phosphorus from the aqueous phase. With the iron oxide-rich mineralogy of bauxite residue, this study investigated the potential of bauxite residue in the removal of aqueous phosphate via retention at concentrations relevant to agriculture runoff. Three types of bauxite residue were tested, exhibiting phosphate retention capacity ranging from 0.93 to 1.58 mg P/g. The parallel-first-order model suggested the phosphate removal process followed two-phase retention. The phosphate removal capacity was found to be affected by sulfate concentration, pH, and initial phosphate concentration. The increase in sulfate concentration and initial phosphate concentration lead to the increase in phosphate removal capacity. The neutralization and acidification of bauxite residue could enhance the phosphate removal.

## Introduction

Bauxite residue is a caustic waste from the process of alumina refining. With the industry development, the estimated production of bauxite residue has been growing rapidly based on the alumina production (Power et al., 2011) and the treatment is hard for bauxite residue due to its high alkalinity, leading to the serious storage problem. Besides acid neutralization, seawater, gypsum, $CO_2$ and $SO_2$ are also used to neutralize bauxite residue (Grafe et al., 2011). The flue gas containing some acid gas is also a promising way to neutralize bauxite residue and the desulfurization happens at the same time (Fois et al., 2007; Wang et al., 2015). After neutralization, the main applications for bauxite residue consist of construction materials and wastewater treatment (Klauber et al., 2011). New approaches for utilizing these bauxite residues should be explored.

The reuse of carbon, nitrogen, and phosphorous is always of great concern for social development and environmental protection, especially phosphorous as a nonrenewable resource. Phosphorus is an essential nutrient for plant growth, however, it is also an important factor for the eutrophication in natural water bodies. Nowadays, the recovery and reuse of phosphorous become more valuable by total value calculation (Mayer et al., 2016). The primary source of the losing phosphorus is the animal waste with the high concentration (Szogi and Vanotti, 2009). Many researchers have verified that the neutralized bauxite residue with the high content of iron oxides can be used to removal the phosphorus via the formation of complex and was considered as a

valid absorbent for phosphorous with relatively high concentration (Li et al., 2006; Liu et al., 2007; Huang et al., 2008; Bhatnagar et al., 2011; Zhao et al., 2012). Based on the previous study (Weaver and Ritchie, 1987), the cost of phosphorous treatment increased rapidly with the decrease of final required phosphorus concentration to less than 4 mg/L, implying that removal of phosphorous with low concentration is a key problem. Moreover, the agriculture runoff and erosion is another important source for the phosphorus capture with the property of high volume and low concentration (Rittmann et al, 2011). The inappropriate runoff can induce the eutrophication in surface as the serious environmental pollution. Only a few researches give some concern to the low concentration of phosphate (Huang et al., 2008). It is necessary for studying removal and recovery of phosphorous from the natural environment with low concentration.

For phosphate removal, activated bauxite residue with acid and heat treatment shows the ideal performance as an inexpensive adsorbent. After acid and heat activation, bauxite residue can show more surface adsorption sites and positive charge in surface area to improve the phosphate adsorption (Li et al., 2006; Yue et al., 2010). Many researches use different acids to treat the bauxite residue, such as HCl, $HNO_3$ (Huang et al., 2008), and $H_2SO_4$ (Koumanova et al., 1997). During the desulfurization, bauxite residue is equal to be acid activated by $H_2SO_3$ or $H_2SO_4$. During the phosphate removal by acid activated bauxite residue, many parameters, such as contact time, pH, temperature, ionic strength,

adsorbent dosage, competing ions, and initial phosphate concentration can have some obvious effects on the phosphate removal (Li et al., 2006; Huang et al., 2008; Zhao et al., 2012; Behera and Das, 2016; Ye et al., 2016). During the desulfurization by bauxite residue, the bauxite residue may be neutralized to different pH and may contain large amounts of sulfate. These parameters may affect the phosphate removal by the neutralized bauxite residue. Additionally, phosphate removal by bauxite residue is related to many mechanisms, so the phosphate removal may be related to the property of bauxite residue. However, there is no study about the comparison of phosphate removal by the bauxite residue in different conditions.

In this study, we investigated the potential of bauxite residue in the removal of aqueous phosphate via retention at concentrations relevant to agriculture runoff. Due to the different sources of raw bauxite, the bauxite residue always has different compositions and characteristics. This study is aimed to the comparison of phosphate removal by three types of bauxite residue and to exploit the optimal operating conditions and the possible retention mechanism under low concentration of phosphate by the neutralized bauxite residue.

## Materials and Methods

### *Bauxite residue*

Three types of bauxite residue from Shandong, Guangxi, Pingguo in China were selected with different characteristics and named by BR1, BR2 and BR3. The bauxite residue (4 g) with 100 ml DI water was neutralized to pH 3, 5, 7 and 9 by

1 N $H_2SO_4$. The $H_2SO_4$ neutralized bauxite residue was used to simulate the desulfurized bauxite residue. The raw sample was gotten without the addition of $H_2SO_4$. After the equilibrium for 24 h, the samples were rinsed with DI water three times.

The phosphate stock solution (1000 mg P/L) was prepared by dissolving the potassium dihydrogen orthophosphate ($KH_2PO_4$) with DI water. The $Na_2SO_4$ stock solution (2 M) was prepared to adjust the concentration of sulfate. Phosphate and sulfate solutions with different concentrations were prepared by diluting the stock solution with DI water.

The solid composition was determined by ICP-AES after the acid digestion ($HNO_3$, HCl, HF). To identify the mineral composition, XRD patterns were collected using a Panalytical Empyrean with Cu Kα radiation at 45 kV and 40 mA. Scanning electron microscope is used to analyze the morphology. The specific surface area was determined by Brunauer–Emmett–Teller (BET)/$N_2$ adsorption method using an automatic specific surface area measurement. pH was measured by pH meter with a combination pH electrode.

***Retention kinetics***

For phosphate retention kinetics, 200 mg of the $H_2SO_4$ neutralized bauxite residue (pH 7) was mixed with 200 mL phosphate solution (2 mg P/L) in a 250 mL Erlenmeyer flask and 0.05 M $Na_2SO_4$ as a background electrolyte was added to adjust the ionic strength. The Erlenmeyer flask was capped with screws by

shaking at 120 rpm at 20 °C with duplicates. 1 ml solution was sampled at 0, 0.1, 0.4, 1, 2, 4, 6, 8, 10, 12.5, 22, 32 and 48 h and then was centrifuged at 16000 g/min for 10 min. A clear aliquot of the supernatant was analyzed for phosphate by Ion Chromatography (Dionex 3000i/SP). The pH value was measured by pH meter during the experiment.

The amount of phosphate retention at equilibrium ($q_e$, mg/g) was calculated based on the equation bellow:

$$q_e = \frac{(C_i - C_e)V}{m} \quad (1)$$

where $C_i$ and $C_e$ are the initial and final (equilibrium) concentrations of the anions in solution (mg/L), $V$ the solution volume (L), and $m$ is the amount of adsorbent (g).

The retention kinetics mainly follow the two-phase retention mechanism, e.g. the initial rapid phase and the second slow phase. A number of nonlinear equations have been applied to simulate the retention mechanism. The following equations were used to simulate the retention kinetics of phosphate in this study.

The pseudo first-order equation:

$$q_t = q_e(1 - e^{-k_1 t}) \quad (2)$$

where $q_t$ (mg/g) is the amount of phosphate adsorbed at time $t$ (h), and $k_1$ is the equilibrium rate constant for pseudo first-order kinetics ($h^{-1}$).

The pseudo second-order equation:

$$\frac{t}{q_t} = \frac{1}{k_2 q_e^2} + \frac{t}{q_e} \quad (3)$$

where $k_2$ is the equilibrium rate constant for pseudo second-order kinetics (g $mg^{-1}$ $h^{-1}$)

The parallel first-order kinetics

$$q_t = q_{e1}(1 - e^{-k_{1a}t}) + q_{e2}(1 - e^{-k_{1b}t}) \quad (4)$$

where $q_{e1}$ and $q_{e2}$ are the amount of phosphate adsorbed at equilibrium (mg/g) in the first and second reactions, respectively, and $k_{1a}$ and $k_{1b}$ ($h^{-1}$) are the equilibrium rate constants for the first and second reactions, respectively.

Intraparticle diffusion equation

$$q_t = k_i t^{0.5} + C_i \quad (5)$$

where $k_i$ is the intraparticle diffusion rate constant (mg $g^{-1}$ $h^{-0.5}$) and $C_i$ is the constant, which is proportional to the boundary layer thickness.

***Batch phosphate removal experiment***

For batch phosphate removal studies, 20 ml solution with 2 mg P/L phosphate and the 1 g/L $H_2SO_4$ neutralized bauxite residue (pH 7) were prepared in 40 ml serum bottle with a background electrolyte of 0.05 M $Na_2SO_4$. The serum bottle was placed on a shaker (150 rpm) at 20 °C for 48 h phosphate for equilibrium. In the end, 1 ml solution was centrifuged at 16000 g/min for 10 min and analyzed for phosphate concentration and pH in solution. Different phosphate concentration (0, 1, 2, 5, 10, 20 mg/L) were set to study the effect of initial phosphate concentration on phosphate removal by fixing other parameters. With the similar procedure, the effect of sulfate concentration on phosphate removal

was examined in a series of experiments with different concentration of $Na_2SO_4$ (0, 0.01, 0.05, 0.1, 0.5, 1 M). Bauxite residue neutralized to pH 3, 5, 7, 9 by $H_2SO_4$ and raw bauxite residue were used to study the effect of bauxite residue pH on phosphate removal. All batch experiments were carried out in triplicates.

***Data analysis***

Fitting of the data to the model was carried out using iterative nonlinear regression by Sigma Plot 14.0. Significance analyses were performed using the Student's t-test by IBM SPSS Statistics 23.0, and the statistical probability $P < 0.05$ was considered significant.

## Results and Discussion

***Characteristics of bauxite residue***

The chemical composition of bauxite residue is shown in Table 3.1 and the principal components were the oxides of Si, Fe, Al, Ca, Ti and Na. pH of these three types of bauxite residue were all closed to 7 in table 3.2. The surface area varied based on the origin of these bauxite residues and decreased following the order, BR1 (38.91 $m^2/g$) < BR2 (15.06 $m^2/g$) < BR3 (11.03 $m^2/g$). The XRD pattern results indicated the remarkable difference among three types of bauxite residue in figure 3.1. BR1 contained more sodalite ($Na_{7.88}(Al_6Si_6O_{24})(CO_3)_{0.93}$), while BR2 and BR3 contained more hematite ($Fe_2O_3$). SEM provided the surface morphology of the bauxite residue in figure 3.2. The BR1 seemed to contain smaller particle than the other two types of bauxite residue.

***Phosphate retention kinetics of bauxite residue***

The dynamic retention of phosphate on the bauxite residue were illustrated in figure 3.3. At initial phosphate concentration of 2 mg P/L, 1g/L of bauxite residue was utilized for removing the phosphorus. After 48 h, the phosphate retention approached the equilibrium and the equilibrium time was apparently longer than equilibrium time (5 min−7 h) of phosphate retention by acid activated bauxite residue in other studies (Li et al., 2006; Liu et al., 2007; Huang et al., 2008; Zhao et al., 2012). However, the equilibrium time of phosphate retention was comparable with phosphate retention by other materials, such as zinc–aluminum layered double hydroxides (Cheng et al., 2009), and amorphous zirconium hydroxide (Chitrakar et al., 2006). In addition, the amount of phosphate removed at equilibrium decreased with the order of BR1 (1.58 mg/g) > BR2 (1.23 mg/g) > BR3 (0.93 mg/g).

Based on these tests, the four different models were used to simulate the retention kinetics and the kinetics parameters were shown in table 3.3. Compared with pseudo-first-order model, pseudo-second-order model showed the better fit of experimental data with the greater regression coefficient and the smaller standard error. Consequently, chemical adsorption may dominate the process of phosphate retention on these bauxite residues due to that the pseudo-second-order model was generally interpreted as chemical adsorption process (Huang et al., 2008).

Besides, the parallel-first-order model was used to simulate the retention kinetics and showed the best fit of experimental data with the greatest regression coefficient ($R^2 > 0.99$) for all three types of bauxite residue among all kinetics model. The model suggested the phosphate retention on the bauxite residue followed the two-phase retention (Huang et al., 2008). At the initial 10 hours, the retention was relatively quick and exceeded 50% of the maximal retention amount, and the second phase was relatively steady. The two-phase retention may be attributed to retention for the two acidic phosphate species namely $H_2PO_4^-$ and $HPO_4^{2-}$, which mainly existed in phosphate solution at pH 7. By comparing the amount of phosphate removed at equilibrium ($q_e$) and the equilibrium rate ($k$) in table 3.3, the retention capacity of BR1 was significantly different from BR2 and BR3. According to XRD and SEM, BR1 was different from BR2 and BR3 in mineral composition and surface morphology.

Intraparticle diffusion model was used to explore the possible impact of intraparticle diffusion resistance on phosphate retention (Mezenner and Bensmaili, 2009). The relative high regression coefficient (table 3.3) indicated that the intraparticle diffusion was involved in the phosphate retention on bauxite residue. The values of $C$ (0.02−0.11) was close to zero, implying the boundary layer effect and intraparticle diffusion may be the rate controlling step (Mezenner and Bensmaili, 2009). The intraparticle diffusion rate constant ($K_i$) for three types of bauxite residue followed the decreasing order of BR1 > BR2 > BR3.

***Effect of sulfate***

During the flue gas desulfurization, the $SO_2$ was absorbed by NaOH solution and transformed into $Na_2SO_3$ and finally oxidized into $Na_2SO_4$, so the concentration of sulfate should be very high when desulfurized bauxite residue was applied to phosphate removal. The effect of different sulfate concentration on phosphate retention was shown in figure 3.4. With the increasing of sulfate concentration, the phosphate retention was enhanced. From sulfate concentration increasing from 0 to 0.5 M, the amount of phosphate removed respectively increased from 0.19 to 1.99 mg P/g BR1, from 0.82 to 1.98 mg P/g BR2 and from 0.68 to 1.96 mg P/g BR3. At relative high sulfate concentration (0.5−1 M), the amount of phosphate removed was almost equal. The amount of phosphate removed with the 0.05−1 M sulfate followed the decreasing order of BR1 > BR2 > BR3. With 0 and 0.01 M sulfate, the amount of phosphate removed by BR1 was minimal.

The enhanced phosphate retention in existing of sulfate may be ascribed to the increasing ionic strength in solution or the direct effect of sulfate as a coexisting anion. For the influence of ionic strength, increasing the ionic strength should increase the surface charge. The phosphate retention on amorphous $ZrO_2$ nanoparticles increased with the increase of the solution ionic strength due to the inner-sphere complex mechanism of phosphate (Su et al., 2013). For influence of coexisting anion, the phosphate retention on synthetic zeolite increased slightly in the presence of chloride, nitrate, or sulfate forming outer-sphere complexes (Onyango et al., 2007). However, other studies showed that

phosphate retention was inhibited in coexisting of sulfate. With the effect of zeta potential, sulfate performed a strong competition adsorption against phosphate on bauxite residue granular adsorbent (Zhao et al., 2012). By forming both inner- and outer-sphere complexes with surface active sites, sulfate could hinder more available retention sites of neutralized bauxite residue (Tor et al., 2006) and hydroxyl–iron–lanthanum doped activated carbon fiber (Liu et al., 2013). Additionally, sulfate as coexisting ion showed no significant effect on phosphate retention by different types of materials, such as neutralized bauxite residue (Akhurst et al., 2006), Fe–Mn binary oxide (Zhang et al., 2009), nanostructured iron(III)–copper(II) binary oxides (Li et al., 2014) and iron hydroxide and iron oxide (Zhang et al., 2016). Therefore, the reason for enhancing the phosphate retention by bauxite residue with increasing sulfate concentration is not clear and it needs to be studied in future.

***Effect of pH***

Phosphate retention on the bauxite residue with different pH was illustrated in figure 3.5. All three types of bauxite residue neutralized to pH 5 performed the greatest phosphate retention capacity with 2.0 mg P/g bauxite residue, which was consistent with other studies (Huang et al., 2008; Zhao et al., 2012). The phosphate retention capacity decreased with pH of bauxite residue increasing and phosphate retention capacity of BR1, BR2 and BR3 was respectively 0.47, 0.87 and 0.68 mg P/g bauxite residue at pH 9. BR2 and BR3 acidified to pH 3 were nearly equal to the phosphate retention capacity of neutralized to pH 5, but

the BR1 acidified to pH 3 performed the low phosphate BR3 acidified with 0.73 mg P/g bauxite residue. In some previous studies, phosphate BR3 acidified capacity of bauxite residue was also considered to have a close relationship with pH value of the phosphate solution.

The effect of bauxite residue pH on the phosphate removal resulted from the change of characteristics of bauxite residue neutralized or acidified into different pH and the effect of different pH in solution on the surface charge and phosphorus species. In this study, pH in solution was measured and the results showed that the pH in solution was slightly higher than pH of bauxite residue (figure 3.5). For the bauxite residue neutralized to pH 7, the pH in solution was around 6.7 and slightly lower than 7. Overall, the pH of bauxite residue affected the pH in solution and the phosphate retention capacity of bauxite residue was correlated with the pH of bauxite residue. The bauxite residue acidified to low pH generally reduced the negative charges and increased more positive charges in the surface of bauxite residue which increased the attraction of the phosphate species by electrostatic forces in solution. Phosphate retention on activated bauxite residue was referred to the inner sphere complex mechanism relating to pH and thus the increased pH caused the decrease of phosphate retention (Pradhan et al., 1998). On the other hand, with the pH in solution decreased, the amount of $H_3PO_4$ decreased and the $H_2PO_4^-$ and $HPO_4^{2-}$ dominated in the solution that consequently resulted in the high phosphate retention. Additionally, sodalite and cancrinite as alkaline mineral could be dissolved by neutralization

and acidification (Grafe et al., 2011), leading to more aluminum or iron oxides exposed in surface of bauxite residue that mainly contributed to the phosphate retention by chemical adsorption and formation of metal phosphate precipitates (Castaldi et al., 2010; Ye et al., 2015).

***Effect of phosphate amount***

The phosphate retention was linearly related to the initial phosphate concentration (figure 3.6). This result suggested that the phosphate retention capacity of bauxite residue remained unsaturated for retention sites and had potential to adsorb more phosphate or another anion. In the previous research, the phosphate retention by bauxite residue could reach to the thousands of mg P/L (Li at el., 2006). So that may result in that sulfate as coexisting ion enhanced the phosphate retention by bauxite residue instead of competition (figure 3.4). The concentration gradient as the driving force played an important role to overcome the mass transfer resistance between the solution and adsorbent surface (Liu et al., 2011; Ye et al., 2016). According to the calculation, the removal efficiency of phosphate with different phosphate concentration was about 50% by neutralized bauxite residue. The result implied that initial phosphate concentration had no significant influence on the phosphate removal efficiency. As same as the study above, the phosphate retention capacity followed the decreasing order, BR1 > BR2 > BR3, indicating that the phosphate retention capacity was related to the characteristics of bauxite residue.

## Conclusion

With the iron oxide-rich mineralogy of bauxite residue, this study investigated the potential of bauxite residue in the removal of aqueous phosphate via retention at concentrations relevant to agriculture runoff. The bauxite residues with different characteristics had different phosphate retention capacity. By comparison of phosphate removal by three types of bauxite residue under different conditions, the phosphate retention capacity all followed the decreasing order, BR1 > BR2 > BR3. By comparing four kinetics model, the pseudo-second-order model, the parallel-first-order model and intraparticle diffusion model could all fit the data well, of which the parallel-first-order model showed the best fitness. The equilibrium time was up to 48 hours. The phosphate retention capacity was subjected to the sulfate concentration as a coexisting anion, pH of bauxite residue and initial phosphate concentration. With increasing of sulfate concentration and initial phosphate concentration, the phosphate retention capacity increased, while the phosphate retention capacity increased with decreasing of pH of bauxite residue and was greatest with bauxite residue neutralized to pH 5. The initial phosphate concentration had no significant influence on the removal efficiency of phosphate.

# References

Akhurst DJ, Jones GB, Clark M, McConchie D. 2006. Phosphate removal from aqueous solutions using neutralised bauxite refinery residues (Bauxsol (TM)). Environ Chem 3(1): 65-74.

Behera RK, Das R. 2016. Adsorptive removal of phosphorus(V) and chromium(VI) oxyanions using thermally treated titanium-rich bauxite. Desalin Water Treat 57(32): 15115-15124.

Bhatnagar A, Vilar VJP, Botelho CMS, Boaventura RAR. 2011. A review of the use of red mud as adsorbent for the removal of toxic pollutants from water and wastewater. Environ Technol 32(3): 231-249.

Castaldi P, Silvetti M, Garau G, Deiana S. 2010. Influence of the pH on the accumulation of phosphate by red mud (a bauxite ore processing waste). J Hazard Mater 182(1-3): 266-272.

Cheng X, Huang XR, Wang XZ, Zhao BQ, Chen AY, Sun DZ. 2009. Phosphate adsorption from sewage sludge filtrate using zinc-aluminum layered double hydroxides. J Hazard Mater 169(1-3): 958-964.

Chitrakar R, Tezuka S, Sonoda A, Sakane K, Ooi K, Hirotsu T. 2006. Selective adsorption of phosphate from seawater and wastewater by amorphous zirconium hydroxide. J Colloid Interf Sci 297(2): 426-433.

Fois E, Lallai A, Mura G. 2007. Sulfur dioxide absorption in a bubbling reactor with suspensions of Bayer red mud. Ind Eng Chem Res 46(21): 6770-6776.

Huang WW, Wang SB, Zhu ZH, Li L, Yao XD, Rudolph V, Haghseresht F. 2008. Phosphate removal from wastewater using red mud. J Hazard Mater 158(1): 35-42.

Klauber C, Grafe M, Power G. 2011. Bauxite residue issues: II. options for residue utilization. Hydrometallurgy 108(1-2): 11-32.

Koumanova B, Drame M, Popangelova M. 1997. Phosphate removal from aqueous solutions using red mud wasted in bauxite Bayer's process. Resour Conserv Recy 19(1): 11-20.

Li GL, Gao S, Zhang GS, Zhang XW. 2014. Enhanced adsorption of phosphate from aqueous solution by nanostructured iron(III)-copper(II) binary oxides. Chem Eng J 235: 124-131.

Li YZ, Liu CJ, Luan ZK, Peng XJ, Zhu CL, Chen ZY, Zhang ZG, Fan JH, Jia ZP. 2006. Phosphate removal from aqueous solutions using raw and activated red mud and fly ash. J Hazard Mater 137(1): 374-383.

Liu CJ, Li YZ, Luan ZK, Chen ZY, Zhang ZG, Jia ZP. 2007. Adsorption removal of phosphate from aqueous solution by active red mud. J Environ Sci-China 19(10): 1166-1170.

Liu JY, Wan LH, Zhang L, Zhou Q. 2011. Effect of pH, ionic strength, and temperature on the phosphate adsorption onto lanthanum-doped activated carbon fiber. J Colloid Interf Sci 364(2): 490-496.

Liu JY, Zhou Q, Chen JH, Zhang L, Chang N. 2013. Phosphate adsorption on hydroxyl-iron-lanthanum doped activated carbon fiber. Chem Eng J 215: 859-867.

Mayer BK, Baker LA, Boyer TH, Drechsel P, Gifford M, Hanjra MA, Parameswaran P, Stoltzfus J, Westerhoff P, Rittmann BE. 2016. Total value of phosphorus recovery. Environ Sci Technol. 50 (13): 6606–6620.

Mezenner NY, Bensmaili A. 2009. Kinetics and thermodynamic study of phosphate adsorption on iron hydroxide-eggshell waste. Chem Eng J 147(2-3): 87-96.

Onyango MS, Kuchar D, Kubota M, Matsuda H. 2007. Adsorptive removal of phosphate ions from aqueous solution using synthetic zeolite. Ind Eng Chem Res 46(3): 894-900.

Power G, Grafe M, Klauber C. 2011. Bauxite residue issues: I. Current management, disposal and storage practices. Hydrometallurgy 108(1-2): 33-45.

Pradhan J, Das J, Das S, Thakur RS. 1998. Adsorption of phosphate from aqueous solution using activated red mud. J Colloid Interf Sci 204(1): 169-172.

Rittmann BE, Mayer B, Westerhoff P, Edwards M. 2011. Capturing the lost phosphorus. Chemosphere 84: 846-853.

Su Y, Cui H, Li Q, Gao SA, Shang JK. 2013. Strong adsorption of phosphate by amorphous zirconium oxide nanoparticles. Water Res 47(14): 5018-5026.

Szogi AA, Vanotti MB. 2009. Removal of phosphorus from livestock effluents. J Environ Qual 38(2): 576-586.

Tor A, Cengeloglu Y, Aydin ME, Ersoz M. 2006. Removal of phenol from aqueous phase by using neutralized red mud. J Colloid Interf Sci 300(2): 498-503.

Wang XK, Zhang YH, Lv FZ, An Q, Lu RR, Hu P, Jiang SB. 2015. Removal of alkali in the red mud by $SO_2$ and simulated flue gas under mild conditions. Environ Prog Sustain 34(1): 81-87.

Weaver DM, Ritchie GSP. 1987. The effectiveness of lime-based amendments and bauxite residues at removing phosphorus from piggery effluent. Environ Pollut 46(3): 163-175.

Ye J, Cong XN, Zhang PY, Hoffmann E, Zeng GM, Liu Y, Fang W, Wu Y, Zhang HB. 2015. Interaction between phosphate and acid-activated neutralized red mud during adsorption process. Appl Surf Sci 356: 128-134.

Ye J, Cong XN, Zhang PY, Zeng GM, Hoffmann E, Wu Y, Zhang HB, Fang W. 2016. Operational parameter impact and back propagation artificial neural network modeling for phosphate adsorption onto acid-activated neutralized red mud. J Mol Liq 216: 35-41.

Yue QY, Zhao YQ, Li Q, Li WH, Gao BY, Han SX, Qi YF, Yu H. 2010. Research on the characteristics of red mud granular adsorbents (RMGA) for phosphate removal. J Hazard Mater 176(1-3): 741-748.

Zhang GS, Liu HJ, Liu RP, Qu JH. 2009. Removal of phosphate from water by a Fe-Mn binary oxide adsorbent. J Colloid Interf Sci 335(2): 168-174.

Zhang L, Gao Y, Xu YF, Liu JY. 2016. Different performances and mechanisms of phosphate adsorption onto metal oxides and metal hydroxides: a comparative study. J Chem Technol Biot 91(5): 1232-1239.

Zhao YQ, Yue QY, Li Q, Xu X, Yang ZL, Wang XJ, Gao BY, Yu H. 2012. Characterization of red mud granular adsorbent (RMGA) and its performance on phosphate removal from aqueous solution. Chem Eng J 193: 161-168.

# Appendix

**Table 3.1. The chemical composition of three types of bauxite residue.**

| Composition | BR1 | BR2 | BR3 |
|---|---|---|---|
| $Al_2O_3$ | 8.43 ± 0.55 | 16.92 ± 2.73 | 13.62 ± 0.87 |
| CaO | 0 ± 0 | 9.18 ± 0.92 | 11.75 ± 0.73 |
| $Fe_2O_3$ | 22.42 ± 0.45 | 31.45 ± 0.12 | 29.62 ± 2.08 |
| $Na_2O$ | 6.93 ± 0.19 | 1.74 ± 0.15 | 1.66 ± 0.27 |
| $SiO_2$ | 17.29 ± 1.65 | 6.91 ± 0.30 | 3.77 ± 1.48 |
| $TiO_2$ | 3.74 ± 0.95 | 4.15 ± 2.76 | 5.77 ± 1.20 |
| LOI (1000 °C) | 14.34 | 15.43 | 12.15 |

**Table 4.2. The major characteristics of three types of bauxite residue.**

| | BR1 | BR2 | BR3 |
|---|---|---|---|
| pH | 6.77 | 6.74 | 6.86 |
| BET surface area ($m^2/g$) | 38.91 | 15.06 | 11.03 |

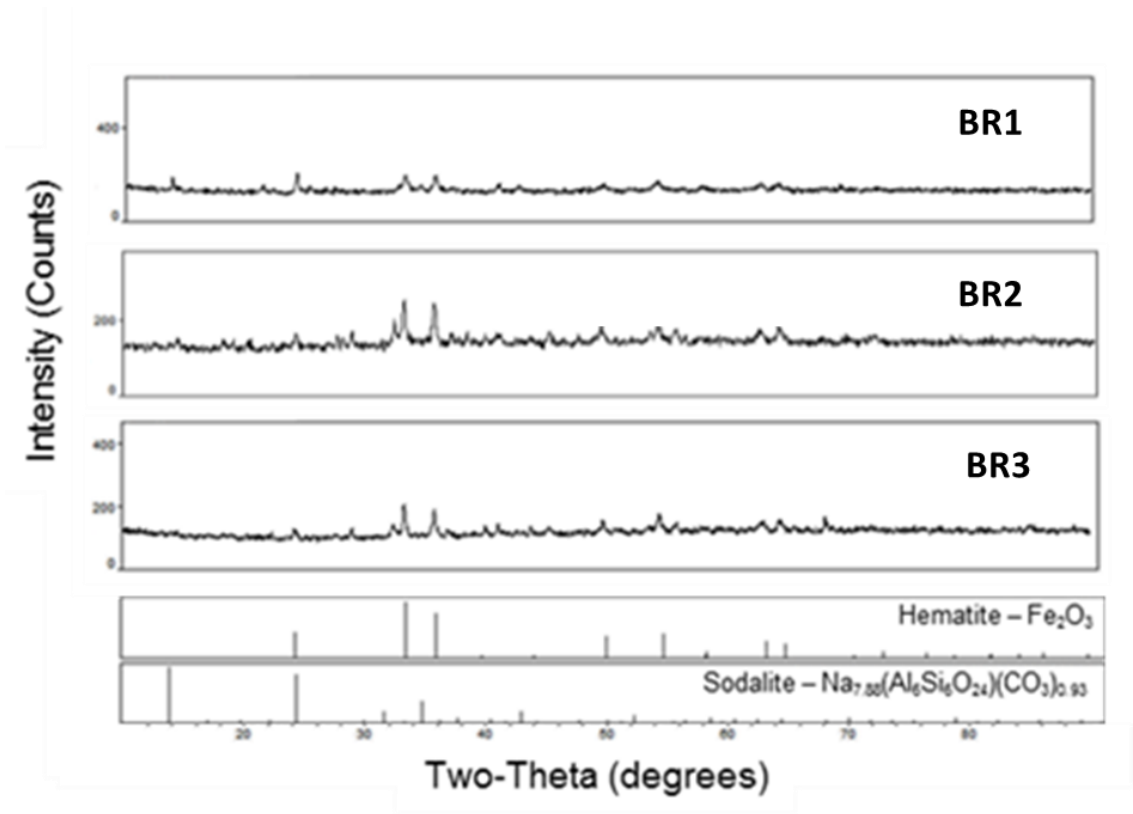


**Figure 3.1. XRD patterns of three types of bauxite residue.**

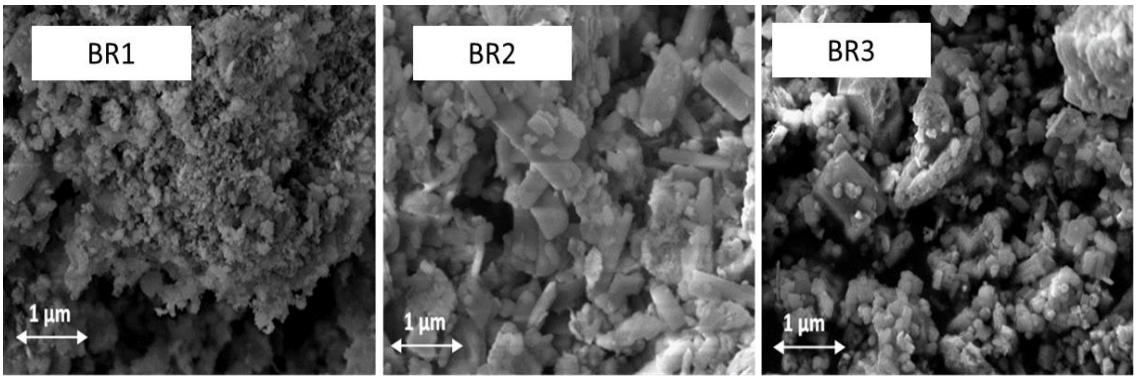


**Figure 3.2. SEM patterns of three types of bauxite residue.**

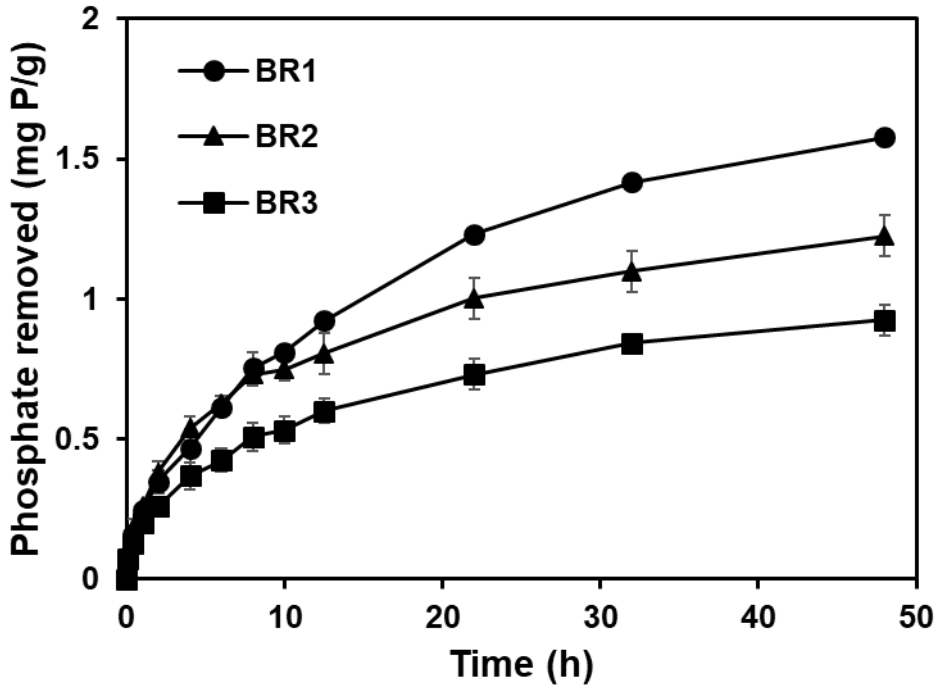


**Figure 3.3. Phosphate retention kinetics by bauxite residue.**

**Table 5.3. Removal kinetics parameters regressed by four different models.**

| Parameters | BR1 | BR2 | BR3 |
|---|---|---|---|
| Pseudo-first-order model | | | |
| $K_1$ | 0.08 ± 0.01 a | 0.14 ± 0.02 a | 0.11 ± 0.02 a |
| $q_e$ | 1.55 ± 0.07 a | 1.11 ± 0.06 b | 0.96 ± 0.05 b |
| $R^2$ | 0.98 | 0.95 | 0.96 |
| Standard error | 0.07 | 0.09 | 0.07 |
| Pseudo-second-order model | | | |
| $K_2$ | 0.04 ± 0.02 a | 0.13 ± 0.01 a | 0.13 ± 0.03 a |
| $q_e$ | 1.97 ± 0.09 a | 1.30 ± 0.06 b | 1.02 ± 0.06 b |
| $R^2$ | 0.99 | 0.98 | 0.98 |
| Standard error | 0.06 | 0.06 | 0.05 |
| Parallel-first-order model | | | |
| $K_{1a}$ | 2.68 ± 0.65 a | 0.94 ± 0.28 a | 2.06 ± 0.63 a |
| $q_{e1}$ | 0.19 ± 0.02 a | 0.37 ± 0.06 a | 0.19 ± 0.02 a |
| $K_{1b}$ | 0.06 ±0.00 a | 0.05 ± 0.01 a | 0.06 ± 0.01 a |
| $q_{e2}$ | 1.49 ± 0.02 a | 0.91 ± 0.05 b | 0.77 ± 0.02 b |
| $R^2$ | 0.999 | 0.99 | 0.997 |
| Standard error | 0.01 | 0.03 | 0.02 |
| Intraparticle diffusion model | | | |
| $K_i$ | 0.24 ± 0.01 a | 0.18 ± 0.01 b | 0.14 ± 0.01 b |
| $C$ | 0.02 ± 0.02 a | 0.11 ± 0.04 a | 0.06 ± 0.02 a |
| $R^2$ | 0.99 | 0.96 | 0.98 |
| Standard error | 0.05 | 0.08 | 0.05 |

*Values followed by different letter in row are significantly different ($p < 0.05$)

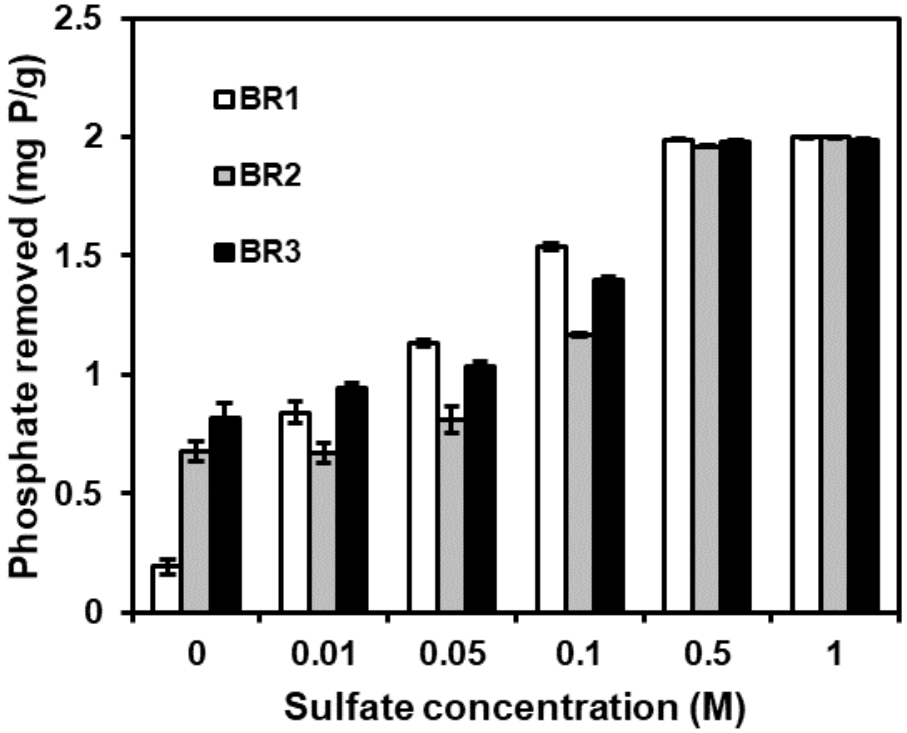


**Figure 3.4. Effect of sulfate on phosphate removal by bauxite residue.**

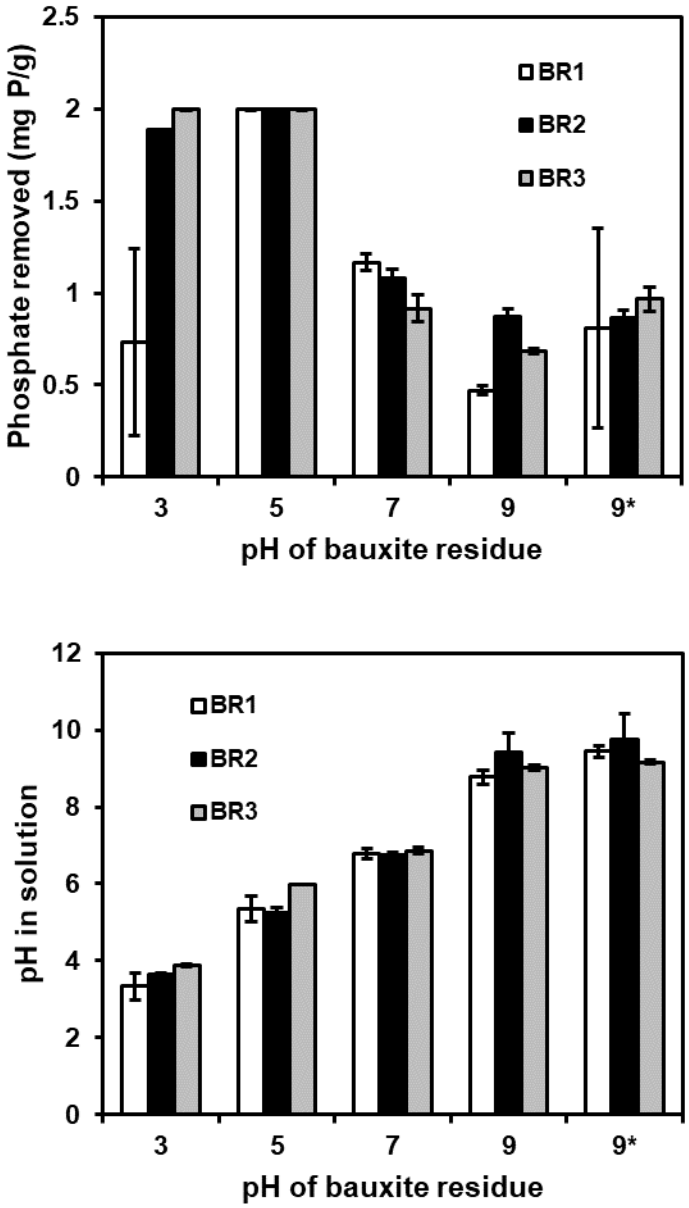


**Figure 3.5. Phosphate removal by bauxite residue with different pH and pH in equilibrium solution.**

*means the pH of raw bauxite residue that is close to 9

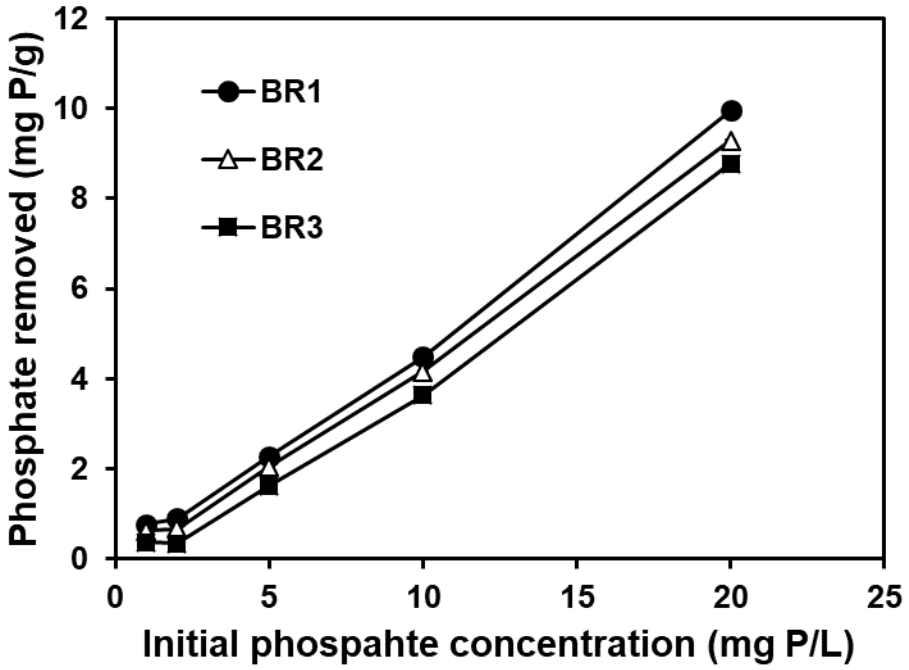


**Figure 3.6. Phosphate removal by bauxite residue with different phosphate concentration.**

# CHAPTER IV
# FEASIBILITY OF BAUXITE RESIDUE FOR THE REMOVAL OF CIPROFLOXAIN IN THE AQUEOUS SOLUTION

## Abstract

Antibiotics are considered as emerging contaminants. Ciprofloxacin (CIP) as one of the synthetic fluoroquinolone antibacterial agents is frequently detected in aquatic environments. Bauxite residue as an alkaline waste stream generated from the alumina refining industry has been proposed for applications in pollution mitigation as an effective sorbent. In this study, two types of bauxite residue were tested for the removal of CIP. Characterization of the CIP retention kinetics revealed that the parallel-first-order model exhibited the best fitness with the equilibrium time of 24 h. Comparing the removal capacity of these two types of bauxite residue, BR1 with higher content of sodium had greater CIP removal capacity than BR2 with greater content of iron oxide and aluminum oxide, indicating that the ion exchange was considered as the main mechanism for CIP retention on bauxite residue. CIP removal exhibited a strong dependence on pH and ionic strength, indicating that a combined mechanism of cation exchange and complexation with iron and aluminum oxides was also responsible for CIP removal. Initial concentration of CIP and operation temperature were the other two important parameters affected CIP removal. The applicability of the Freundlich model provided a better fitting than the Langmuir model. In conclusion, bauxite residue could be utilized for the effective removal of CIP from the aqueous phase, expanding the utility of bauxite residue for the removal of aqueous pollutants.

## Introduction

Bauxite residue is the solid residue from the production of alumina. As the alkaline waste, there is no ideal approach for disposal and the storage problems also induce a variety of environmental and safety problems. Some concerns and researches focus on exploring the efficient solution for the storage and disposal of bauxite residue (Klauber et al., 2011). The current neutralization approaches included utilization of seawater, gypsum, mineral acids, $CO_2$ and $SO_2$ (Grafe et al., 2011). The desulfurization of flue gas by bauxite residue is a promising way by integrating the desulfurization of flue gas and neutralization of bauxite residue (Wang et al., 2015) and has been applied for industrial practice in some countries (Grafe et al., 2011). After neutralization, the bauxite residue was applied for the environmental pollutant treatment. The bauxite residue shows the excellent removal performance for the inorganic material, such as phosphate (Li et al., 2006, Huang et al., 2008), heavy metal (Gupta and Sharma, 2002, Nadaroglu et al., 2010) and organic materials, such as dye (Wang et al., 2005, Shirzad-Siboni et al., 2014), phenolic compounds (Gupta et al., 2004, Tor et al., 2006). However, the utilization of bauxite residue is limited. Additionally, due to the different origin of bauxite mineral, the different bauxite residues have different characteristics that can lead to the different efficiency for the environmental application (Snars and Gilkes, 2009). Thus, it is necessary to explore more environmental applications according to the characteristics of bauxite residue.

Antibiotics as the emerging pollutant due to antibiotics abuse have been detected in different environments, thereafter the related environmental problems have persisted for several years all around the world (Fatta-Kassinos et al., 2011, Michael et al., 2013, Zhang et al., 2015), and the bacterial resistance is becoming one of the most important environmental problems. Ciprofloxacin (CIP) is a type of synthetic fluoroquinolone antibacterial agents and is widely used for human and animals (Zhang et al., 2015). CIP is frequently detected in natural environments, such as wastewater, river water, sediments and soil (Golet et al., 2002, Golet et al., 2002, Liu and Wong, 2013). Environmental concentration of CIP in surface waters ranged between 14.4 and 9660 ng/L, while it ranged between 8 and 720 ng/L in wastewater effluents (Fatta-Kassinos et al., 2011). The hospital wastewater can be detected with a higher concentration (Van Doorslaer et al., 2014). CIP can be removed efficiently in wastewater treatment plant by adsorption on the sludge (Michael et al., 2013), thus CIP concentration in sewage sludge ranges from 1.40 to 2.42 mg/kg of dry matter (Golet et al., 2002).

CIP can be removed by adsorption (Gu and Karthikeyan, 2005), photolysis (Wei et al., 2013), and biodegradation (Girardi et al., 2011). Adsorption as an efficient retention approach has been studied widely. The carbon-based materials, such as nonporous carbons (Li et al., 2017), graphene oxide (Chen et al., 2015), activated carbon, carbon xerogel and carbon nanotubes (Carabineiro et al., 2012, Yu et al., 2016), have been verified as an efficient absorbent for CIP

removal. Besides, some inorganic absorbents have been used for CIP adsorption, such as aluminum and iron hydrous oxides (Gu and Karthikeyan, 2005), montmorillonite (Wang et al., 2010, Wu et al., 2010), and kaolinite (Li et al., 2011). $pK_{a1}$ and $pK_{a2}$ values for CIP are 6.1 and 8.7 respectively and its species are different under different pH, thus CIP adsorption is a strong pH-dependent behavior (Gu and Karthikeyan, 2005). The mechanisms of CIP on soil mineral clay include cation exchange (Wang et al., 2010, Li et al., 2011) and surface complexation (Gu and Karthikeyan, 2005, Pei et al., 2010). Many exchangeable basic cations exist in the surface of bauxite residue contributing its cation exchange capacity (Liu et al., 2007). Additionally, due to that the bauxite residue is a mixture of minerals including various oxides of Fe, Al, Si, Ca (Klauber et al., 2011), it may form the complexation with CIP. Although there is no study about the retention of CIP by bauxite residue, it has the possible potential for the removal of CIP by bauxite residue.

This study aims to explore the feasibility of bauxite residue for removal of CIP from the aqueous solution and compare the removal efficiency of two types of bauxite residue. Using bauxite residue from two sources, we studied the retention kinetics, factors affecting the retention (pH, ionic strength, CIP concentration, and temperature) and isotherm curve.

## Methods and Materials

### *Materials*

CIP (purity >=98%) was purchased from Sigma-Aldrich Co. and stored at room temperature. Two types of bauxite residues with different characteristics were respectively collected from Shandong and Guangxi, China, which were denoted as BR1 and BR2. All air-dried samples were grounded and sieved by a 140-mesh sieve. The bauxite residue (4 g) with 100 ml DI water was neutralized by 1 N $H_2SO_4$. The $H_2SO_4$ neutralized bauxite residue represented the bauxite residue after the desulfurization of flue gas. After the equilibrium for 24 h, the samples were rinsed with DI water for three times. The raw sample with pH 10 was gotten without the addition of $H_2SO_4$. The rinsed samples with final pH 9 were rinsed with DI water for three times. The acidified samples were gotten with the similar method of neutralized samples by acidifying with different amounts of $H_2SO_4$ and the final pH of acidified samples were 3 and 5. The chemical composition of raw materials and neutralized bauxite residue were listed in table 3.1.

### *Retention kinetics*

For retention kinetics, 1 g of the $H_2SO_4$ neutralized bauxite residue (pH 7) was mixed with 500 mL CIP solution (0.1 mM $\approx$ 34 mg/L) in a 1 L amber glass bottle and 0.1 M NaCl as a background electrolyte was added to adjust the ionic strength. The amber glass bottles were capped with screws by shaking at 120 rpm and 20 °C with duplicates. 3 ml solution was sampled at 0, 0.25, 0.5, 1, 2, 4, 6, 8, 12, 24 and 48 h and then was centrifuged at 16000 g/min for 10 min. A clear

aliquot of the supernatant was analyzed for CIP concentration by spectrophotometer (as below). The pH value was measured by a pH meter during the experiment.

***Batch removal study***

For batch removal studies, 20 ml CIP solution (0.1 mM) with the $H_2SO_4$ neutralized bauxite residue (2 g/L) were prepared in 40 ml amber serum bottle and NaCl (0.1 M) as a background electrolyte was added to adjust the ionic strength. The amber serum bottles were placed on a shaker at 120 rpm and 20 °C for 48 h. In the end, 3 ml solution was centrifuged at 16000 g/min for 10 min and analyzed for CIP concentration and pH in solution. The various amounts of NaCl were added to investigate the effect of ionic strength on the CIP retention by neutralized bauxite residue. Bauxite residue neutralized and acidified to different pH by $H_2SO_4$ were used to study the effect of bauxite residue pH on CIP removal. Different concentration of CIP solution was prepared to study the effect of initial CIP concentration on CIP removal by neutralized bauxite residue. All batch experiments were carried out in duplicates.

***Adsorption isotherm***

Adsorption isotherm studies were carried out in 40 ml amber serum bottle with different initial concentrations of CIP and a fixed concentration of neutralized bauxite residue (2 g/L). The amber serum bottles were placed on a shaker with different temperatures (20, 30 and 40 °C) at 120 rpm for 48 h. Other operation parameters were as same as the batch retention study above.

***Analysis methods***

The CIP concentration was determined by a ThermoFisher Scientific Evolution 600 UV/Vis spectrophotometer (Madison, WI 53711, US) with a detection wavelength at 275 nm. The CIP concentration was determined by the standard curve ranging from 0 to 50 mg/L. The solution without CIP was measured as control and the results showed that it had no interference on the CIP measurement. The mineralogical composition of bauxite residue was determined by XRD with Cu Kα radiation and a step/time scan mode of 0.75°/min and the crystalline phase was analyzed by the software MDI JADE with comparing standards in the powder diffraction file (PDF2) database. The specific surface areas of bauxite residue were obtained by BET/$N_2$ adsorption methods using an automatic specific surface area measurement (Belsorp-max, MicrotracBEL, Japan). To determine pH of bauxite residue, 1 g of air-dried bauxite residue sample was stirred with 5 mL of deionized water for 5 minutes, and after settling for 30 minutes, the aqueous phase was used for pH measurement using a combination pH electrode (Oakton pH 700, U.S.). The point of zero charge ($pH_{PZC}$) of bauxite residue was measured by batch equilibrium method. 0.1 g dried red mud sample was mixed with 20 mL of 0.1 M NaCl solution of a known initial pH in a glass vial, then was shaken at 250 rpm for 24 h. Initial pH was adjusted in a wide pH range (from 1 to 11) using different volumes of 0.1 M HCl or 0.1 M NaOH. Final pH values were plotted against initial pH and the $pH_{PZC}$ was determined from the plateau of the graph.

***Data analysis***

*Kinetics model*

The CIP removal capacity at equilibrium ($q_e$, mg/g) was calculated based on the equation bellow:

$$q_e = \frac{(C_i - C_e)V}{m} \quad (1)$$

where $C_i$ and $C_e$ are the initial and final (equilibrium) concentrations of CIP in solution (mg/L), $V$ the solution volume (L), and $m$ is the amount of bauxite residue (g).

The removal kinetics were fitted to the three types of kinetic models as below:

The pseudo first-order equation:

$$q_t = q_e(1 - e^{-k_1 t}) \quad (2)$$

where $q_t$ (mg/g) is the amount of CIP removed at time $t$ (h), and $k_1$ is the equilibrium rate constant for pseudo first-order kinetics ($h^{-1}$).

The pseudo second-order equation:

$$\frac{t}{q_t} = \frac{1}{k_2 q_e^2} + \frac{t}{q_e} \quad (3)$$

where $k_2$ is the equilibrium rate constant for pseudo second-order kinetics (g $mg^{-1}$ $h^{-1}$)

The parallel first-order kinetics:

$$q_t = q_{e1}(1 - e^{-k_{1a} t}) + q_{e2}(1 - e^{-k_{1b} t}) \quad (4)$$

where $q_{e1}$ and $q_{e2}$ are the amount of CIP removed at equilibrium (mg/g) in the first and second reactions, respectively, and $k_{1a}$ and $k_{1b}$ ($h^{-1}$) are the equilibrium rate constants for the first and second reactions, respectively.

*Isotherm model*

Langmuir and Freundlich isotherms, were applied to describe the equilibrium retention of CIP by the neutralized bauxite residue (pH 7) from liquid solution. The Langmuir isotherm assumes the sorption process at specific homogeneous sites for monolayer adsorption. The Freundlich isotherm is an empirical equation employed to describe heterogeneous system.

Langmuir isotherm

$$Q = \frac{kQ_m C_{eq}}{1+kC_{eq}} \quad (5)$$

where $Q$ is the amount of CIP removed at equilibrium (mg/g), $C_{eq}$ is the equilibrium concentration of CIP in solution (mg/L), $Q_m$ is the monolayer retention capacity (mg/g) and $k$ is a constant related to the free energy of retention (L/mg).

Freundlich isotherm

$$Q = KC_{eq}^{1/n} \quad (6)$$

where $K$ is a constant ((mg/g)(L/mg)$^{1/n}$ ) that indicates the extent of the retention and $n$ is a constant, which indicates the nonlinearity between solution concentration and the retention.

Fitting of the data to the model was carried out using iterative nonlinear regression by SigmaPlot 14.0. Significance analyses were performed using the Student's t-test by IBM SPSS Statistics 23.0, and the statistical probability $p < 0.05$ was considered significant.

## Results and Discussion

### *Retention kinetics*

Retention kinetics of CIP on the two types of bauxite residue were shown in figure 4.1. To evaluate the removal performance, three retention kinetics models, first-order model, parallel-first-order model, second-order-model were used to fit the removal process. The kinetics parameters were listed in Table 4.1. According to the R-squared, parallel-first-order model was fitted better with the $R^2$ of 0.99 for the removal of CIP on both two types of bauxite residue. The parallel-first-order model showed the retention of CIP followed two-phase process, quick retention ($K_{1a}$ = 2.67 for BR1 and 1.37 for BR2) and slow retention ($K_{1b}$ = 0.18 for BR1 and 0.05 for BR2). Some retention studies of CIP on the soil minerals had demonstrated that piperazinyl amine enabled CIP retention with cation exchange and the carboxylic acid group could interact with iron oxides, aluminum oxides and aluminosilicate by complexation or bridging (Gu and Karthikeyan, 2005, Carrasquillo et al., 2008, Mackay and Seremet, 2008). The cation exchange was confirmed as the primary retention mechanism of CIP on some clay minerals, such as montmorillonite (Wu et al., 2010), kaolinite (Li et al., 2011) and rectorite (Wang et al., 2011) based on the quantitative desorption study of the

exchangeable cation. Based on our results, the removed amount of CIP at equilibrium $q_{e1}$ (4.36 for BR1 and 1.53 for BR2) is greater than $q_{e2}$ (2.33 for BR1 and 1.17 for BR2), which indicate the quick retention process was the dominant process. For two types of bauxite residue, the quick retention could be completed within 8 h and total equilibrium time was up to 24 h.

Compared with the BR1 and BR2, the retention capacity of BR1 (4.36 for $q_{e1}$ and 2.33 for $q_{e2}$) at equilibrium was significantly greater than BR2 (1.53 for $q_{e1}$ and 1.17 for $q_{e2}$). Although the content of iron oxide and aluminum oxide in BR2 was greater than BR1, the result of retention capacity was opposite, suggesting that the complexation was not the main mechanism for CIP retention. Therefore, the cation exchange was supposed to the dominant mechanism. As exchangeable cations, sodium content of BR2 was the greater than BR2 in table 4.1. Sodium in bauxite residue mainly consists of the sodium carbonate, sodium bicarbonate, sodium hydroxide and some minerals (sodalite, cancrinite, dawsonite) (Grafe et al., 2011). For BR1, the main mineral form of sodium was sodalite, and it transferred into tamarugite after the acidifying process, while the sodalite was much less for BR2 in figure 3.1. By quantitative desorption study, sodium was verified as primary cation to contribute to cation exchange during the CIP adsorption in the previous study (Wu et al., 2010, Li et al., 2011). Thus, BR1 with higher sodium content was inferred that had the greater ion exchange capacity than BR2. The cation exchange may follow the equilibrium as below:

$$\equiv RM^{-} - Na^{+} + CIP^{+} \leftrightarrow \equiv RM^{-} - CIP^{+} + Na^{+} \quad (7)$$

On the other hand, the specific surface area of BR1 (38.91 $m^2/g$) was obviously greater than BR2 (15.06 $m^2/g$), indicating that BR1 had more exchangable sites than BR2. The average of the specific surface area of bauxite residue was 32.7 $m^2/g$ for thirty different kinds of samples based on the previous review study (Grafe et al., 2011). During the neutralization, the specific surface area of bauxite residue changed depended on the origin of bauxite residue. For BR1, the specific surface area increased from the 32.17 $m^2/g$ to 38.91 $m^2/g$, while it decreased from 19.16 $m^2/g$ to 15.06 $m^2/g$ for BR2 in table 4.1. Therefore, neutralization had different effects on the specific surface area of bauxite residue with different origins.

***The effect of some parameters in batch removal experiment***

*Effect of ionic strength*

The retention capacity of CIP on bauxite residue decreased with the increasing of ionic strength from 0 to 0.5 M in figure 4.2. The CIP retention to aluminum and iron hydrous oxides was insensitive to ionic strength (Gu and Karthikeyan, 2005). Thus, the ionic strength could affect the ion exchange instead of complexation or bridging as described in equation 7. Due to the NaCl as a background electrolyte to adjust the ionic strength, the existence of sodium would compete for the exchangeable sites with the $CIP^+$ and decrease the retention of CIP on the surface of bauxite residue. The decrease of ion exchange induced by the increase of ionic strength had been verified before (Li et al., 2009). Moreover, the

inhibition effect of ionic strength was found during the CIP retention on graphene oxide due to the electrostatic forces (Chen et al., 2015).

*Effect of pH*

Bauxite residues were neutralized or acidified into different pH, and then they were used to study the retention capacity of bauxite residue with different pH. The solution of bauxite residue with different treatments had different pH after the CIP retention. Thus, the CIP adsorption capacity was depended on the solution pH as shown in figure 4.3. The CIP retention had the greatest capacity at pH 7.66 for BR1 and 6.28 for BR2. Between pH 6.1 ($pK_{a1}$) and 8.7 ($pK_{a2}$), CIP existed primarily in zwitterionic species that played an important role on the interaction of CIP and material surface (Gu and Karthikeyan, 2005, Wang et al., 2010, Li et al., 2011). When the cation exchange was considered as the CIP retention mechanism, the cation species of CIP at low pH should be favorable for retention. Some studies showed that the retention of CIP decreased with increase of pH (Mackay and Seremet, 2008, Pei et al., 2010). Besides, based on the $pH_{pzc}$ in table 4.1, the two types of bauxite residue were different from each other. When the pH in solution was lower than $pH_{pzc}$, the surface of bauxite residue dominated with cation, and the cation could expel with the bauxite residue by electrostatic interaction, while the anion could appeal to the bauxite residue. Although the cation exchange may be the dominant mechanism for CIP retention, the function of complexation and bridging should be not neglected completely. With the limited availability of cation exchange sites, the CIP

retention on soil initially increased with pH and decreased at pH > 8 (Vasudevan et al., 2009). It was studied that retention of CIP on iron and aluminum hydrous oxides due to complexation reached the plateau in the circumneutral pH range (Gu and Karthikeyan, 2005). Therefore, due to the high content of iron and aluminum oxides in bauxite residue (table 4.1), adsorption of CIP on bauxite residue was not only correlated with the cation exchange but also related with the complexation with the iron and aluminum oxides.

*Effect of initial concentration of CIP and temperature*

Retention capacity increased with increasing of initial concentration in figure 4.4. Bauxite residue showed the favorable removal capacity of CIP with the concentration ranged from 1.76-35.21 mg/L. This result indicated that the CIP retention on bauxite residue kept unsaturated, and it had the capacity to remove more CIP. However, with the increase of the initial concentration of CIP, removal efficiency decreased significantly. For BR1, CIP removal efficiency decreased from the 75% to 32% with CIP initial concentration increase from 1.76 mg/L to 35.21 mg/L and decreased from 64% to 24% for BR2. Therefore, to achieve the high removal efficiency, the wastewater with high concentration of CIP requires to be treated by bauxite residue for several times.

With the increase of temperature from 20 °C to 40 °C, CIP retention capacity decreased for BR2 in table 4.3. From 20 °C to 40 °C, there was no significant difference for BR1. Based on these results, the high temperature was

unfavorable for CIP retention on bauxite residue. Therefore, at room temperature, the CIP retention capacity of bauxite residue was excellent.

***Adsorption isotherm***

The adsorption isotherm at 20 °C, 30 °C, and 40 °C were fitted with Freundlich and Langmuir model, and the parameters were shown in table 4.3. The Freundlich model was significantly fitted better than Langmuir model with greater $R^2$. The Freundlich model indicated various sites on the heterogeneous surface of bauxite residue. The cation exchange sites and metal oxides on the surface of bauxite residue both provided the retention sites. On the other hand, the different types of metal oxides and mineral morphology lead to the heterogeneous surface of bauxite residue. For different types of bauxite residue, the morphology differed from each other. Therefore, the CIP retention on bauxite residue was different from other mineral materials, e.g. montmorillonite (Wu et al., 2010) and kaolinite (Li et al., 2011), which could be fitted well with Langmuir model.

## Conclusion

Two types of bauxite residue were tested for the removal of CIP as one of the typical antibiotics. For CIP removal kinetics, the parallel-first-order model with equilibrium time of 24 h showed better fitness than first-order model and second-order-model. Comparing the removal capacity of these two types of bauxite residue, BR1 with higher content of sodium had greater CIP removal capacity than BR2 with greater content of iron oxide and aluminum oxide. The CIP retention on bauxite residue showed a strong pH and ionic strength dependent

behavior. Neutral pH and low ionic strength supported the CIP removal. Increasing the initial concentration of CIP could obviously decrease the removal efficiency of CIP and increasing temperature was also unfavorable for CIP removal. The Freundlich isotherm model was fitted better for CIP removal than the Langmuir isotherm model.

# References

Carabineiro SAC, Thavorn-amornsri T, Pereira MFR, Serp P, Figueiredo JL. 2012. Comparison between activated carbon, carbon xerogel and carbon nanotubes for the adsorption of the antibiotic ciprofloxacin. Catal Today 186(1): 29-34.

Carrasquillo AJ, Bruland GL, Mackay AA, Vasudevan D. 2008. Sorption of ciprofloxacin and oxytetracycline zwitterions to soils and soil minerals: influence of compound structure. Environ Sci Technol 42(20): 7634-7642.

Chen H, Gao B, Li H. 2015. Removal of sulfamethoxazole and ciprofloxacin from aqueous solutions by graphene oxide. J Hazard Mater 282: 201-207.

Fatta-Kassinos D, Meric S, Nikolaou A. 2011. Pharmaceutical residues in environmental waters and wastewater: current state of knowledge and future research. Anal Bioanal Chem 399(1): 251-275.

Girardi C, Greve J, Lamshoft M, Fetzer I, Miltner A, Schaeffer A, Kastner M. 2011. Biodegradation of ciprofloxacin in water and soil and its effects on the microbial communities. J Hazard Mater 198: 22-30.

Golet EM, Alder AC, Giger W. 2002. Environmental exposure and risk assessment of fluoroquinolone antibacterial agents in wastewater and river water of the Glatt Valley Watershed, Switzerland. Environ Sci Technol 36(17): 3645-3651.

Golet EM, Strehler A, Alder AC, Giger W. 2002. Determination of fluoroquinolone antibacterial agents in sewage sludge and sludge-treated soil using accelerated solvent extraction followed by solid-phase extraction. Anal Chem 74(21): 5455-5462.

Grafe M, Power G, Klauber C. 2011. Bauxite residue issues: III. Alkalinity and associated chemistry. Hydrometallurgy 108(1-2): 60-79.

Gu C, Karthikeyan KG. 2005. Sorption of the antimicrobial ciprofloxacin to aluminum and iron hydrous oxides. Environ Sci Technol 39(23): 9166-9173.

Gupta VK, Ali I, Saini VK. 2004. Removal of chlorophenols from wastewater using red mud: an aluminum industry waste. Environ Sci Technol 38(14): 4012-4018.

Gupta VK, Sharma S. 2002. Removal of cadmium and zinc from aqueous solutions using red mud. Environ Sci Technol 36(16): 3612-3617.

Huang WW, Wang SB, Zhu ZH, Li L, Yao XD, Rudolph V, Haghseresht F. 2008. Phosphate removal from wastewater using red mud. J Hazard Mater 158(1): 35-42.

Klauber C, Grafe M, Power G. 2011. Bauxite residue issues: II. options for residue utilization. Hydrometallurgy 108(1-2): 11-32.

Li JX, Hu J, Sheng GD, Zhao GX, Huang Q. 2009. Effect of pH, ionic strength, foreign ions and temperature on the adsorption of Cu(II) from aqueous solution to GMZ bentonite. Colloid Surface A 349(1-3): 195-201.

Li SQ, Zhang XD, Huang YM. 2017. Zeolitic imidazolate framework-8 derived nanoporous carbon as an effective and recyclable adsorbent for removal of ciprofloxacin antibiotics from water. J Hazard Mater 321: 711-719.

Li YZ, Liu CJ, Luan ZK, Peng XJ, Zhu CL, Chen ZY, Zhang ZG, Fan JH, Jia ZP. 2006. Phosphate removal from aqueous solutions using raw and activated red mud and fly ash. J Hazard Mater 137(1): 374-383.

Li ZH, Hong HL, Liao LB, Ackley CJ, Schulz LA, MacDonald RA, Miheliche AL, Emard SM. 2011. A mechanistic study of ciprofloxacin removal by kaolinite. Colloid Surface B 88(1): 339-344.

Liu JL, Wong MH. 2013. Pharmaceuticals and personal care products (PPCPs): A review on environmental contamination in China. Environ Int 59: 208-224.

Liu Y, Lin CX, Wu YG. 2007. Characterization of red mud derived from a combined Bayer Process and bauxite calcination method. J Hazard Mater 146(1-2): 255-261.

Mackay AA, Seremet DE. 2008. Probe compounds to quantify cation exchange and complexation interactions of ciprofloxacin with soils. Environ Sci Technol 42(22): 8270-8276.

Michael I, Rizzo L, McArdell CS, Manaia CM, Merlin C, Schwartz T, Dagot C,Fatta-Kassinos D. 2013. Urban wastewater treatment plants as hotspots for the release of antibiotics in the environment: A review. Water Res 47(3): 957-995.

Nadaroglu H, Kalkan E, Demir N. 2010. Removal of copper from aqueous solution using red mud. Desalination 251(1-3): 90-95.

Nikraz HR, Bodley AJ, Cooling DJ, Kong PYL, Soomro M. 2007. Comparison of physical properties between treated and untreated bauxite residue mud. J Mater Civil Eng 19(1): 2-9.

Pei ZG, Shan XQ, Kong JJ, Wen B, Owens G. 2010. Coadsorption of ciprofloxacin and Cu(II) on montmorillonite and kaolinite as affected by solution pH. Environ Sci Technol 44(3): 915-920.

Shirzad-Siboni M, Jafari SJ, Giahi O, Kim I, Lee SM, Yang JK. 2014. Removal of acid blue 113 and reactive black 5 dye from aqueous solutions by activated red mud. J Ind Eng Chem 20(4): 1432-1437.

Snars K, Gilkes RJ. 2009. Evaluation of bauxite residues (red muds) of different origins for environmental applications. Appl Clay Sci 46(1): 13-20.

Tor A, Cengeloglu Y, Aydin ME, Ersoz M. 2006. Removal of phenol from aqueous phase by using neutralized red mud. J Colloid Interf Sci 300(2): 498-503.

Van Doorslaer X, Dewulf J, Van Langenhove H, Demeestere K. 2014. Fluoroquinolone antibiotics: An emerging class of environmental micropollutants. Sci Total Environ 500: 250-269.

Vasudevan D, Bruland GL, Torrance BS, Upchurch VG, MacKay AA. 2009. pH-dependent ciprofloxacin sorption to soils: Interaction mechanisms and soil factors influencing sorption. Geoderma 151(3-4): 68-76.

Wang CJ, Li ZH, Jiang WT. 2011. Adsorption of ciprofloxacin on 2:1 dioctahedral clay minerals. Appl Clay Sci 53(4): 723-728.

Wang CJ, Li ZH, Jiang WT, Jean JS, Liu CC. 2010. Cation exchange interaction between antibiotic ciprofloxacin and montmorillonite. J Hazard Mater 183(1-3): 309-314.

Wang SB, Boyjoo Y, Choueib A, Zhu ZH. 2005. Removal of dyes from aqueous solution using fly ash and red mud. Water Res 39(1): 129-138.

Wang XK, Zhang YH, Lv FZ, An Q, Lu RR, Hu P, Jiang SB. 2015. Removal of alkali in the red mud by $SO_2$ and simulated flue gas under mild conditions. Environ Prog Sustain 34(1): 81-87.

Wei XX, Chen JW, Xie Q, Zhang SY, Ge LK, Qiao XL. 2013. Distinct photolytic mechanisms and products for different dissociation species of ciprofloxacin. Environ Sci Technol 47(9): 4284-4290.

Wu QF, Li ZH, Hong HL, Yin K, Tie LY. 2010. Adsorption and intercalation of ciprofloxacin on montmorillonite. Appl Clay Sci 50(2): 204-211.

Yu F, Sun SN, Han S, Zheng J, Ma J. 2016. Adsorption removal of ciprofloxacin by multi-walled carbon nanotubes with different oxygen contents from aqueous solutions. Chem Eng J 285: 588-595.

Zhang QQ, Ying GG, Pan CG, Liu YS, Zhao JL. 2015. Comprehensive evaluation of antibiotics emission and fate in the river basins of China: source analysis, multimedia modeling, and linkage to bacterial resistance. Environ Sci Technol 49(11): 6772-6782.

# Appendix

**Table 4.1. The major characteristics of two types of raw and neutralized bauxite residue.**

| parameters | BR1 | Neutralized BR1 | BR2 | Neutralized BR2 |
|---|---|---|---|---|
| Specific Surface Area, A ($m^2/g$) | 32.17 | 38.91 | 19.16 | 15.06 |
| $pH_{pzc}$ | | 7.7 | | 8.3 |

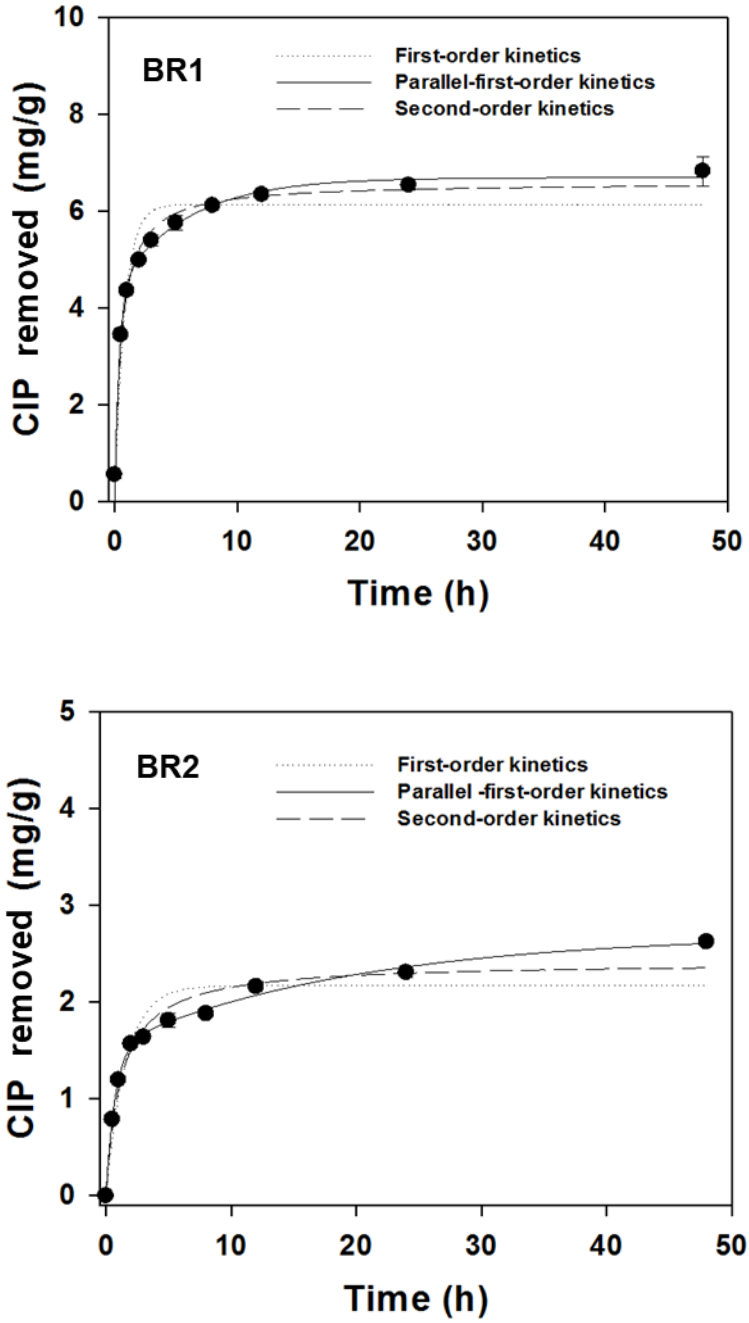


**Figure 4.1. CIP retention kinetics by bauxite residue. The line was the data fitted by first-order kinetics, parallel-first-order kinetics and second order kinetics.**

**Table 4.2. Retention kinetics parameters on bauxite residue.**

| Parameters | BR1 | BR2 |
|---|---|---|
| First-order model | | |
| $q_t = q_e(1 - e^{-k_1 t})$ | | |
| $K_1$ | 1.25 ± 0.23 | 0.64 ± 0.14 |
| $q_e$ | 6.13 ± 0.22 | 2.17 ± 0.12 |
| $R^2$ | 0.93 | 0.91 |
| Standard error | 0.53 | 0.25 |
| Second-order model | | |
| $\frac{t}{q_t} = \frac{1}{k_2 q_e^2} + \frac{t}{q_e}$ | | |
| $K_2$ | 0.29 ± 0.03 | 0.34 ± 0.02 |
| $q_e$ | 6.59 ± 0.15 | 2.41 ± 0.01 |
| $R^2$ | 0.98 | 0.98 |
| Standard error | 0.28 | 0.06 |
| Parallel-first-order model | | |
| $q_t = q_{e1}(1 - e^{-k_{1a} t}) + q_{e2}(1 - e^{-k_{1b} t})$ | | |
| $K_{1a}$ | 2.67 ± 0.68 | 1.37± 0.14 |
| $q_{e1}$ | 4.36 ± 0.48 | 1.53 ± 0.07 |
| $K_{1b}$ | 0.18 ± 0.07 | 0.05 ± 0.01 |
| $q_{e2}$ | 2.33 ± 0.45 | 1.17 ± 0.09 |
| $R^2$ | 0.99 | 0.99 |
| Standard error | 0.25 | 0.05 |

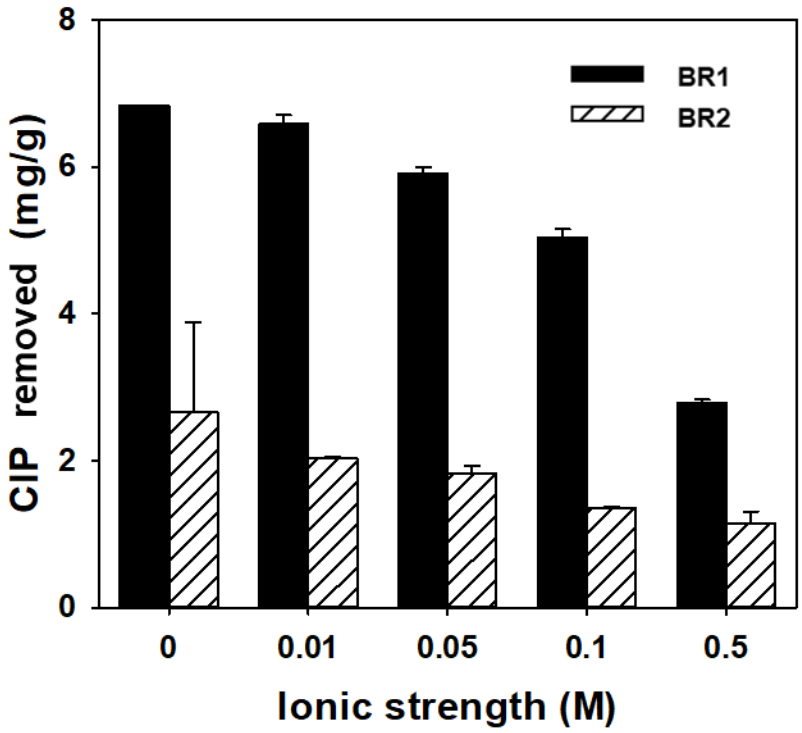


**Figure 4.2. The effect of ionic strength on CIP removal by bauxite residue.**

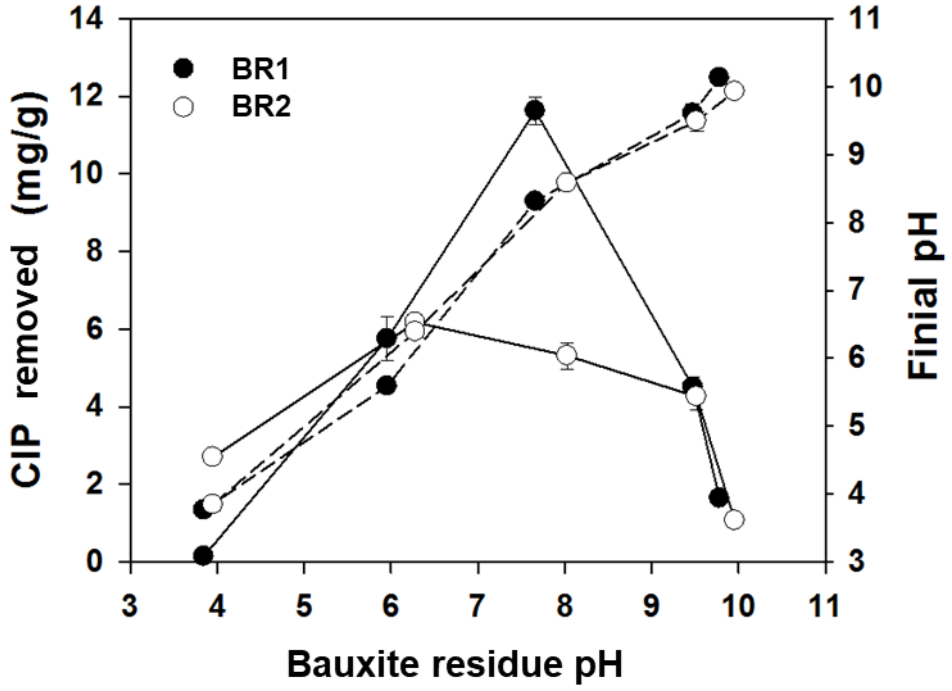


**Figure 4.3. The effect of pH on CIP removal (left axis) and final solution pH (right axis). The solid lines represent the amount of CIP removed and dash lines represent the final solution pH, respectively.**

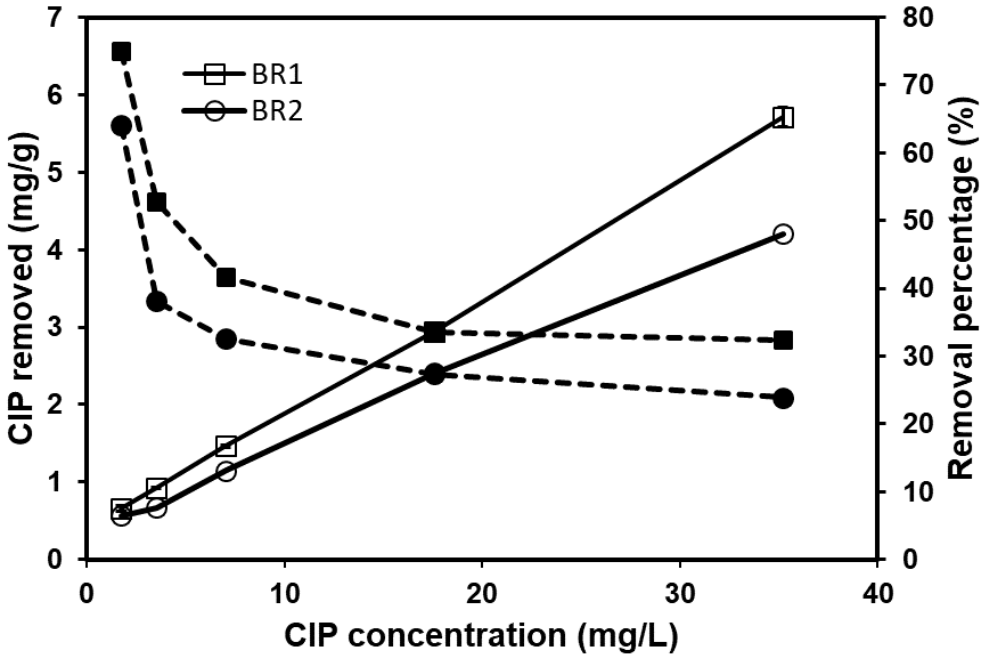


**Figure 4.4. The effect of CIP concentration on CIP removal amount (left axis) and removal percentage (right axis). The solid lines represent the amount of CIP removed and dash lines represent the removal percentage, respectively.**

**Table 4.3. Adsorption isotherm parameters on bauxite residue.**

| Sample | Temperature (°C) | Langmuir model | | | Freundlich model | | |
|---|---|---|---|---|---|---|---|
| | | k | $Q_m$ | $R^2$ | K | 1/n | $R^2$ |
| BR1 | 20 | 0.08 | 7.71 | 0.72 | 0.51 | 0.75 | 0.98 |
| | 30 | 0.07 | 8.44 | 0.75 | 0.52 | 0.77 | 0.99 |
| | 40 | 0.05 | 9.59 | 0.83 | 0.52 | 0.75 | 0.99 |
| BR2 | 20 | 0.07 | 6.14 | 0.76 | 0.40 | 0.71 | 0.99 |
| | 30 | 0.01 | 13.70 | 0.19 | 0.29 | 0.79 | 0.99 |
| | 40 | 0.02 | 10.26 | 0.73 | 0.18 | 0.89 | 0.99 |

# CHAPTER V
# EFFECTS OF BAUXITE RESIDUE AS AN ADDITIVE ON BIOGAS PRODUCTION AND PHOSPHORUS RECOVERY IN ANAEROBIC DIGESTER

## Abstract

Anaerobic digestion is a proven technology for the treatment of organic waste and production of biogas as a renewable energy source. Challenges to the broad application of anaerobic digestion include the need to improve treatment efficiency and management of nutrients in the digestate, such as phosphorus. In this study, the bauxite residue as an alkaline solid waste was applied to the anaerobic digestion as an additive. It was hypothesized that the addition of iron-rich bauxite residue could increase the availability of iron, which is commonly considered as a limiting trace metal nutrient in anaerobic digestion. Using two bauxite residues of different minerology, the effect of bauxite residue on the biogas production and phosphorus (P) availability in anaerobic digester was investigated. The modified Gompertz model was found to fit the cumulative methane production well. The dosage of bauxite residue was shown to be critical for biogas production, with the addition of 8% bauxite residue significantly prolonging the lag time. Addition of BR1 with lower dosages amounts (0.5%, 2% and 4%) improved the biogas production, while the addition of BR2 had no impact on biogas production. It is also found that the addition of bauxite residue increased the levels of dissolved sodium (Na) and iron (Fe) in the digestion liquor. The increase in Na concentration is typically considered to be undesirable for anaerobic digestion processes. However, increased Fe following bauxite residue addition was beneficial for methane production and $H_2S$ elimination. Moreover, the addition of bauxite residue increased the relative abundance of

non-apatite inorganic phosphorus (NAIP), indicative of enhanced availability of phosphorus in the digestate. Therefore, the addition of bauxite residue at proper dosages could simultaneously enhance methane production and increase the availability of phosphorus in the digestate, providing an innovative strategy for the reuse of bauxite residue to support waste treatment and resource management.

## Introduction

With the rapid development of economy and society, the bio-solid waste production increases rapidly all around the world. The intensified animal production causes the large amounts of production of animal waste. Anaerobic digestion is a valid approach for waste stabilization and reduction as well as for converting the solid waste to bioenergy in the form of methane. Besides, the solid residue after the anaerobic digestion, e.g. anaerobic digestate, can be used as fertilizer with the high content of nitrogen and phosphorus (Insam et al., 2015). Land application of digestate can bring various benefits, such as nutrient recycling, reduction of mineral fertilizer consumption, and water pollution mitigation (Holm-Nielsen et al., 2009).

Optimizing of operation is the primary way to maintain the stability of anaerobic digestion. Some biological or chemical additives are utilized to enhance biogas yield in anaerobic digestion or reduce the inhibition. Mao et al. (2015) summered some biological additives, such as microbial consortium and enzymes, and chemical additives, such as alkali reagent, acid reagent and oxidative reagent can be used to increase the availability of cellulose, hemicellulose, and lignocelluloses, which were reluctant for microbial utilization. The addition of macronutrients and trace elements can stimulate the treatment efficiency by stimulating the growth of microorganisms (Banks et al., 2012). Adding rusty scrap iron into anaerobic digestion was also proposed to enhance anaerobic sludge digestion as induced microbial iron reduction accelerated the

anaerobic hydrolysis–acidification processes (Zhang et al., 2014). Moreover, some adsorbents, such as zeolite, glauconite, activated carbon, and biochar, were considered to mitigate the inhibition and supply a habitat for the methanogenic microflora (Yenigun and Demirel, 2013, Mumme et al., 2014, Fagbohungbe et al., 2016).

Besides high alkalinity and high salinity, bauxite residue as a kind of industrial waste from the alumina refining process is the iron oxide-rich mineral solid. Recently, bauxite residue with the high content of hematite was innovatively used as an additive in the anaerobic digestor (Ye et al., 2018, Ye et al., 2018, Ye et al., 2018). Firstly, the high alkalinity of bauxite residue promoted the hydrolysis-acidification reaction. Secondly, the higher conductivity enhanced the electron transfer between the syntrophic bacteria and methanogens. Additionally, the multivalent cations from hematite effectively promoted the formation of compact aggregates. All these performances obviously enhanced the biogas production. On the other hand, pH of bauxite residue can be neutralized during the anaerobic digestion, where the fermentative microbial community was verified for bioremediation of alkaline bauxite residue by producing organic acids and $CO_2$ from an organic carbon substrate (Santini et al., 2016). Although the addition of bauxite residue in the anaerobic digestion had some advantages, it is not clear that the different kinds of bauxite residue had the same function in the anaerobic digester.

Bauxite residue has been verified as a valid absorbent of phosphorus, especially for the acid neutralized bauxite residue (Li et al., 2006, Liu et al., 2007, Huang et al., 2008, Zhao et al., 2012). The adsorption mechanism was suggested to include the chemical adsorption on Fe-Al phases of bauxite residue, and the formation of metal phosphate precipitates (Castaldi et al., 2010, Bhatnagar et al., 2011). Due to the decrease of phosphorus reserve, the recovery and reuse of phosphorous become more valuable based on the total value calculation (Mayer et al., 2016). Animal waste with high phosphorus concentration was the primary source for phosphorus recovery (Rittmann et al., 2011). Therefore, the digestate from the anaerobic digestion was considered as the important resource of fertilizer. Separation of the liquid and solid fraction may shift phosphorus contents into the solid part, thus the availability of phosphorus in the digestate is critical as fertilizer. However, due to the addition of bauxite residue, it is not clear whether the availability of phosphorus in digestate can change.

The aim of this study to the investigate and compare the impact of two bauxite residues with different minerology on the anaerobic digestion. First, we study the effect of the addition of different dosages of bauxite residue on the biogas production and explore the possible reason. Second, we study the phosphorus availability in the digestate after the separation of the liquid and solid fraction.

## Materials and Methods

### *Materials*

The bauxite residue from Shandong and Guangxi in China were selected with different characteristics and denoted by BR1 and BR2. Before use, the bauxite residue was crushed and passed through 60 mesh (0.25 mm) sieve. The characteristics of two types of bauxite residue were listed in table 5.1.

Dairy waste slurry was collected from the waste storage tank of a dairy farm located in Loudon County, Tennessee, USA. The dairy waste slurry raw dairy manure and wastewater discharges. The inoculum was gotten from the subsequent laboratory-scale anaerobic digester with waste activated sludge as feedstock. All waste substrates were stored at 4 °C in the closed container before use.

### *Batch experiment*

Batch experiments were conducted in the 120 ml glass vessels with 50 ml mixture of dairy waste slurry (61 g TS/L, pH 6.84) and 10 ml inoculum (5 g TS/L, pH 7.05). The bauxite residue was spiked into the vessel with the dosage of 0.5% (0.3 g), 2% (1.2 g), 4% (2.4 g) and 8% (4.8 g). The control treatment was set up without the addition of bauxite residue. All vessels were flushed with nitrogen gas for 10 min and then sealed with rubber stopper and aluminum crimp cap. All digesters were incubated in the shaking incubator with a setting of 80 rpm at 35 °C. Duplicates were set up in each experiment.

### *Analytic method*

Biogas production was determined by a modified water displacement method. Methane content in biogas was measured with a Hewlett Packard 5890 Series gas chromatograph with a thermal conductivity detector (TCD). When the biogas production was over, 2 ml suspension sample was collected from the vessel. Then the suspension sample was centrifuged, and the supernatant was acidified by $HNO_3$. The supernatant was used for analysis of pH, VFA, soluble phosphorus and cation concentration, and the precipitate was used for analysis of phosphorus fraction. The pH was measured with a pH meter (Thermo Scientific Orion model 720-A). VFA was analyzed by a Hewlett Packard 5890 gas chromatograph equipped with a flame ionization detector (FID) and a Restek Stabilwax-DA column. Soluble cation was quantified by inductively coupled atomic emission spectrometry (Thermo Electron Intrepid II ICP-AES). Soluble phosphorus was quantified by ICP-AES and spectrophotometer.

### *Phosphorus fraction*

Phosphorus in the solid was extracted according to the SMT protocol from the European Commission, through the Standards, Measurements and Testing (SMT) Program (Ruban et al., 1999). Briefly, the solid sample was calcinated in 450 °C for 3 h, and then extracted by 3.5 M HCl. The phosphorus concentration by this step was denoted as the total phosphorus (TS). Inorganic phosphorus (IP) was analyzed by extraction with 1 M HCl, and the residue that was considered as organic phosphorus (OP) was calcinated at 450 °C for 3 h and then extracted by

1 M HCl. IP was furtherly divided by non-apatite inorganic phosphorus (NAIP) and apatite phosphorus (AP) by extraction with 1 M NaOH. Soluble phosphorus was measured by the stannous chloride method based on the *Standard Methods for the Examination of Water and Wastewater* (APHA, 2005).

***Data analysis***

Modified Gompertz model was selected to model the cumulative methane production as below (Nopharatana et al., 2007):

$$G_t = G_0 \times exp\left\{-exp\left[\frac{U \times e}{G_0}(\lambda - \mathrm{t}) + 1\right]\right\}$$

$G_t$ is cumulative of specific biogas production, ml; $G_o$ is biogas production potential, ml; $U$ is the maximum biogas production rate (ml/day); $\lambda$ lag phase period (minimum time to produce biogas), days; and $t$ accumulative time for biogas production, days; $e$ is the exp(1) = 2.7183.

The experimental data were analyzed by SigmaPlot 14.0. To the differences in these parameters were analyzed using one-way analysis of variance (ANOVA). Significant differences in these parameters between different process stages were indicated by a probability value ($p$) less than 0.05 in ANOVA analysis with fish LSD test.

## Results and Discussion

***Impact of bauxite residue on the methane production***

The modified Gompertz equation was fit well to the cumulative methane production with addition of the different amount of bauxite residue. The parameters of $G_0$, $U$ and $\lambda$ were summarized in Table 5.2. The modified equation can be used to fit the methane production process with correlation coefficients from 0.996 to 0.999. For methane production potential, the addition of BR1 with 0.5%, 2% and 4% increased the methane production potential and the increased ranged from 2.66% to 4.79%. However, the methane production potential did not significantly change with the addition of 8% BR1 and different amounts of BR2. This result was different from a previous study (Ye et al., 2018), in which the addition of 2% bauxite residue resulted in an obvious increase with 35.5% methane production due to the promoted the hydrolysis-acidification reaction and the enhanced electrical conductivity. The enhanced hydrolysis-acidification by alkali was verified by some studies (Su et al., 2013). For the maximum methane production rate, with increasing amount of bauxite residue, the maximum methane production rate increased, except the addition of 2% BR1, suggesting that more readily degraded organic matter is available due to the possible enhanced the hydrolysis. For the lag time, the large amounts of bauxite residue increased the lag time for 8% BR1, and 4% and 8% BR2. Especially, the addition of 8% BR2 significantly increased the lag time by 3.37 times relative to the control. This result was attributed to the high pH of bauxite residue and the limited buffer capacity of the fermentation liquor. The addition of bauxite residue

could increase the initial pH in the anaerobic digester that affected the microbial acclimatization time.

Although the initial pH could be affected, the final pH kept steady ranging from 7.7 to 7.9 in figure 5.1, indicating the bauxite residue could be neutralized by the anaerobic digestion with the increase of buffer capacity due to the production of VFA and $CO_2$. Therefore, the up to 8% of the bauxite residue could be neutralized by the anaerobic digestion. There was no significant accumulation of VFA, except for the addition of 8% BR2. The primary composition of VFA was acetate here, thus the accumulated acetate was not consumed by methanogen that was affected by the addition of 8% BR2.

***The content of soluble cation in the anaerobic digester***

Bauxite residue contained lots of the aluminum (Al), iron (Fe), calcium (Ca), sodium (Na), silica (Si), and titanium (Ti) for the BR1 and BR2 in Table 5.1. The NaOH, $Na_2CO_3$, and sodalite could all release sodium. Potassium (K), Calcium (Ca), Sodium (Na), Magnesium (Mg) were the primary elements in the digestion liquor in figure 5.2. Compared with control, Na concentration significantly increased with the increased addition amounts of bauxite residue. The Na concentration in control was 773 mg/L, while Na concentration was respectively 5186 mg/L and 6841 mg/L with the addition of 8% BR1 and BR2. K concentration decreased with the increasing addition of BR1, while K concentration kept steady with the increasing addition of BR2. For Ca and Mg, the concentration relatively decreased with increasing addition of bauxite residue. In sum, the addition of

bauxite residue increased the salinity in the solution. The salt was necessary for microbial growth; however, the high salt could cause microbial cells to dehydrate due to osmotic pressure (Chen et al., 2008). Thus, the increase of salinity was detrimental to methane production. However, the bauxite residue from different sources had different Na content (Grafe et al., 2011), and the effect of the increase of salinity was subjected to the different sources of bauxite residue.

The addition of iron-rich bauxite residue could also increase the availability of Fe in the reducing condition, which is commonly considered as a limiting trace metal nutrient in anaerobic digestion. In figure 5.3, increase addition of bauxite residue increased the Fe concentration in the digestion liquor. For BR1, the Fe concentration increased from 1.77 mg/L for control to 3.52 mg/L, while for BR2, Fe concentration increased from 1.77 mg/L for control to 10.41 mg/L. The difference may be ascribed into the different content of Fe for two different types of bauxite residue. BR2 contained 29.53% of Fe, which was greater than 21.32% for BR1. Besides of the dissolved Fe, the bauxite residue contained high content of hematite. Ye et al. (Ye et al., 2018, Ye et al., 2018) explained the reason that the addition of bauxite residue with the high content of hematite increased methane production. On the one hand, multivalent cations from hematite effectively promoted the formation of large and compact aggregates that lead to the direct electron exchange. On the other hand, Fe released from bauxite residue as a redox-active mediator could take part in the interspecies electron transfer process between syntrophic bacteria and methanogenic archaea.

Furthermore, the ferric iron reduction could be considered as an important pathway for enhancing organic matter decomposition (Lovley, 1987, Liu et al., 2015). The release of Fe not only affected the methane production but also eliminated the potential sulfide production as well as the possible $H_2S$ emission in the by iron-sulfide precipitation (Liu et al., 2015). Therefore, the increase of Fe by addition of bauxite residue would be beneficial for the anaerobic digester.

***Impact of bauxite residue on the bioavailability of phosphorus in the digestate***

The phosphorus concentration was determined by UV-Vis spectrophotometry and ICP-AES, which represent the soluble reactive phosphorus and the total phosphorus (Pardo et al., 2004). The difference between these two values represented the organic phosphorus. Addition of BR1 decreased the concentration of IP in figure 5.4, indicating IP was adsorbed by BR1. However, the concentration of IP and OP increased with the addition of BR2, especially for the addition of 8% BR2. The result implied that the addition of bauxite residue promoted the release of the soluble P.

Besides of the soluble phosphorus, over 94% of TP was bound in the digestate. SMT for analyzing the phosphorus fractionation had been applied for the sewage sludge and sediment samples (Medeiros et al., 2005). According to the SMT method, the phosphorus in the solid was divided into OP and IP that consisted of NAIP and AP. NAIP represented the adsorbed by exchange site and associated with Al, Fe and Mn oxide and hydroxides, while AP represented the

Ca-bound compounds (Ruban et al., 1999). In figure 5.5, with the increase amounts of bauxite residue, relative abundance of NAIP increased from 32% for control to 66% for BR1 and 61% for BR2, while relative abundance of AP decreased from 48% for control to 16% for BR1 and 26% for BR2. This result suggested that AP was transferred into NAIP with the addition of bauxite residue and availability of phosphorus in the digestate increased with the addition of bauxite residue. It was postulated that organic acid and $CO_2$ could promote the dissolution of apatite. The digestate with bauxite residue had the potential as the P resource for substitution of P fertilizer from the P rock. Furthermore, the digestate as fertilizer could play an important role in the organic amendment (Tambone et al., 2009).

## Conclusion

Using two types of bauxite residues with the different minerology, the effect of bauxite residue on the biogas production and phosphorus (P) availability in anaerobic digester was investigated. The modified Gompertz model was found to fit the cumulative methane production well. The dosage of bauxite residue was shown to be critical for biogas production, with the addition of 8% bauxite residue significantly prolonging the lag time with accumulation of acetate in anaerobic digester. Addition of BR1 with lower dosages amounts (0.5%, 2% and 4%) improved the biogas production with 2.66% to 4.79%, while the addition of B2 had no impact on biogas production. At the end, pH in anaerobic digester was similar from 7.7 to 7.9 with different dosage of bauxite residue. It is also found

that the addition of bauxite residue increased the levels of dissolved Na and Fe in the digestion liquor. The increase in Na concentration is typically considered to be undesirable for anaerobic digestion processes. However, increased Fe following bauxite residue addition was beneficial for methane production and $H_2S$ elimination. Moreover, the addition of bauxite residue increased the relative abundance of non-apatite inorganic phosphorus (NAIP), indicative of enhanced availability of phosphorus in the digestate. Therefore, the addition of bauxite residue at proper dosages could simultaneously enhance methane production and increase the availability of phosphorus in the digestate, providing an innovative strategy for the reuse of bauxite residue to support waste treatment and resource management.

# References

American Public Health Association (APHA). 2005. Standard methods for the examination of water and wastewater, 21 edn. APHA, AWWA, WEF, Washington, DC.

Bhatnagar A, Vilar VJP, Botelho CMS, Boaventura RAR. 2011. A review of the use of red mud as adsorbent for the removal of toxic pollutants from water and wastewater. Environ Technol 32(3): 231-249.

Castaldi P, Silvetti M, Garau G, Deiana S. 2010. Influence of the pH on the accumulation of phosphate by red mud (a bauxite ore processing waste). J Hazard Mater 182(1-3): 266-272.

Chen Y, Cheng JJ, Creamer KS. 2008. Inhibition of anaerobic digestion process: A review. Bioresource Technol 99(10): 4044-4064.

Fagbohungbe MO, Herbert BMJ, Hurst L, Li H, Usmani SQ, Semple KT. 2016. Impact of biochar on the anaerobic digestion of citrus peel waste. Bioresource Technol 216: 142-149.

Grafe M, Power G, Klauber C. 2011. Bauxite residue issues: III. Alkalinity and associated chemistry. Hydrometallurgy 108(1-2): 60-79.

Holm-Nielsen JB, Al Seadi T, Oleskowicz-Popiel P. 2009. The future of anaerobic digestion and biogas utilization. Bioresource Technol 100(22): 5478-5484.

Huang WW, Wang SB, Zhu ZH, Li L, Yao XD, Rudolph V, Haghseresht F. 2008. Phosphate removal from wastewater using red mud. J Hazard Mater 158(1): 35-42.

Insam H, Gomez-Brandon M, Ascher J. 2015. Manure-based biogas fermentation residues - Friend or foe of soil fertility? Soil Biol Biochem 84: 1-14.

Li YZ, Liu CJ, Luan ZK, Peng XJ, Zhu CL, Chen ZY, Zhang ZG, Fan JH, Jia ZP. 2006. Phosphate removal from aqueous solutions using raw and activated red mud and fly ash. J Hazard Mater 137(1): 374-383.

Liu CJ, Li YZ, Luan ZK, Chen ZY, Zhang ZG, Jia ZP. 2007. Adsorption removal of phosphate from aqueous solution by active red mud. J Environ Sci-China 19(10): 1166-1170.

Liu YW, Wang QL, Zhang YB, Ni BJ. 2015. Zero valent iron significantly enhances methane production from waste activated sludge by improving biochemical methane potential rather than hydrolysis rate. Sci Rep 5, 8263.

Lovley DR. 1987. Organic-matter mineralization with the reduction of ferric iron - a review. Geomicrobiol J 5(3-4): 375-399.

Mao CL, Feng YZ, Wang XJ, Ren GX. 2015. Review on research achievements of biogas from anaerobic digestion. Renew Sust Energ Rev 45: 540-555.

Mayer BK, Baker LA, Boyer TH, Drechsel P, Gifford M, Hanjra MA, Parameswaran P, Stoltzfus J, Westerhoff P, Rittmann BE. 2016. Total value of phosphorus recovery. Environ Sci Technol 50 (13): 6606–6620.

Medeiros JJG, Cid BP, Gomez EF. 2005. Analytical phosphorus fractionation in sewage sludge and sediment samples. Anal Bioanal Chem 381(4): 873-878.

Mumme J, Srocke F, Heeg K, Werner M. 2014. Use of biochars in anaerobic digestion. Bioresource Technol 164: 189-197.

Nopharatana A, Pullammanappalli PC, Clarke WP. 2007. Kinetics and dynamic modelling of batch anaerobic digestion of municipal solid waste in a stirred reactor. Waste Manage 27(5): 595-603.

Pardo P, Rauret G, Lopez-Sanchez JF. 2004. Shortened screening method for phosphorus fractionation in sediments - A complementary approach to the standards, measurements and testing harmonised protocol. Anal Chim Acta 508(2): 201-206.

Rittmann BE, Mayer B, Westerhoff P, Edwards M. 2011. Capturing the lost phosphorus. Chemosphere 84(6): 846-853.

Ruban V, Lopez-Sanchez JF, Pardo P, Rauret G, Muntau H, Quevauviller P. 1999. Selection and evaluation of sequential extraction procedures for the determination of phosphorus forms in lake sediment. J Environ Monitor 1(1): 51-56.

Santini TC, Malcolm LI, Tyson GW, Warren LA. 2016. pH and organic carbon dose rates control microbially driven bioremediation efficacy in alkaline bauxite residue. Environ Sci Technol 50(20): 11164-11173.

Su GQ, Huo MX, Yuan ZG, Wang SY, Peng YZ. 2013. Hydrolysis, acidification and dewaterability of waste activated sludge under alkaline conditions: Combined effects of NaOH and $Ca(OH)_2$. Bioresource Technol 136: 237-243.

Tambone F, Genevini P, D'Imporzano G, Adani F. 2009. Assessing amendment properties of digestate by studying the organic matter composition and the degree of biological stability during the anaerobic digestion of the organic fraction of MSW. Bioresource Technol 100(12): 3140-3142.

Ye J, Hu A, Cheng X, Lin W, Liu X, Zhou S, He Z. 2018. Response of enhanced sludge methanogenesis by red mud to temperature: Spectroscopic and electrochemical elucidation of endogenous redox mediators. Water Res. 143: 240-249.

Ye J, Hu AD, Ren GP, Chen M, Tang JH, Zhang PY, Zhou SG, He Z. 2018. Enhancing sludge methanogenesis with improved redox activity of extracellular polymeric substances by hematite in red mud. Water Res 134: 54-62.

Ye J, Hu AD, Ren GP, Zhou T, Zhang GM, Zhou SG. 2018. Red mud enhances methanogenesis with the simultaneous improvement of hydrolysis-acidification and electrical conductivity. Bioresource Technol 247: 131-137.

Yenigun O, Demirel B. 2013. Ammonia inhibition in anaerobic digestion: a review. Process Biochem 48(5-6): 901-911.

Zhao YQ, Yue QY, Li Q, Xu X, Yang ZL, Wang XJ, Gao BY, Yu H. 2012. Characterization of red mud granular adsorbent (RMGA) and its performance on phosphate removal from aqueous solution. Chem Eng J 193: 161-168.

# Appendix

**Table 5.1. The major composition of two types of bauxite residue.**

| Composition | BR1 | BR2 |
|---|---|---|
| $Al_2O_3$ | 18.05 ± 2.97 | 18.34 ± 0.02 |
| CaO | 2.22 ± 0.22 | 12.48 ± 4.74 |
| $Fe_2O_3$ | 21.32 ± 3.41 | 29.53 ± 3.76 |
| $Na_2O$ | 11.70 ± 1.70 | 5.63 ± 3.29 |
| $SiO_2$ | 12.51 ± 8.99 | 3.13 ± 3.84 |
| $TiO_2$ | 4.29 ± 5.80 | 3.13 ± 2.75 |
| LOI (1000 °C) | 11.25 | 16.86 |

**Table 5.2. Parameters of methane production calculated from Gompertz equation.**

| | | $G_0$ (ml) | U (ml/day) | λ (days) |
|---|---|---|---|---|
| Control | 0% | 781.43 ± 8.35 a | 36.96 ± 1.26 a | 4.43 ± 0.36 a |
| BR1 | 0.5% | 818.88 ± 8.48 c | 39.70 ± 1.35 ab | 4.27 ± 0.35 a |
| | 2% | 803.05 ± 7.02 bc | 42.67 ± 1.34 cd | 4.65 ± 0.30 a |
| | 4% | 802.24 ± 7.24 b | 40.84 ± 1.26 bc | 4.89 ± 0.31 a |
| | 8% | 773.93 ± 3.63 a | 44.05 ± 0.77 de | 6.60 ± 0.16 c |
| BR2 | 0.5% | 794.06 ± 6.64 ab | 42.44 ± 1.29 cd | 4.59 ± 0.29 a |
| | 2% | 786.89 ± 5.09 ab | 44.45 ± 1.10 bcd | 4.84 ± 0.23 a |
| | 4% | 792.59 ± 5.68 ab | 46.34 ± 1.29 ef | 5.79 ± 0.25 b |
| | 8% | 766.82 ± 9.41 a | 47.68 ± 2.00 f | 14.93 ± 0.32 d |

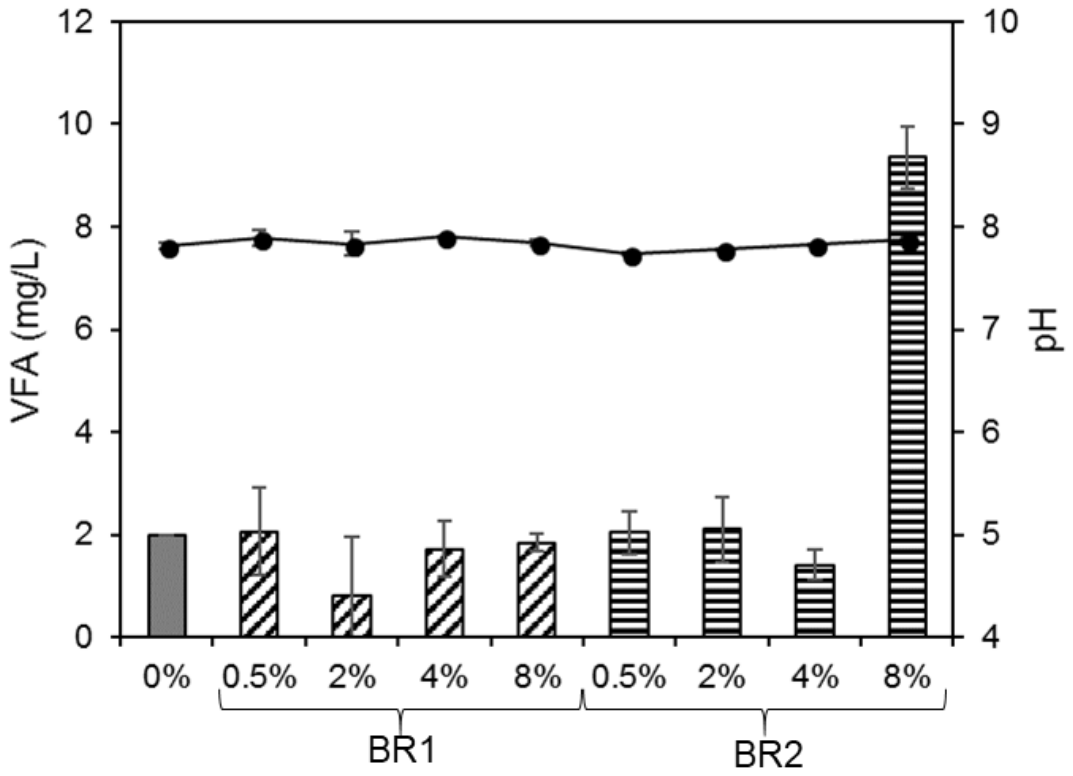


**Figure 5.1. Influence of the addition of different dosages of bauxite residue on the VFA (left axis) and pH (dotted line, right axis) in the anaerobic digester. The error bars indicate the standard deviation with duplicates.**

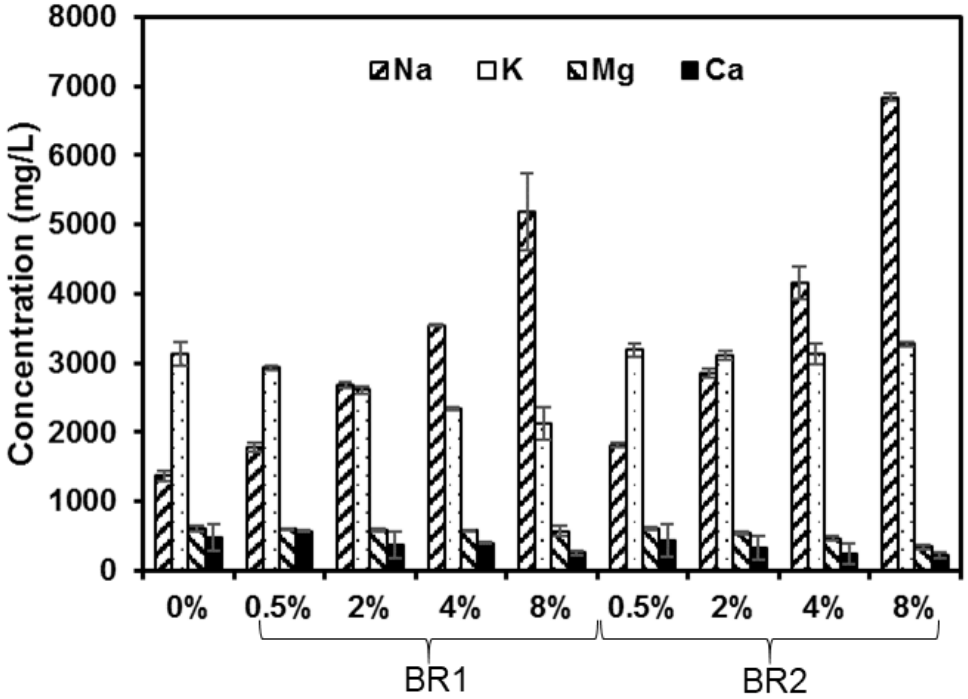


**Figure 5.2. Influence of the addition of different dosages of bauxite residue on soluble cations in the anaerobic digester. The error bars indicate the standard deviation with duplicates.**

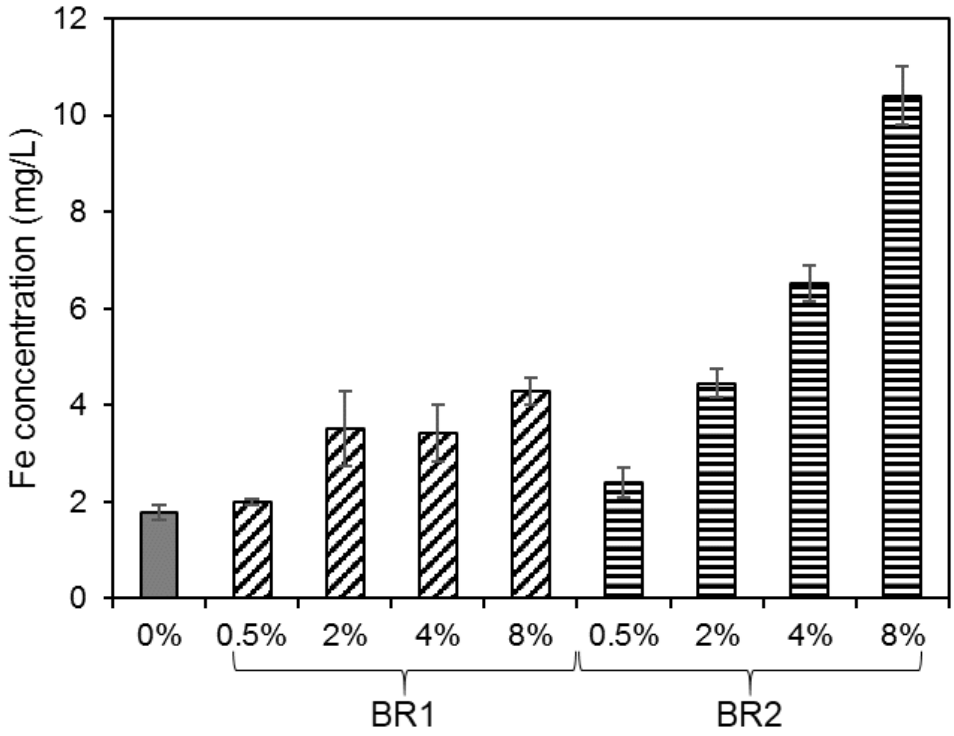


**Figure 5.3. Influence of the addition of different dosages of bauxite residue on Fe in the anaerobic digester. The error bars indicate the standard deviation with duplicates.**

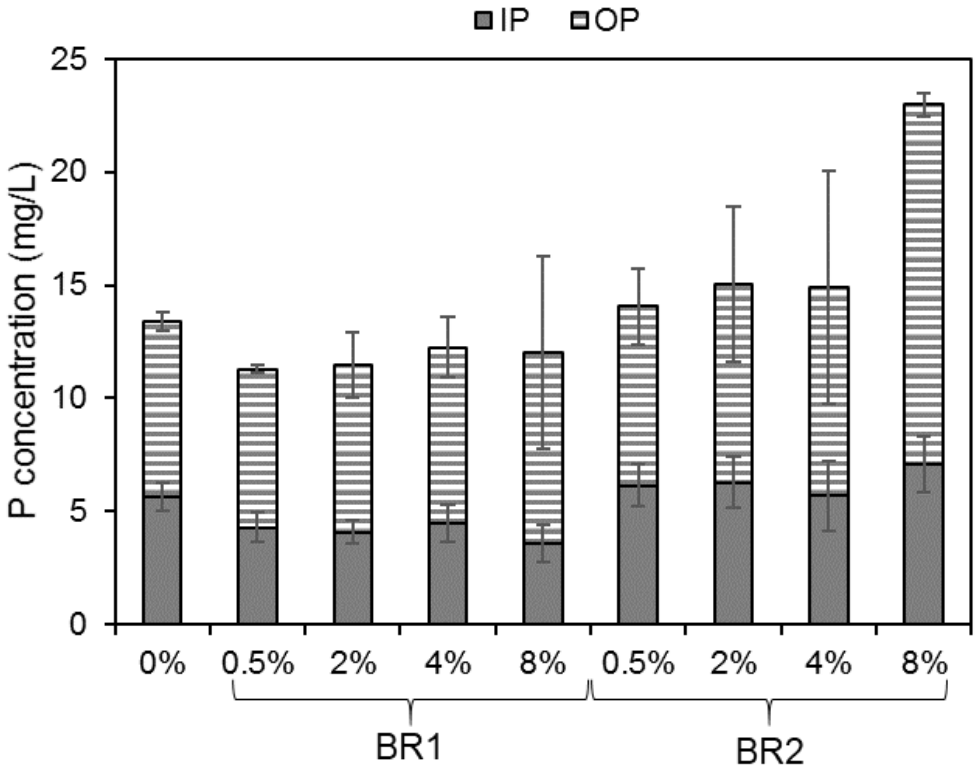


**Figure 5.4. Influence of the addition of different dosages of bauxite residue on P concentration in the liquid of anaerobic digester. The error bars indicate the standard deviation with duplicates.**

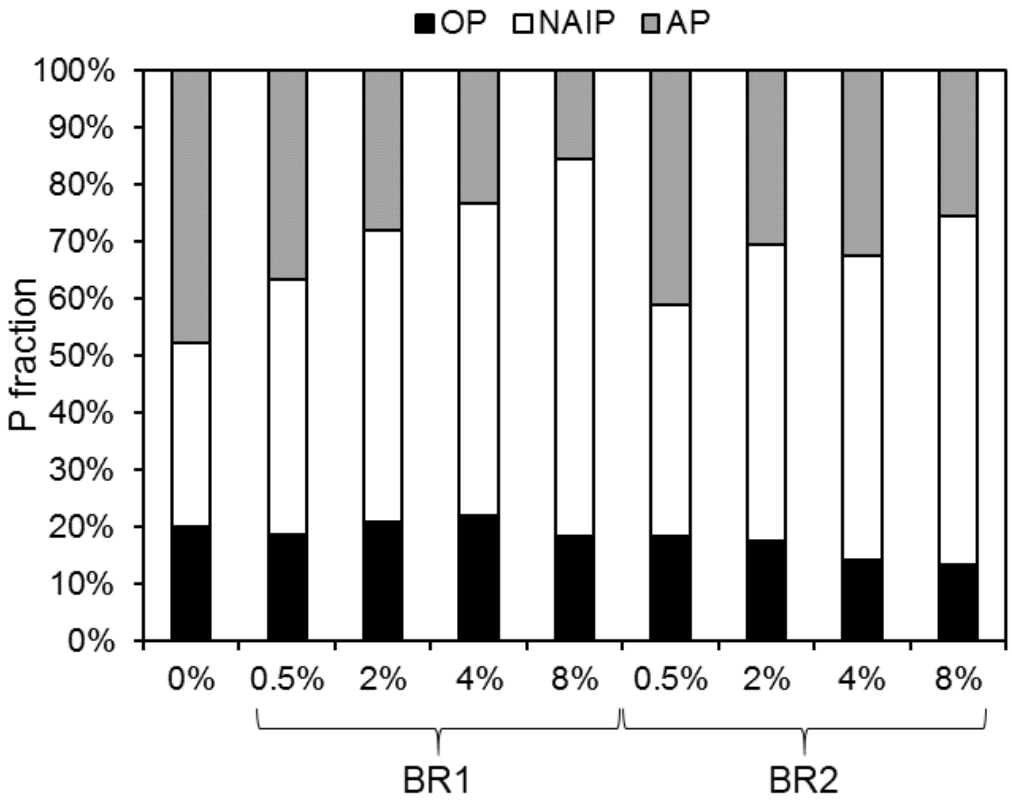


**Figure 5.5. Influence of the addition of different dosages of bauxite residue on P fraction in the digestate.**

# CHAPTER VI
# SUMMARY

Bauxite residue is an industrial waste generated from the alumina refining industry, raising great concerns for environmental pollution. The primary problem for bauxite residue is its high alkalinity and salinity. Flue gas desulfurization as a valid approach has verified to neutralize the alkalinity of bauxite residue with the acidity in flue gas. This beneficial reuse of bauxite residue is desirable for the sustainable management of this waste stream. In this study, it was first identified the linkage between the characteristics of the bauxite residues and their acid neutralization capacity (ANC). Further options of beneficial use were investigated according to the characteristics of bauxite residues. With the iron oxide-rich mineralogy, bauxite residue exhibited excellent capabilities to remove aqueous phosphate at environmentally relevant concentrations. Given that phosphate is an important nutrient, the removal and concentration of phosphorus with bauxite residue could be a strategy for the recovery of phosphorus as a resource. Moreover, bauxite residues were also found to be able to remove ciprofloxacin as an extensively used antibiotics and potential water pollutant. These findings show that bauxite residues could be used as feasible materials for pollution mitigation as well as resource recovery. The utility of bauxite residues was further demonstrated in the utilization of bauxite residues as an additive in anaerobic digestion, which is frequently implemented for the stabilization of organic waste and the production of biogas as a renewable energy source. My work shows that bauxite residues could be readily neutralized by the buffering capacity of the digestate in the anaerobic digestion without negatively impacting process

performance. More importantly, the addition of bauxite residue could enhance the availability of phosphorus in the digestate which is desirable for the land application of anaerobic digestate as a soil supplement.

The significance of this application of bauxite residue could be further illustrated at the nexus of water, energy, and food. High strength wastewater, such as dairy farm wastewater, is treated with the anaerobic digestion technology with the production of biogas as a renewable energy source. Additionally, the digestate derived from anaerobic digestion is suitable for land application as a fertilizer to support crops. Subsequently, crops are used as food for human consumption or as feedstock for livestock. Organic waste from the livestock industry or human consumption can be again used in anaerobic digestion treatment to produce biogas as a renewable energy source and digestate for land application as fertilizers, providing a closed-loop framework with high levels of sustainability that could serve as a model for the development of sustainable environmental management practices in other industries.

# VITA

Yongfeng Wang was born in Zibo, Shandong, China on October 15, 1987. He attended Shandong University for his undergraduate study and earned his Bachelor of Science in Environmental Science in 2010. Then he started his master's thesis studying about the fate of nitro-nonylphenol in soil and sludge under the instruction of Dr. Rong Ji and then attained his Master of Science in Environmental Science in 2013 at Nanjing University. After graduation, he worked as postmaster in Dr. Rong Ji's lab and focused on studying the synthesis of some organic matters. In August 2015, he enrolled on the FEED program and started to pursue a Doctor of Philosophy degree in Environmental Engineering at the University of Tennessee, Knoxville. Under the guidance of Dr. Qiang He, his research focused on the reuse of industrial solid waste and anaerobic digestion.